Vibration Fatigue Testing of Socket Welds (PWRMRP-07)



PWR Materials Reliability Project (PWRMRP)

Effective December 6, 2006, this report has been made publicly available in accordance with Section 734.3(b)(3) and published in accordance with Section 734.7 of the U.S. Export Administration Regulations. As a result of this publication, this report is subject to only copyright protection and does not require any license agreement from EPRI. This notice supersedes the export control restrictions and any proprietary licensed material notices embedded in the document prior to publication.

SINGLE USER LICENSE AGREEMENT

THIS IS A LEGALLY BINDING AGREEMENT BETWEEN YOU AND THE ELECTRIC POWER RESEARCH INSTITUTE, INC. (EPRI). PLEASE READ IT CAREFULLY BEFORE BREAKING OR TEARING THE WARNING LABEL AND OPENING THIS SEALED PACKAGE.

BY OPENING THIS SEALED REPORT YOU ARE AGREEING TO THE TERMS OF THIS AGREEMENT. IF YOU DO NOT AGREE TO THE TERMS OF THIS AGREEMENT, PROMPTLY RETURN THE UNOPENED REPORT TO EPRI AND THE PURCHASE PRICE WILL BE REFUNDED.

1. GRANT OF LICENSE

EPRI grants you the nonexclusive and nontransferable right during the term of this agreement to use this report only for your own benefit and the benefit of your organization. This means that the following may use this report: (I) your company (at any site owned or operated by your company); (II) its subsidiaries or other related entities; and (III) a consultant to your company or related entities, if the consultant has entered into a contract agreeing not to disclose the report outside of its organization or to use the report for its own benefit or the benefit of any party other than your company.

This shrink-wrap license agreement is subordinate to the terms of the Master Utility License Agreement between most U.S. EPRI member utilities and EPRI. Any EPRI member utility that does not have a Master Utility License Agreement may get one on request.

2. COPYRIGHT

This report, including the information contained in it, is either licensed to EPRI or owned by EPRI and is protected by United States and international copyright laws. You may not, without the prior written permission of EPRI, reproduce, translate or modify this report, in any form, in whole or in part, or prepare any derivative work based on this report.

3. RESTRICTIONS

You may not rent, lease, license, disclose or give this report to any person or organization, or use the information contained in this report, for the benefit of any third party or for any purpose other than as specified above unless such use is with the prior written permission of EPRI. You agree to take all reasonable steps to prevent unauthorized disclosure or use of this report. Except as specified above, this agreement does not grant you any right to patents, copyrights, trade secrets, trade names, trademarks or any other intellectual property, rights or licenses in respect of this report.

4. TERM AND TERMINATION

This license and this agreement are effective until terminated. You may terminate them at any time by destroying this report. EPRI has the right to terminate the license and this agreement immediately if you fail to comply with any term or condition of this agreement. Upon any termination you may destroy this report, but all obligations of nondisclosure will remain in effect.

5. DISCLAIMER OF WARRANTIES AND LIMITATION OF LIABILITIES

NEITHER EPRI, ANY MEMBER OF EPRI, ANY COSPONSOR, NOR ANY PERSON OR ORGANIZATION ACTING ON BEHALF OF ANY OF THEM:

(A) MAKES ANY WARRANTY OR REPRESENTATION WHATSOEVER, EXPRESS OR IMPLIED, (I) WITH RESPECT TO THE USE OF ANY INFORMATION, APPARATUS, METHOD, PROCESS OR SIMILAR ITEM DISCLOSED IN THIS REPORT, INCLUDING MERCHANTABILITY AND FITNESS FOR A PARTICULAR PURPOSE, OR (II) THAT SUCH USE DOES NOT INFRINGE ON OR INTERFERE WITH PRIVATELY OWNED RIGHTS, INCLUDING ANY PARTY'S INTELLECTUAL PROPERTY, OR (III) THAT THIS REPORT IS SUITABLE TO ANY PARTICULAR USER'S CIRCUMSTANCE; OR

(B) ASSUMES RESPONSIBILITY FOR ANY DAMAGES OR OTHER LIABILITY WHATSOEVER (INCLUDING ANY CONSEQUENTIAL DAMAGES, EVEN IF EPRI OR ANY EPRI REPRESENTATIVE HAS BEEN ADVISED OF THE POSSIBILITY OF SUCH DAMAGES) RESULTING FROM YOUR SELECTION OR USE OF THIS REPORT OR ANY INFORMATION, APPARATUS, METHOD, PROCESS OR SIMILAR ITEM DISCLOSED IN THIS REPORT.

6. EXPORT

The laws and regulations of the United States restrict the export and re-export of any portion of this report, and you agree not to export or re-export this report or any related technical data in any form without the appropriate United States and foreign government approvals.

7. CHOICE OF LAW

This agreement will be governed by the laws of the State of California as applied to transactions taking place entirely in California between California residents.

8. INTEGRATION

You have read and understand this agreement, and acknowledge that it is the final, complete and exclusive agreement between you and EPRI concerning its subject matter, superseding any prior related understanding or agreement. No waiver, variation or different terms of this agreement will be enforceable against EPRI unless EPRI gives its prior written consent, signed by an officer of EPRI.

Vibration Fatigue Testing of Socket Welds (PWRMRP-07)

PWR Materials Reliability Project (PWRMRP)

TR-113890

Final Report, December 1999

EPRI Project Manager
R. Carter

EPRI • 3412 Hillview Avenue, Palo Alto, California 94304 • PO Box 10412, Palo Alto, California 94303 • USA
800.313.3774 • 650.855.2121 • askepri@epri.com • www.epri.com

DISCLAIMER OF WARRANTIES AND LIMITATION OF LIABILITIES

THIS DOCUMENT WAS PREPARED BY THE ORGANIZATION(S) NAMED BELOW AS AN ACCOUNT OF WORK SPONSORED OR COSPONSORED BY THE ELECTRIC POWER RESEARCH INSTITUTE, INC. (EPRI). NEITHER EPRI, ANY MEMBER OF EPRI, ANY COSPONSOR, THE ORGANIZATION(S) BELOW, NOR ANY PERSON ACTING ON BEHALF OF ANY OF THEM:

(A) MAKES ANY WARRANTY OR REPRESENTATION WHATSOEVER, EXPRESS OR IMPLIED, (I) WITH RESPECT TO THE USE OF ANY INFORMATION, APPARATUS, METHOD, PROCESS, OR SIMILAR ITEM DISCLOSED IN THIS DOCUMENT, INCLUDING MERCHANTABILITY AND FITNESS FOR A PARTICULAR PURPOSE, OR (II) THAT SUCH USE DOES NOT INFRINGE ON OR INTERFERE WITH PRIVATELY OWNED RIGHTS, INCLUDING ANY PARTY'S INTELLECTUAL PROPERTY, OR (III) THAT THIS DOCUMENT IS SUITABLE TO ANY PARTICULAR USER'S CIRCUMSTANCE; OR

(B) ASSUMES RESPONSIBILITY FOR ANY DAMAGES OR OTHER LIABILITY WHATSOEVER (INCLUDING ANY CONSEQUENTIAL DAMAGES, EVEN IF EPRI OR ANY EPRI REPRESENTATIVE HAS BEEN ADVISED OF THE POSSIBILITY OF SUCH DAMAGES) RESULTING FROM YOUR SELECTION OR USE OF THIS DOCUMENT OR ANY INFORMATION, APPARATUS, METHOD, PROCESS, OR SIMILAR ITEM DISCLOSED IN THIS DOCUMENT.

ORGANIZATION(S) THAT PREPARED THIS DOCUMENT

Structural Integrity Associates, Inc.
Pacific Gas and Electric Company

ORDERING INFORMATION

Requests for copies of this report should be directed to the EPRI Distribution Center, 207 Coggins Drive, P.O. Box 23205, Pleasant Hill, CA 94523, (800) 313-3774.

Electric Power Research Institute and EPRI are registered service marks of the Electric Power Research Institute, Inc. EPRI. POWERING PROGRESS is a service mark of the Electric Power Research Institute, Inc.

Copyright © 1999 Electric Power Research Institute, Inc. All rights reserved.

CITATIONS

This report was prepared by

Structural Integrity Associates, Inc.
3315 Almaden Expressway, Suite 24
San Jose, CA 95118

Principal Investigators
P. Riccardella
P. Hirschberg
S. Pan

Pacific Gas and Electric Company
Technical and Ecological Services
3400 Crow Canyon Road
San Ramon, CA 94583

Principal Investigators
M. Sullivan
J. Schletz

EPRI Repair and Relpacement Applications Center
1300 W.T. Harris Blvd.
Charlotte, NC 28262

Principal Investigator
G. Frederick

This report describes research sponsored by EPRI.

The report is a corporate document that should be cited in the literature in the following manner:

Vibration Fatigue Testing of Socket Welds (PWRMRP-07): PWR Materials Reliability Project (PWRMRP), EPRI, Palo Alto, CA: 1999. TR-113890.

REPORT SUMMARY

Failures of small bore piping connections continue to occur frequently at nuclear power plants in the United States, resulting in degraded plant systems and unscheduled plant downtime. Socket welds are used extensively for small bore piping and fittings (less than 2 inches (5.08 cm) nominal pipe size) in nuclear power plant systems. This study was undertaken to improve socket weld design and fabrication practices to allow these welds to better resist high cycle fatigue.

Background

Fatigue-related failures are generally detected as small cracks or leaks before major pressure boundary ruptures occur. However, in many cases, the leak locations are not isolable from the primary reactor coolant system and result in forced plant outages. EPRI report TR-104534 indicated that the majority of fatigue failures are caused by vibration of socket welds. Analytical results reported in EPRI TR-107455 have demonstrated that the socket weld leg size configuration can have an important effect on its high cycle fatigue resistance, with longer legs along the pipe side of the weld greatly increasing its predicted fatigue resistance. Other potentially important factors influencing fatigue life include residual stress, weld root and toe condition, loading mode, pipe size, axial and radial gaps, and materials of construction.

Objectives

- To confirm the analytical predictions reported in EPRI TR-107455
- To quantify the effects of the factors listed above on the fatigue strength of socket welds
- To test methods of *in situ* modification or repair of socket welds

Approach

Fifty-four socket weld specimens of various designs were tested by bolting them to a vibration shaker table and shaking them near their resonant frequencies to produce the desired stress amplitudes and cycles. Researchers examined the effect of the weld leg size on fatigue resistance by testing samples fabricated with oversized legs on the pipe side and comparing them to control samples of nominal Code dimensions. Other parameters that were tested included axial radial gaps, the effects of residual stress, toe condition, pipe size, materials, and last pass weld improvement, a technique in which an additional weld pass is added at the toe on the pipe side of a normal ASME Code socket weld. Repair of leaking welds by a weld overlay and modification of standard Code welds by buildup of the pipe side leg length were tested to determine whether the original fatigue strength of welds subjected to fatigue cycling could be restored *in situ*. Some butt welds were also tested for comparison purposes.

Results

It is concluded that socket welds with a 2 to 1 weld leg configuration (weld leg along the pipe side of the weld equal to twice the Code-required weld leg dimension) offer a significant high cycle fatigue improvement over standard ASME Code socket welds. This weld design offers a superior improvement in fatigue resistance than does replacement of socket-welded fittings with butt-welded fittings. Because vibration fatigue of socket welds has been a significant industry problem, it is recommended that this improved configuration be used for all socket welds in vibration-critical applications.

The majority of the test failures occurred due to cracks that initiated at weld roots. However, toe-initiated failures occurred in tests at higher stress levels and were premature in comparison with identical tests in which root failures prevailed. Therefore, care must be taken with socket welds to avoid metallurgical or geometric discontinuities at the toes of the welds (such as undercut or non-smooth transitions). Such discontinuities promote a tendency for toe failure, which greatly reduces fatigue life.

The ASME Code-required axial gap in socket welds [1/16-inch (.16 cm)] appears to have little or no effect on high cycle fatigue resistance and post-weld heat treatment (PWHT) appears to increase the fatigue resistance of standard Code specimens. Although post-weld heat treatment consistently showed improved results, it has the downside of potentially sensitizing austenitic welds for intergranular stress corrosion cracking (IGSCC) in certain environments. Therefore, PWHT is not recommended for situations where IGSCC might be an active damage mechanism.

Testing of modification and repair concepts indicated that these approaches were successful in improving the strength of already-installed socket welds without having to replace them with butt welds. Code standard 1x1 welds that were built up to a 2x1 profile performed as well as new 2x1 welds. Weld overlay repairs of leaking standard welds not only provided enough fatigue resistance for the welds to last to the next outage, but also actually improved their fatigue strength to better than new standard Code welds.

EPRI Perspective

Vibration fatigue is the leading cause of piping failures in nuclear power plants, accounting for more than one-third of all piping failures. Such failures cause unplanned or extended outages and have a significant cost impact on the industry. The results obtained in this study are expected to lead to improvements in socket weld design, fabrication, and integrity management.

TR-113890

Keywords

Piping systems
Pipe joints
Fatigue (materials)
Fatigue testing
Welded joints

ABSTRACT

Failures of small bore piping connections continue to occur frequently at nuclear power plants in the United States, resulting in degraded plant systems and unscheduled plant downtime. Fatigue-related failures are generally detected as small cracks or leaks but, in many cases, the leak locations are not isolable from the primary reactor coolant system and result in forced plant outages. Because socket welds are used extensively for small bore piping and fittings, this study was undertaken to improve socket weld design and fabrication practices to allow these welds to better resist high cycle fatigue. EPRI report TR-104534 indicated that the majority of fatigue failures are caused by vibration of socket welds. Analytical results reported in EPRI TR-107455 have demonstrated that the socket weld leg size configuration can have an important effect on its high cycle fatigue resistance, with longer legs along the pipe side of the weld greatly increasing its predicted fatigue resistance. Other potentially important factors influencing fatigue life include residual stress, weld root and toe condition, pipe size, axial and radial gaps, and materials of construction.

The purpose of this project was to perform high cycle testing of socket welds of various designs in order to quantify the effects of these factors upon fatigue strength. Another objective was to test methods of *in situ* modification or repair of socket welds to provide an alternative to replacement with butt welds. 54 socket weld specimens of various designs were tested by bolting them to a vibration shaker table and shaking them near their resonant frequencies to produce the desired stress amplitudes and cycles. The effect of the weld leg size on fatigue resistance was examined by testing samples fabricated with oversized legs on the pipe side and comparing them to control samples of nominal Code dimensions. Other parameters that were tested included the effects of residual stress, toe condition, pipe size, materials, and last pass weld improvement, a technique in which an additional weld pass is added at the toe on the pipe side of a normal ASME Code socket weld. Tests were also conducted to determine the potential effect of eliminating the Code-required axial gap from an otherwise standard Code weld. Repair of leaking welds by a weld overlay, and modification of standard Code welds by buildup of the pipe side leg length, were tested to determine whether the original fatigue strength of welds subjected to fatigue cycling could be restored *in situ.*

Results are presented that include comparisons of the various socket weld designs with standard Code socket welds, butt welds, ASME mean failure data, and recent test data from Japan. Fatigue strength reduction factors (FSRFs) are calculated based on the testing results. On the basis of the testing, it is concluded that socket welds with a 2 to 1 weld leg configuration offer a significant high cycle fatigue improvement over standard ASME Code socket welds.

CONTENTS

_1_ INTRODUCTION 1-1

_2_ BACKGROUND AND APPROACH 2-1

2.1 Fatigue Strength Reduction Factors and ASME Code Stress Indices 2-1

2.2 Weld Geometry Effects 2-2

2.3 Dynamic Load Factors in Vibration Loading 2-7

_3_ TEST PROGRAM 3-1

3.1 Testing Arrangement 3-1

3.2 Parameters Tested 3-4

3.3 Data Analysis 3-11

_4_ TEST RESULTS 4-1

4.1 General Observations 4-1

4.2 Effect of Weld Size 4-7

4.3 Toe Condition 4-10

4.4 Weld Process Enhancements 4-12

4.5 3/4-Inch (1.91 cm) Pipe Diameter Tests 4-15

4.6 Modified and Repaired Welds 4-17

4.7 Fatigue Strength Reduction Factors 4-19

4.8 Dynamic Load Factors (DLFs) 4-21

_5_ CONCLUSIONS AND RECOMMENDATIONS 5-1

_6_ REFERENCES 6-1

_A_ TEST ASSEMBLY A-1

A.1 Socket Weld Flange A-2

A.2 Pipe Section A-3

A.3 Slip-On Flange and Blind Flange A-3

_B_ WELD SPECIFICATIONS B-1

B.1 Standard 1x1 Configuration B-4

B.2 2x1 Modified Configuration B-6

B.3 Last Pass Improved (LPI) B-9

B.4 Post-Weld Heat Treat (PWHT) B-11

B.5 No Axial Gap Configuration B-11

B.6 Welds with Toe Discontinuity B-13

B.7 1x1 to 2x1 Modified Configuration B-13

B.8 Overlay Repair Weld Configuration B-16

B.9 Standard Butt Weld Configuration B-28

B.10 Butt Weld with Flaw B-31

LIST OF FIGURES

Figure 2-1 Comparison of ASME Mean Failure Curve with Markl Correlation 2-3
Figure 2-2 DLF vs. Damping and Frequency 2-8
Figure 3-1 Overall Test Setup 3-1
Figure 3-2 Test Specimen Detail 3-2
Figure 3-3 Test Apparatus 3-3
Figure 3-4 Test Specimen Configurations 3-4
Figure 3-5 1 x 1 Weld Built Up to 2 x 1 3-8
Figure 3-6 Weld Overlay Design 3-8
Figure 3-7 Standard Weld with PWHT 3-9
Figure 3-8 Standard Weld Built Up to 2x1 3-10
Figure 3-9 Weld Overlay Repair 3-10
Figure 4-1 Root Failure 4-3
Figure 4-2 Toe Failure 4-3
Figure 4-3 2" (5.08 cm) Stainless Steel Weld Sizes 4-7
Figure 4-4 2" (5.08 cm) Carbon Steel Weld Sizes 4-8
Figure 4-5 Butt Weld Failure 4-10
Figure 4-6 Toe Conditions 4-11
Figure 4-7 Polished Toe Failure 4-12
Figure 4-8 2" (5.08 cm) Stainless Steel Weld Enhancements 4-13
Figure 4-9 2" (5.08 cm) Carbon Steel Weld Enhancements 4-14
Figure 4-10 3/4" (1.91 cm) Stainless Steel Tests 4-15
Figure 4-11 Comparison of 3/4" (1.91 cm) and 2" (5.08 cm) Data 4-16
Figure 4-12 Weld Overlay of Toe Crack 4-18
Figure 4-13 Weld Overlay of Root Crack 4-18
Figure A-1 Drawing of Typical Test Specimen for Vibration Fatigue Test Evaluation A-1
Figure A-2 Socket-Welded Flange Specifications for 3/4-Inch (1.91 cm) Test Specimens A-2
Figure A-3 Socket-Welded Flange Specifications for 2-Inch (5.08 cm) Test Specimens A-2
Figure A-4 Blind Flange for 2-Inch (5.08 cm) Test Specimens with O-Ring Groove A-4
Figure A-5 Blind Flange for 3/4-Inch (1.91 cm) Test Specimens with O-Ring Groove A-4

Figure B-1 Drawing of Standard Weld Sequence with Equal Leg Lengths B-5
Figure B-2 Drawing of Modified Weld Sequence for Vibration Fatigue Test Matrix with Fillet Weld Leg L2 > L1 for 2-Inch (5.08 cm) Specimen B-7
Figure B-3 Drawing of Modified Weld Sequence with Unequal Fillet Weld Leg Length (L2 = 2 x L1) for 3/4-Inch (1.91 cm) Test Specimen B-8
Figure B-4 Drawing of Modified Weld Sequence with Last-Pass-Improved Weld Pass on the Pipe Side B-10
Figure B-5 Drawing of Standard Weld Sequence with Equal Leg Lengths B-12
Figure B-6 Drawing of Modified Weld Geometry from the Standard L1 = L2 to L2 = 2L1 ..... B-15
Figure B-7 Weld Sequence for 1x1 to 2x1 Modified Configuration B-16
Figure B-8 Geometry for Repair Overlay Sequence for Standard 1x1 Weld B-19
Figure B-9 Seal Welds for Cracked Specimen B3-2CS-1 ..... B-20
Figure B-10 Overlay Sequence for Cracked Specimen B3-2CS-1 ..... B-21
Figure B-11 Seal Welds for Cracked Specimen B3-2CS-2 ..... B-22
Figure B-12 Overlay Sequence for Cracked Specimen B3-2CS-2 ..... B-23
Figure B-13 Seal Welds for Cracked Specimen B2-2SS-2 ..... B-24
Figure B-14 Overlay Sequence for Cracked Specimen B2-2SS-2 ..... B-25
Figure B-15 Seal Welds for Cracked Specimen B2-2SS-8 ..... B-26
Figure B-16 Overlay Sequence for Cracked Specimen B2-2SS-8 ..... B-27
Figure B-17 Drawing of Typical Mockup Configuration with Standard Weld Neck Flange for Butt Weld Evaluation B-29
Figure B-18 Drawing of Standard Weld Sequence for Butt Weld Geometry B-30
Figure B-19 Drawing of Standard Weld Sequence for Butt Weld Geometry with Flaw B-32

LIST OF TABLES

Table 3-1 Phase I Test Matrix 3-6
Table 3-2 Phase II Test Matrix 3-7
Table 4-1 Phase I Test Results 4-2
Table 4-2 Phase II Test Results 4-5
Table 4-3 Fatigue Strength Reduction Factors 4-20
Table B-1 Test Matrix—Weld Categories B-2
Table B-2 Weld Specifications for Standard 1x1 Configuration B-4
Table B-3 Weld Specifications for 2x1 Modified Configuration B-6
Table B-4 Weld Specifications for LPI Configuration B-9
Table B-5 Weld Specifications for 1x1 to 2x1 Modified Configuration B-14
Table B-6 Weld Specifications for Overlay and Seal Weld Repair Configuration B-18
Table B-7 Weld Specifications for Standard Butt Weld Configurations B-28

1
INTRODUCTION

Failures of small bore piping connections continue to occur frequently at nuclear power plants in the United States, resulting in degraded plant systems and unscheduled plant downtime. Fatigue-related failures are generally detected as small cracks or leaks before major pressure boundary ruptures occur. However, in many cases, the leak locations are not isolable from the primary coolant system and result in forced plant outages. Most of the recent failures have been small bore piping connections to the primary coolant system and were first noticed as an increase in unidentified leakage. However, other systems, such as main steam and electro-hydraulic control systems, have also experienced similar failures.

Prior research [1] has indicated that the majority of such failures are caused by vibration fatigue of socket welds. In order to better understand and characterize this phenomenon, investigations have been performed in the United States [1,2,3] and overseas [4,5,6]. Analytical results reported in EPRI TR-107455 [3] have demonstrated that the socket weld leg size configuration can have an important effect on its high cycle fatigue resistance, with longer legs along the pipe side of the weld greatly increasing its predicted fatigue resistance. Other factors that potentially influence socket weld fatigue life are residual stress, weld root and toe condition, loading mode, pipe size, axial and radial gaps, and materials of construction.

The test program documented in this report was initiated in 1997 to study the importance of these factors and to confirm the analytical predictions reported in EPRI TR-107455 [3]. The program continued through 1999. A large number of socket weld samples were vibration-fatigue tested to failure on a high frequency shaker table. The objectives of the testing were to:

- Improve the industry's understanding and characterization of the high cycle fatigue resistance of socket welds
- Develop appropriate fatigue strength reduction factors for socket welds that reflect the effects of the factors listed above that prove to be significant

The ultimate goal of this research is to develop recommended design and fabrication practices that can be used to enhance socket weld fatigue resistance in vibration-sensitive locations, as well as to provide guidelines for screening out and preventing vibration fatigue failures in existing welds.

The testing program was carried out in two phases. The first phase [7], completed in 1998, investigated the variation in high cycle fatigue resistance as a function of weld leg length, pipe diameter, and piping material. The effect of an additional weld pass, post-weld heat treatment, and eliminating the ASME Code-required axial gap were also studied. The second phase investigated remedial actions for existing socket welds in order to determine their effectiveness in extending the useful life of socket-welded joints in lieu of making expensive modifications.

The effect of varying toe conditions was also studied in Phase II and additional data at higher loads was collected to further quantify the benefit of increased weld leg length. This report describes the entire test program (Phases I and II), including testing procedure, results, and conclusions.

2
BACKGROUND AND APPROACH

The purpose of this work was to provide experimental confirmation of several important effects observed in the analytical studies reported in EPRI TR-107455 [3], which could have a major influence on how socket welds are designed and fabricated for vibration-critical applications. Based on the results, the intent is to propose practical evaluation tools, design and fabrication methods, and remedial measures for socket welds in vibration-critical applications.

2.1 Fatigue Strength Reduction Factors and ASME Code Stress Indices

The ASME Boiler and Pressure Vessel Code, Section III [8], requires that the design of Class 1 piping account for the possibility of fatigue as a cause of failure. Welded joints are common locations for the origination of fatigue cracks because they produce discontinuities in geometry and stiffness, which result in local stress concentrations. The surface of the weld can also contain small flaws that might eventually lead to cracking. The probability of fatigue failure is a function of many considerations: type of weld, weld profile, material, weld size, wall thickness, heat treatment, grinding after welding, and so on. Socket welds are commonly used in small bore piping (2-inch (5.08 cm) and under) joints due to their ease of assembly but their fatigue strength is generally considered to be less than that of a butt weld. The Fatigue Strength Reduction Factor (FSRF) is defined in Article NB-3200 of Section III of the Code as a stress intensification factor that accounts for the effect of a local structural discontinuity on the fatigue strength of the joint. It is defined as the fatigue strength of the component without the discontinuity divided by the fatigue strength with the discontinuity. The FSRF is a way of measuring the relative resistance to fatigue damage of variations in the geometric configuration of the weld joint or other structural detail. It accounts for local effects that are typically not part of the piping stress analysis. The FSRF is usually determined by test and is generally calculated by dividing the endurance limit of the ASME mean failure curve by the endurance limit of the joint in question. The endurance limit is used because the FSRF varies with fatigue life; the value at the endurance limit is bounding. (For practical reasons, the endurance limit is often defined as the fatigue strength at some large, predefined number of cycles, such as 10^7.)

Appendix I of the ASME Code provides design fatigue curves that relate allowable cyclic stress amplitude to the number of loading cycles. These curves include a factor of safety of two on stress or twenty on cycles, whichever is more conservative, to account for data scatter, size effects, testing environment, and strain rate effects [10]. (The factor of safety of two on stress governs in the high cycle fatigue range.) Article NB-3600 of Section III, which provides rules for the design of Class 1 piping, accounts for the variation in fatigue strength between different welds and fittings by multiplying the calculated alternating stress by stress indices, before entering the fatigue curves. For primary plus secondary bending moment loading, the applicable

stress index is the product of C_2 and K_2. C_2K_2 is essentially an FSRF. For socket welds (1998 Edition of the Code),

$K_2 = 2.0$

$C_2 = 2.1 (t_n/C_x)$ but > 1.3

where t_n = nominal pipe thickness

C_x = weld leg length = 1.09 t_n for a Code minimum weld

Therefore $C_2 = 1.93$ for a Code minimum weld, and the product C_2K_2 is 3.86, or essentially an FSRF of 4 for a socket weld.

For Class 2 piping, the ASME Code uses stress intensification factors (i factors) instead of stress indices. The i factors are based on Markl's testing where the mean trend of the fatigue data on carbon steel welds was represented by

$iS = 490{,}000\ N^{-0.2}$

An i of 1.0 corresponds to a butt weld. A socket weld has an i of 2.1 (t_n/C_x). Stress indices for Class 1 piping can be generally related to stress intensification factors for Class 2 piping by

$i = C_2K_2 / 2$

The above relationship is not strictly true because the Class 1 indices are indexed to the mean failure curve for smooth bar specimens [11], while the Class 2 intensification factors are indexed to a fit of butt weld test data that is a straight line on a log-log plot. Although there is a good correlation between the two for a fatigue life of up to 10^6 cycles, the ASME smooth bar failure curve exhibits an endurance limit and, thus, diverges from the Markl straight line in the high cycle fatigue regime (Figure 2-1). The Class 1 approach is more appropriate for fatigue-critical components because it invokes a rigorous fatigue usage factor analysis. The Class 2 approach includes a caveat that it is not intended for highly fatigue-critical applications.

The testing program described herein determined FSRFs for each test specimen by dividing the alternating stress at the endurance limit ($2x10^7$ cycles) from the applicable smooth bar mean failure curve, by the apparent endurance limit of the test specimen.

2.2 Weld Geometry Effects

While the ASME piping design Code provides stress indices for socket welds, these represent the predicted fatigue strength of standard weld designs. This test program included welds of the standard Code design as well as several variations in weld design. The following is an overview of the parameters being studied.

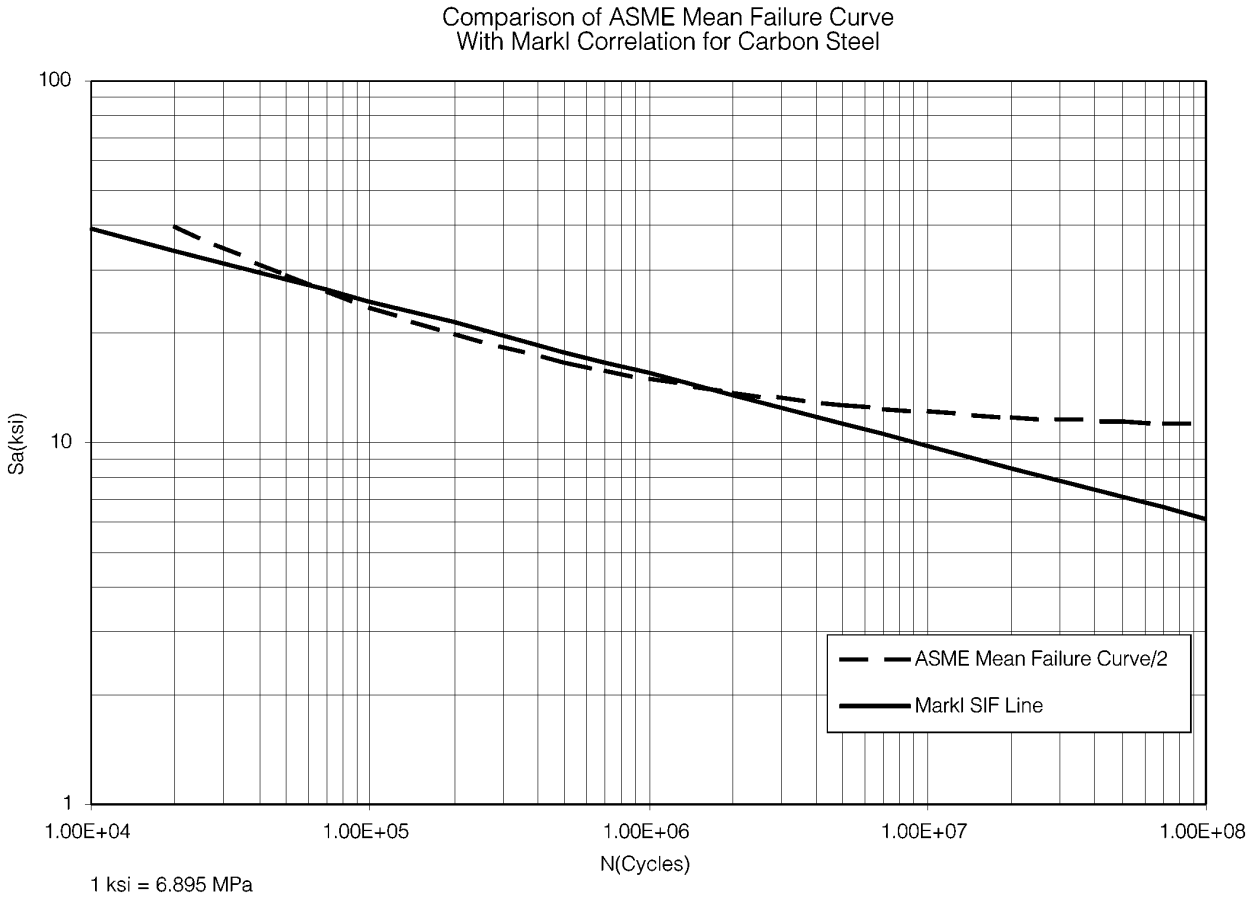


Figure 2-1
Comparison of ASME Mean Failure Curve with Markl Correlation

Weld Leg Size

Analysis described in Reference [3], and testing reported in Reference [9], have identified variations in socket weld design that can significantly affect the fatigue life of the joint under high cycle loading. One of the most important factors is the weld leg size. The Code partially accounts for this in that the primary plus secondary stress index C_2 is inversely proportional to the weld leg length. However, the formula for the index is based on the shortest leg length. Extending the weld leg length along the pipe side of the weld by a factor of two over the Code minimum of 1.09 t_n (where t_n is the nominal pipe wall thickness) has resulted in significant benefit in previous testing. The Code stress index, in its current formulation, is not reduced, however, for this weld geometry from that of a standard weld because the fitting side leg length is still 1.09 t_n. In this testing program, the effect of weld size on fatigue resistance was studied by testing samples fabricated with oversized legs on the pipe side and comparing them to control samples at nominal Code dimensions. Testing was also done to study how conventional small bore butt welded fittings compare to new 2 x 1 welds and to 1 x 1 welds modified to 2 x 1 weld dimensions, under comparable loading conditions.

Residual Stress

The residual stress in the weld can have an important effect on fatigue life in the high cycle regime. Residual stress acts as a mean stress, which reduces the allowable number of cycles at a particular alternating stress. This is more important in the high cycle region than in low cycle fatigue, where the effects of plasticity act to relieve the mean stress. The ASME Code fatigue curve for austenitic steel accounts for mean stress effects in the high cycle regime, as the curve splits into three curves above 10^6 cycles, using a Goodman diagram approach [10] to account for the mean stress.

The Goodman diagram is used to determine the equivalent alternating stress that produces the same fatigue damage at zero mean stress as the actual alternating stress produces with the actual mean stress. The relationship is the following:

$$S_{eq} = \frac{S_{alt}}{1 - \frac{S_{mean}}{S_u}}$$

Where: S_{eq} = Alternating stress adjusted for mean stress

S_{alt} = Actual alternating stress

S_{mean} = Mean stress

S_u = Material ultimate stress

The adjustment of the ASME Code fatigue curve to account for the maximum effect of mean stress can be represented by the following equation:

$$S_{N'} = S_N \left[\frac{S_u - S_y}{S_u - S_N} \right]$$

Where: S_N = Allowable alternating stress at N cycles

$S_{N'}$ = Adjusted allowable stress at N cycles

S_y = Yield stress

The residual stress in a socket weld can be altered by varying the welding technique, such as by adding a final cover weld pass. Last pass improvement refers to a technique in which a normal Code socket weld is improved by adding a last pass on the pipe side of the weld, which theoretically changes the residual stress in the weld root to compressive. Tests were conducted to determine the amount of benefit gained by this process.

Post-Weld Heat Treatment

Post-weld heat treatment (PWHT) is another method for reducing the residual stress in a weld. The ASME Code requires PWHT for most ferritic steel welds but exempts socket welds and austenitic steels. One of the reasons is that heating austenitic steels can sensitize them to Intergranular Stress Corrosion Cracking (IGSCC). However, in view of the importance of residual stresses in high cycle fatigue life, applying PWHT to socket welds in vibration-sensitive locations that are not exposed to an IGSCC-conducive environment can be a viable means of reducing residual stress. Several specimens were post-weld heat treated and tested to quantify the benefit.

Axial Gap

The ASME Code requires that an axial gap of 1/16-inch (.16 cm) be provided between the pipe end and the socket. The reason is that, if the pipe carries hot fluid, differential thermal expansion between the pipe and the fitting might add significant stress to the weld if there is no gap. Also, without the gap, shrinkage of the fillet weld could produce residual stresses in the weld, pipe, and fitting wall. However, some recent testing [4] has indicated that the absence of a gap has a negligible effect, or even some benefit, on the fatigue life. Four specimens were fabricated without the Code-required axial gap and tested.

Weld Profile and Toe Condition

The profile of the weld and the condition of the weld toe can have a significant effect on socket weld fatigue life. The ideal toe condition is for the weld to blend smoothly with the pipe with no discontinuity or undercut. Premature toe failures are generally the result of a discontinuity or small flaw in the toe, which propagates through the base metal. Grinding the weld can help by removing small surface imperfections, which could be sites for crack initiation. Conversely,

heavy “abusive” grinding can worsen the situation by leaving a cold worked condition and tensile residual stresses. In the first phase of testing, several specimens exhibited toe failures prior to the expected number of cycles. When toe failures occurred, they were generally associated with minor welding discontinuities at the toe, which would normally be acceptable by Code and workmanship standards. In the second phase, samples with polished toes, smooth as-welded toes, and intentionally poor toes were tested to quantify the effect of the toe condition. Some last-pass-improved samples were included in the Phase II testing because these tended to be more susceptible to toe failure in the Phase I tests.

Pipe Size

The ASME Code design fatigue curves do not reflect any differences in fatigue strength as a function of pipe diameter. However, the testing done by Higuchi et al. [4,5,6] showed that pipe diameter has a definite effect on socket weld fatigue life. In this test program, most of the tests were done using 2-inch (5.08 cm) diameter specimens because these had lower fatigue strength in the Higuchi work. However, a series of tests were performed using 3/4-inch (1.91 cm) diameter pipe to compare the fatigue strength of standard Code welds to the 2-inch (5.08 cm) results, and to assess the degree of benefit of the various improved designs.

Piping Material

The ASME fatigue curves for stainless and carbon steels begin to diverge above 10^5 cycles. Although the endurance limit of carbon steel is lower than that of stainless, previous test data has indicated that some of the fatigue strength reduction factors for stainless steel are higher. While the majority of the samples tested in this program were stainless steel, one-third of the 2-inch (5.08 cm) specimens were carbon steel. The purpose was to note whether any of the modifications to socket weld design are more or less effective in carbon steel than in stainless.

Weld Modification and Repair

An important purpose of the testing program was to study repair or modification actions that could be taken to improve the fatigue resistance of an existing socket welded joint without first removing it. Repair concepts for leaking socket welds that would allow plants to continue operating until the next outage before implementing a permanent repair were also tested. Weld overlay repairs were applied to four of the welds that developed leaks in the first phase of testing, and the repaired welds were vibration-fatigue tested to determine whether such a repair concept could be used for temporary or short term repairs. Another remedial approach that was tested is the modification of existing standard Code welds to a 2 x 1 leg length configuration after they have been fatigue-cycled in their original configuration, but before any obvious cracking or fatigue damage was observed. Testing compared the degree of improvement for the modified welds relative to new 1 x 1 and 2 x 1 welds.

2.3 Dynamic Load Factors in Vibration Loading

High cycle fatigue failures have generally been attributed to two types of vibration: (1) a mechanical source such as a pump, oscillating at a frequency in resonance with a natural frequency of the piping, or (2) flow-induced vibration including cavitation, which produces broad band vibration over a range of frequencies. The configuration most sensitive to vibration failure is a small bore vent or drain connected to a large bore header pipe that is near a pump. The vent or drain, being a simple cantilever, generally responds primarily at one natural frequency. The excitation force, which originates at the pump, is also significant at a single frequency (or a multiple, such as the vane pass frequency). The damping of a small bore cantilever attachment is low, typically 0.5% -1%. Damping of complex piping systems with pipe supports is generally higher, on the order of 5%, as the supports dissipate some of the energy of the vibratory motion. The low damping and single natural frequency of the cantilever and the distinct excitation frequency of the pump, can combine to produce a very high amplification of the forcing function. The dynamic load factor (DLF) is the ratio of the response acceleration to the excitation acceleration. The DLF is a function of the frequency of the pipe, the forcing frequency, and the damping [1]:

$$DLF = \frac{1}{\sqrt{\left[1-\left(\frac{\Omega^2}{\omega^2}\right)\right]^2 + \left[2\xi\left(\frac{\Omega}{\omega}\right)\right]^2}}$$

Where: Ω = forcing frequency

ω = natural frequency

ξ = percent of critical damping

At resonance, $\Omega = \omega$, and the maximum DLF is equal to $\frac{1}{2\xi}$. For a piping system with 5% damping, the DLF at resonance is 10. However, for a cantilevered vent or drain with damping of 0.5%, the maximum DLF is 100. Thus, the source acceleration can be magnified by a factor of 100 in the attached vent or drain. The relationship between damping, frequency, and DLF for an excitation frequency of 100 Hz is illustrated in Figure 2-2.

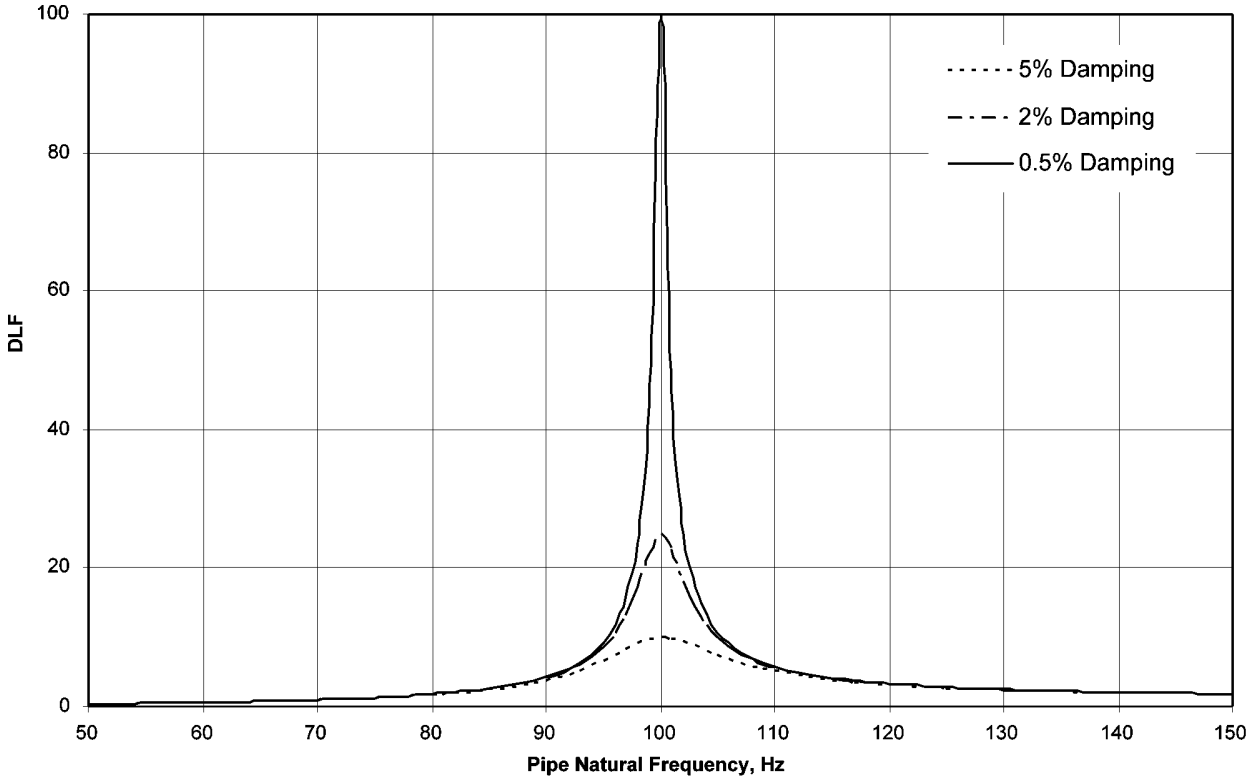


Figure 2-2
DLF vs. Damping and Frequency
Excitation Frequency = 100 Hz

As the forcing frequency and the natural frequency begin to differ from each other, the DLF drops quickly. For example, for a vent being shaken by a pump at a frequency of 100 Hz, if the vent natural frequency is 100 Hz and the damping is 0.5%, the DLF is 100. But if the natural frequency is 95 Hz, the DLF reduces to 9.2. At 90 Hz, the DLF reduces to 4.3. For a complex piping system with 5% damping, the DLFs are 10, 6.6, and 3.3 at 100 Hz, 95 Hz, and 90 Hz, respectively. Clearly, damping and natural frequency are significant factors in the response of a piping system to vibration loading.

The Phase I testing results indicated that, as the specimen began to crack, its natural frequency began to decline. The decline in frequency caused a reduction in acceleration response. Because small changes in frequency can produce large reductions in acceleration, it is possible that for a vent or drain initially at resonance, once it begins to leak, the shift in frequency away from resonance will reduce the response so that further crack growth will be much slower. As part of this testing program, the shift in frequency was examined, as well as whether there was any correlation with the type of weld or location of failure.

3
TEST PROGRAM

3.1 Testing Arrangement

The testing was carried out in six sets, with each set containing nine specimens. The specimen sets grouped common nominal pipe sizes (3/4-inch (1.91 cm) or 2-inch (5.08 cm) NPS) and/or material (stainless steel or carbon steel), or common theme (that is, toe conditions). All specimens were fabricated from Schedule 80 piping and compatible components. For the study of many of the parameters, pipe size was kept at 2-inch (5.08 cm) NPS in order to reduce the number of variables.

Loading amplitudes were selected based on fatigue data available in the literature. The levels of loading used in the tests were roughly 1/3, 1/2, or 2/3 of the ASME mean failure curve for the particular material, with the target of generating failures in approximately 10^6 to 10^7 cycles. As a large number of run-outs were obtained in the first phase of testing, the stress levels in the second phase of testing were increased.

The testing method was displacement controlled, peak-to-peak, with the specimens vertically cantilevered on a shaker table. An efficient testing scheme was devised for the program. Each set of nine socket weld specimens was bolted to the shaker table and shaken simultaneously near their resonant frequencies to produce the desired stress amplitudes and cycles. This is illustrated schematically in Figure 3-1.

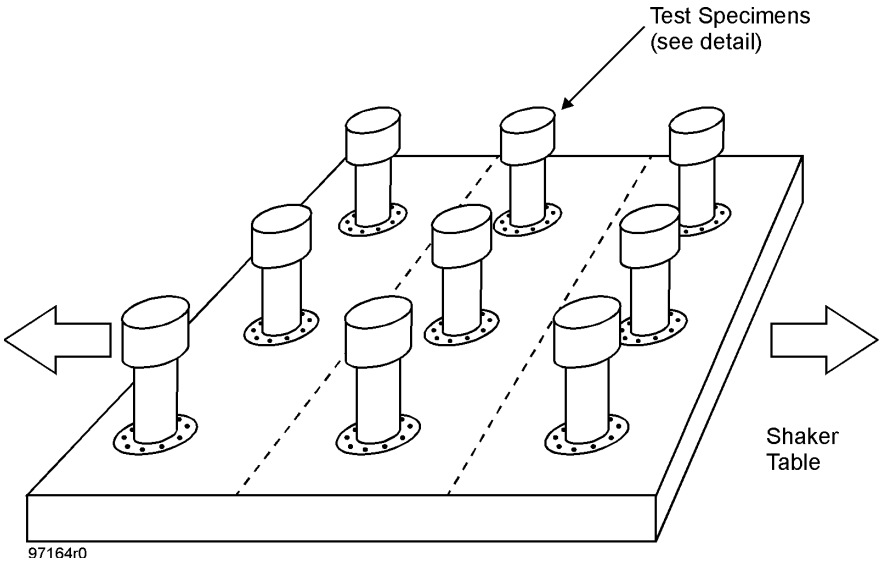


Figure 3-1
Overall Test Setup

A cantilevered specimen of the type illustrated in Figure 3-2 was used, with the test weld being the weld at the lower end of the specimen between the pipe and the flange used to bolt the specimen to the table.

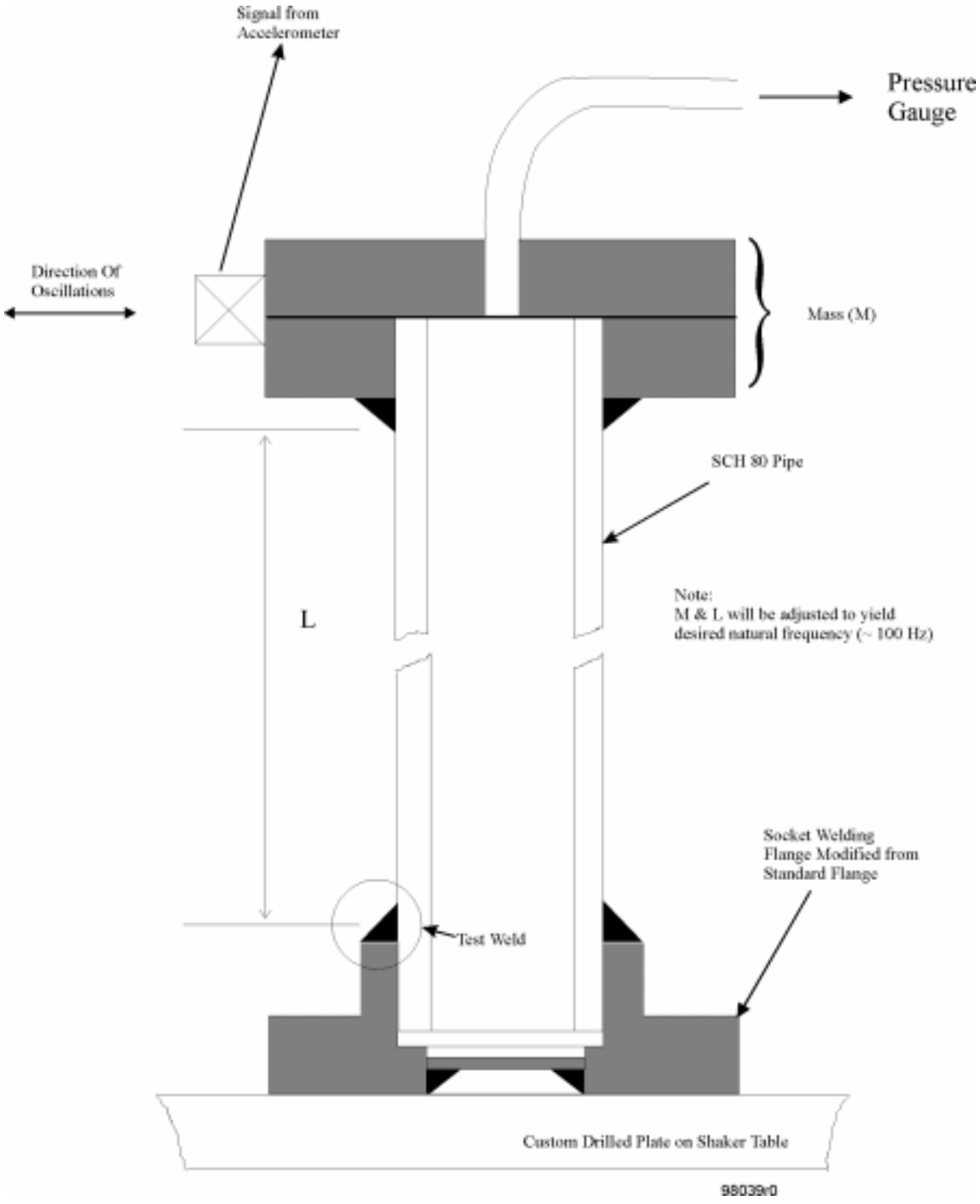


Figure 3-2
Test Specimen Detail

Different load amplitudes were able to be applied to different samples in the same test by fine-tuning the specimen natural frequencies relative to the shaker table excitation frequency. The shaker table typically ran at 100-110 Hz and the test specimens had natural frequencies that were nominally 4-8 Hz lower than the excitation frequency. By adding or subtracting small masses, such as nuts and washers, the frequencies of the test specimens were moved enough off resonance to adjust each individual response acceleration (as described in Section 2.3). The flange configurations were modified to produce socket weld details typical of the socket welded fittings used on small bore piping in nuclear plants (tees, elbows, weldolets, couplings, and so on).

Each specimen was instrumented as illustrated in Figure 3-2, with an accelerometer and a pressure gauge, and the instruments were monitored continuously during testing. The specimens were pressurized with air to a moderate pressure of approximately 50 psig (344.75 kPa). When depressurization occurred, indicating a failure, the specimen was removed from the table at the next convenient test stoppage, and the testing was then resumed with only the remaining specimens. This test method is directly comparable with the plant loading mechanism of concern (vibration fatigue), whereas conventional fatigue testing techniques (rotating beam or four point bending) can have considerable variability with respect to each other [5,6], and possibly with respect to in-plant vibration.

Figure 3-3 illustrates the actual test apparatus. Six of nine 2-inch (5.08 cm) specimens are shown mounted on the shaker table in this photograph. The tubes and wires are leads for the strain gages and pressure transducers, which were relayed to the test control computer (right side of figure). The desired stress level for each test specimen was precalculated as a top mass acceleration. The shaker table amplitude was computer-controlled to achieve a preset accelerometer amplitude on one of the nine samples. The accelerometer amplitude was recorded for all nine samples and used to determine the tested stress amplitude for each specimen.

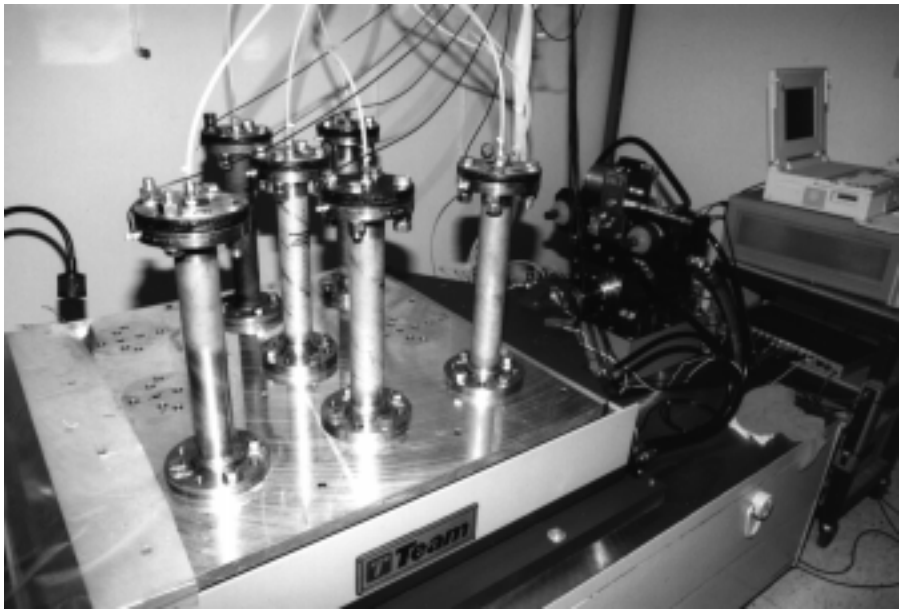


Figure 3-3
Test Apparatus (six of nine specimens shown - test control computer on right)

3.2 Parameters Tested

The various socket weld configurations (specimen types) used to test the potentially significant factors mentioned in Section 2.2 are illustrated in Figure 3-4.

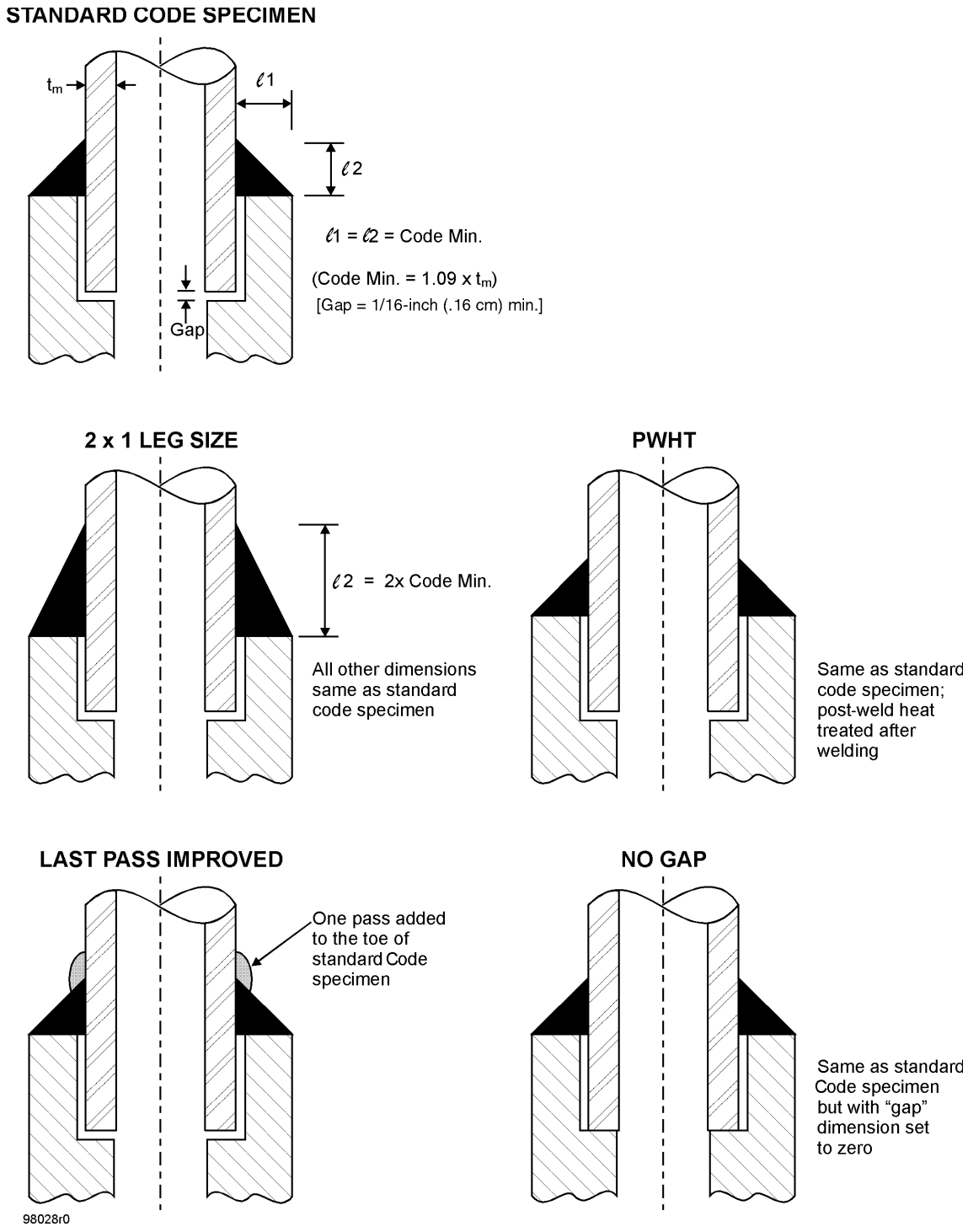


Figure 3-4
Test Specimen Configurations

The complete Phase I test matrix, summarized in Table 3-1, included three test series of nine specimens each, for a total of 27 tests. The first test series included two standard ASME Code specimens (1 x 1 leg sizes, where 1 = the Code minimum of 1.09 times the pipe nominal thickness), three weld specimens with pipe side legs extended to twice the ASME Code requirement (2 x 1 leg sizes), two last-pass-improved specimens, one specimen without the Code-required 1/16-inch (.16 cm) axial gap, and one post-weld heat treated specimen. All Test Series 1 specimens were 3/4-inch (1.91 cm) NPS stainless steel. Test Series 2 was identical to 1 but used 2-inch (5.08 cm) NPS stainless steel specimens. Test Series 3 was similar, but with seven 2-inch (5.08 cm) NPS carbon steel specimens (testing standard Code welds, 2 x 1 welds, post-weld heat treated, and no axial gap welds), and two additional 2-inch (5.08 cm) NPS stainless steel specimens (testing post-weld heat treated and no axial gap welds). Appendix A gives additional details of how the test specimens were fabricated.

Table 3-1
Phase I Test Matrix

Test Series 1 – 3/4" (1.91 cm) – SS			
Spec #	NPS*	Material	Specimen Description
B1-3/4SS-1	¾"	Stainless Steel	Standard Code
B1-3/4SS-2	¾"	Stainless Steel	Standard Code
B1-3/4SS-3	¾"	Stainless Steel	2 x 1 Leg Sizes
B1-3/4SS-4	¾"	Stainless Steel	2 x 1 Leg Sizes
B1-3/4SS-5	¾"	Stainless Steel	2 x 1 Leg Sizes
B1-3/4SS-6	¾"	Stainless Steel	PWHT
B1-3/4SS-7	¾"	Stainless Steel	Last Pass Improved
B1-3/4SS-8	¾"	Stainless Steel	Last Pass Improved
B1-3/4SS-9	¾"	Stainless Steel	No Axial Gap
Test Series 2 - 2" (5.08 cm) NPS – SS			
Spec #	NPS*	Material	Specimen Description
B2-2SS-1	2"	Stainless Steel	Standard Code
B2-2SS-2	2"	Stainless Steel	Standard Code
B2-2SS-3	2"	Stainless Steel	2 x 1 Leg Sizes
B2-2SS-4	2"	Stainless Steel	2 x 1 Leg Sizes
B2-2SS-5	2"	Stainless Steel	2 x 1 Leg Sizes
B2-2SS-6	2"	Stainless Steel	PWHT
B2-2SS-7	2"	Stainless Steel	Last Pass Improved
B2-2SS-8	2"	Stainless Steel	Last Pass Improved
B2-2SS-9	2"	Stainless Steel	No Axial Gap
Test Series 3 - 2" (5.08 cm) NPS – CS			
Spec #	NPS*	Material	Specimen Description
B3-2CS-1	2"	Carbon Steel	Standard Code
B3-2CS-2	2"	Carbon Steel	Standard Code
B3-2CS-3	2"	Carbon Steel	2 x 1 Leg Sizes
B3-2CS-4	2"	Carbon Steel	2 x 1 Leg Sizes
B3-2CS-5	2"	Carbon Steel	2 x 1 Leg Sizes
B3-2CS-6	2"	Carbon Steel	PWHT
B3-2CS-7	2"	Carbon Steel	No Axial Gap
B3-2SS-8	2"	Stainless Steel	PWHT
B3-2SS-9	2"	Stainless Steel	No Axial Gap

* To convert inches to centimeters, multiply the unit by 2.54.

The Phase II test matrix is summarized in Table 3-2.

Table 3-2
Phase II Test Matrix

Test Series 4 - Repair/ Modification Series - SS & CS				
Specimen #	Orig. Specimen	NPS*	Material	Comments
B2-2SS-1	Code 1x1	2"	Stainless Steel	Build-up 2x1
B3-2SS-8	PWHT 1x1	2"	Stainless Steel	Build-up 2x1
B2-2SS-6	PWHT 1x1	2"	Stainless Steel	Runout
B3-2CS-6	PWHT 1x1	2"	Carbon Steel	Build-up 2x1
B3-2CS-7	No gap 1x1	2"	Carbon Steel	Build-up 2x1
B3-2CS-1	Code 1x1	2"	Carbon Steel	Weld Overlay on Root Failure
B3-2CS-2	Code 1x1	2"	Carbon Steel	Weld Overlay on Root Failure
B2-2SS-8	LP	2"	Stainless Steel	Weld Overlay on Toe Failure
B2-2SS-2	Code 1x1	2"	Stainless Steel	Weld Overlay on Root Failure
Test Series 5 - Toe Condition Series – SS				
Specimen #	Type	NPS*	Material	Comments
B5-2SS-1	1x1	2"	Stainless Steel	Smooth, as welded
B5-2SS-2	1x1	2"	Stainless Steel	Smooth, as welded
B5-2SS-3	1x1	2"	Stainless Steel	Poor, as welded
B5-2SS-4	1x1	2"	Stainless Steel	Poor, as welded
B5-2SS-5	1x1	2"	Stainless Steel	Polished toe
B5-2SS-6	1x1	2"	Stainless Steel	Polished toe
B5-2SS-7	LP	2"	Stainless Steel	Smooth, as welded
B5-2SS-8	LP	2"	Stainless Steel	Smooth, as welded
B5-2SS-9	LP	2"	Stainless Steel	Smooth, as welded
Test Series 6 - Butt Weld vs. 2 x 1 Series - SS & CS				
Specimen	Type	NPS*	Material	Comments
B6-2SS-1	Butt	2"	Stainless Steel	Weld neck flange
B6-2SS-2	Butt	2"	Stainless Steel	Weld neck flange
B6-2CS-3	Butt	2"	Carbon Steel	Weld neck flange
B6-2CS-4	Butt	2"	Carbon Steel	Weld neck flange
B6-2SS-5	Butt	2"	Stainless Steel	Butt weld w/undercut
B6-2SS-6	2x1	2"	Stainless Steel	2x1 socket, high load
B6-2SS-7	2x1	2"	Stainless Steel	2x1 socket, high load
B6-2CS-8	2x1	2"	Carbon Steel	2x1 socket, high load
B6-2CS-9	2x1	2"	Carbon Steel	2x1 socket, high load

* To convert inches to centimeters, multiply the unit by 2.54.

The first objective of the Phase II testing was to evaluate proposed modifications or repairs to previously fatigued specimens. The modifications consisted of building up 1 x 1 Code weld leg length specimens from Test Series 2 or 3, in which runouts were obtained, to 2 x 1 configurations (Figure 3-5). A runout is defined as a test to a large number of cycles (>2 x 10^7) where no evidence of failure occurred. These modified specimens were then retested at higher loads in Test Series 4.

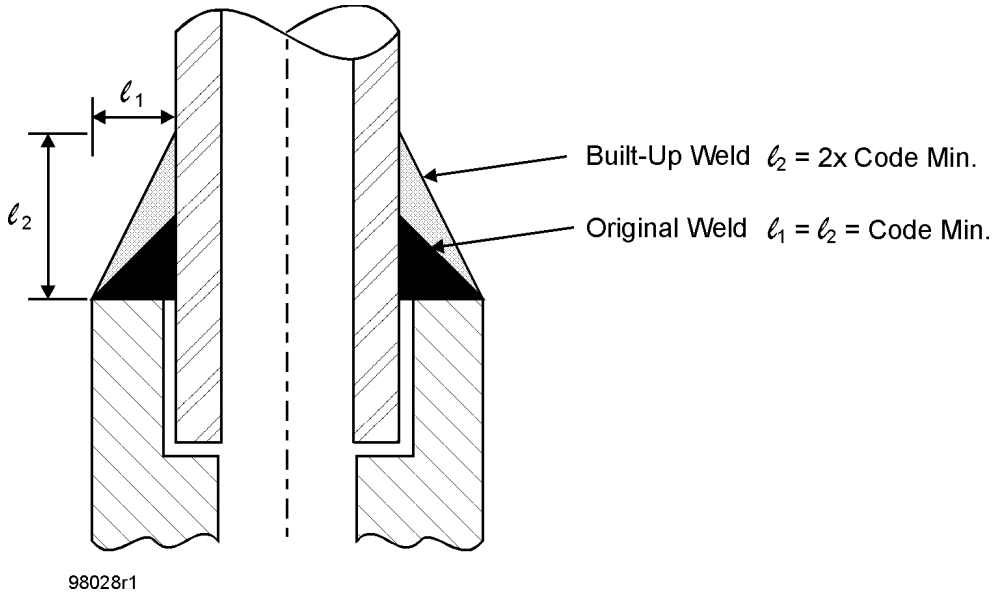


Figure 3-5
1 x 1 Weld Built Up to 2 x 1

Tests were done of weld overlay repairs of specimens that had failed in the first phase of testing. The leaks were peened with water in the pipe under pressure and a seal weld was applied when the leak stopped. The seal weld tended to reopen the leak, and it took several iterations of peening and sealing before the weld overlays were applied. The weld overlay design is shown in Figure 3-6.

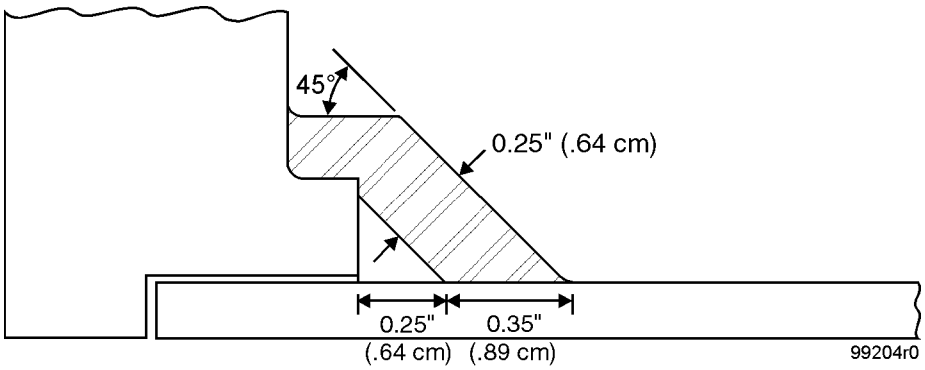


Figure 3-6
Weld Overlay Design

This design applied sufficient additional reinforcement to cover the possibility of either a toe or a root failure having occurred. The overlay added 1/4-inch (.64 cm) to the weld throat across the entire profile, from the pipe side toe to the fitting side toe. It was applied by shielded metal arc welding (SMAW) to simulate the most likely welding process that would be used for a temporary repair in a power plant. The pipe side toe of the weld did not have a blending radius, producing a sharp transition, as would likely be found in a field repair. More details of the weld overlay procedure can be found in Appendix B.

The repaired welds were tested at their original load levels to determine if they could survive until the next outage or convenient time for a permanent repair. Specimens chosen for these tests included carbon and stainless steel welds that had experienced root and toe failures. Another test was run on an unmodified, previously tested specimen (B2-2SS-6) that was a runout, applying 50% higher loads. Figure 3-7 shows a photograph of this specimen, which was a Code standard weld with PWHT. Figure 3-8 shows a standard weld built up to 2x1, and Figure 3-9 shows a specimen with a weld overlay repair.

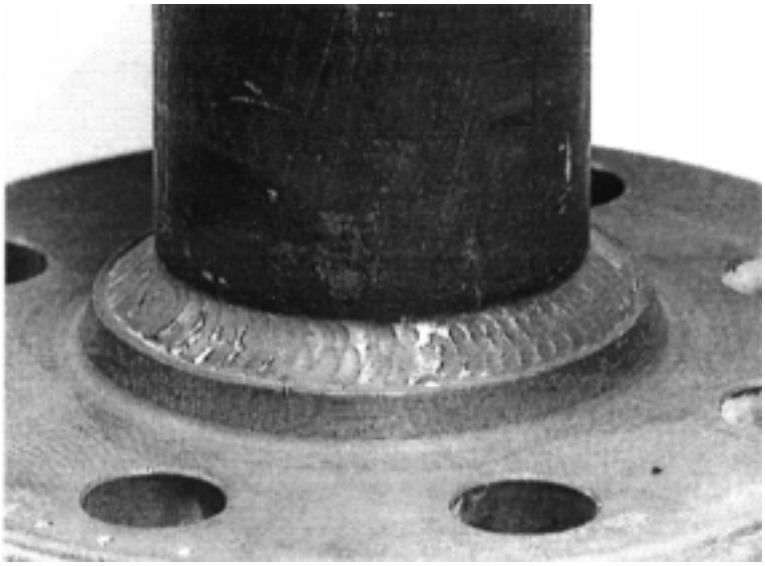


Figure 3-7
Standard Weld with PWHT (B2-2SS-6)

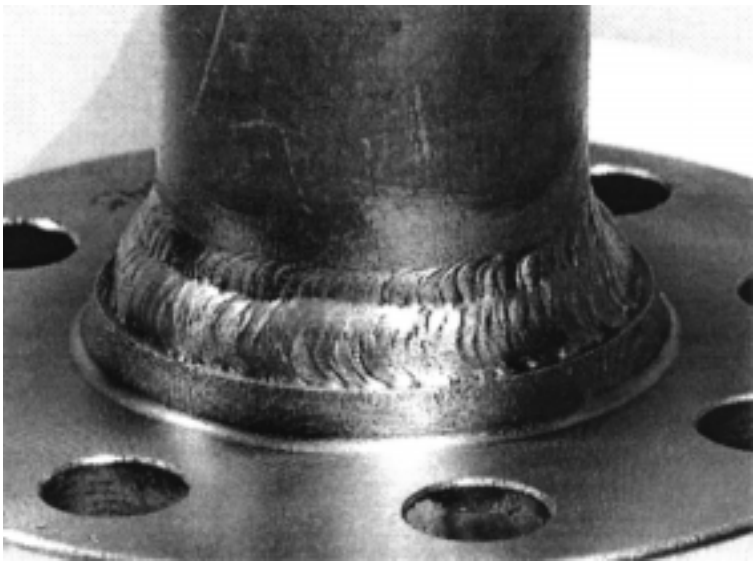


Figure 3-8
Standard Weld Built Up to 2x1 (B2-2SS-1)

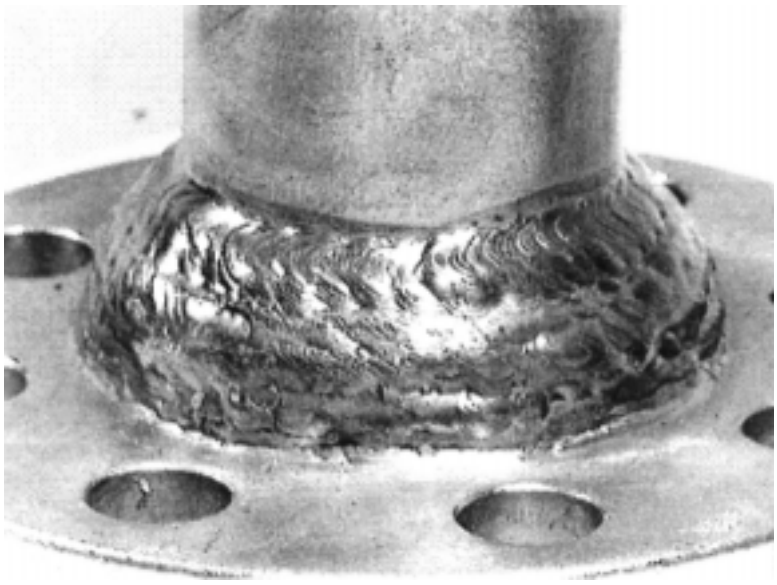


Figure 3-9
Weld Overlay Repair (B2-2SS-2)

Additional testing at higher loads was also performed in Test Series 5 and 6 on new 1 x 1 specimens (B5-2SS-1, B5-2SS-2) and new 2 x 1 specimens (B6-2SS-6, B6-2SS-7, B6-2CS-8, B6-2CS-9). Through this multiplicity of tests, the modified welds were directly compared to new 1 x 1, 2 x 1, and previously tested 1 x 1 specimens under comparable, severe loading conditions.

Test Series 5 involved testing specimens to determine the effects of various toe discontinuities, in order to define an acceptance criteria for toe conditions. These were conducted with specimens specially fabricated with varying toe conditions. They included some last-pass-improved specimens (B5-2SS-7, -8, and –9) because these appeared to be more sensitive to toe failures in the first phase of testing. They also included some intentionally poor toe conditions as well as some smooth as-welded and polished toe conditions for comparison. To minimize the number of test parameters, all Test Series 5 specimens were 2-inch (5.08 cm) diameter stainless steel and were tested at high load levels. This also allowed the smooth toe specimens to double as benchmark 1 x 1 specimens for the tests of the modified welds.

The purpose of Test Series 6 was to further evaluate new 2 x 1 weld configurations at higher loads and to compare them to conventional, butt-welded specimens at comparable loads. These tests were conducted with both carbon and stainless steel specimens and included one butt weld specimen with an intentionally poor toe condition to see if this is also a concern for butt welds. The butt-welded specimens consisted of pipes welded to standard weld neck flanges, which is analogous to a typical method used in power plants for upgrading socket-welded fittings when vibration problems have been experienced.

3.3 Data Analysis

The testing instrumentation recorded the accelerations of the specimen top mass and the shaker table as a function of number of cycles. Measurements of the specimen length and weights of the top mass and pipe were recorded for calculating the stress produced at the weld. The formula for a cantilever beam with a concentrated end mass was not entirely valid for this application as the mass of the pipe was not small compared to the top mass. The relationship between top mass acceleration and stress at the weld was derived from standard beam formulas as follows:

$$x = \frac{m_t L^3}{3EI} + \frac{m_p L^3}{8EI} \qquad M = m_t L + \frac{m_p L}{2}$$

$$S = \frac{M \frac{D_0}{2}}{I} \qquad x = \frac{a}{(2\pi f)^2}$$

$$S = a\left[\frac{1}{(2\pi f)^2}\frac{3}{2}\frac{gED_0}{L^2}\frac{m_t + \frac{m_p}{2}}{m_t + \frac{3m_p}{8}}\right]$$

Where:

x	= displacement, in. (cm)
M	= moment, in.-lb. (N-m)
S	= stress at socket weld, psi (kPa)
I	= moment of inertia, $in.^4$ (cm^4)
A	= acceleration of top mass plus shaker table, g
f	= shaker table frequency, Hz
g	= acceleration due to gravity = 386.4 in/sec^2 (cm/sec^2)
E	= Young's modulus, psi (kPa)
D_o	= pipe outside diameter
L	= distance from weld to accelerometer, in. (cm)
m_t	= top mass (weight), lb. (kg)
m_p	= mass of pipe, lb. (kg)

The test results were plotted on conventional S-N log-log plots and compared to socket weld data from the literature, as well as to standard material S-N curves. Approximate fatigue strength reduction factors (FSRFs) were calculated by graphically estimating the endurance limit stress of each sample and dividing the endurance limit stress of the ASME mean failure curve for the material by this stress. For the specimens where a dropoff in acceleration was observed as the specimen began to fail, the shift in frequency was determined either by calculation of dynamic load factors or by direct measurement. Measurements were also taken of the specimen damping by the half-power and log-decrement methods to determine whether any change in damping occurred as the specimen began to fail.

4
TEST RESULTS

4.1 General Observations

A tabulation of the applied stress amplitudes and resulting cycles to failure for the first three test series is given in Table 4-1. (The stress levels shown in this table are revised from those that had been previously reported in the Interim Report [7].)

Table 4-1
Phase I Test Results

Test Series 1 – 3/4" (1.91 cm) NPS - SS			
Specimen	Sa(ksi)*	Nf	Comments
1 – Code	16.1	1.13E+07	Root Failure
2 – Code	16.5	3.36E+06	Toe Failure
3 – 2x1 Leg	20.3	2.90E+06	Root Failure
4 – 2x1 Leg	17.3	1.81E+06	Root Failure
5 – 2x1 Leg	19.4	2.97E+06	Root Failure
6 – PWHT	16.2	2.44E+06	Root Failure
7 – Last Pass	20.5	6.27E+06	Root Failure
8 – Last Pass	18.2	1.06E+06	Toe Failure
9 – No Gap	17.7	2.80E+06	Root Failure
Test Series 2 - 2" (5.08 cm) NPS – SS			
Specimen	Sa(ksi)*	Nf	Comments
1 – Code	10.4	2.28E+07	Runout (No Failure)
2 – Code	10.4	9.83E+06	Root Failure
3 – 2x1 Leg	13.5	2.28E+07	Runout (No Failure)
4 – 2x1 Leg	13.8	2.28E+07	Runout (No Failure)
5 – 2x1 Leg	13.4	2.28E+07	Runout (No Failure)
6 – PWHT	11.8	2.28E+07	Runout (No Failure)
7 – Last Pass	11.7	2.28E+07	Runout (No Failure)
8 – Last Pass	11.5	1.02E+07	Toe Failure
9 – No Gap	10.5	8.12E+06	Root Failure
Test Series 3 - 2" (5.08 cm) NPS - CS			
Specimen	Sa(ksi)*	Nf	Comments
1 – Code	8.0	1.09E+07	Root Failure
2 – Code	7.8	7.40E+06	Root Failure
3 – 2x1 Leg	11.0	2.42E+07	Runout (No Failure)
4 – 2x1 Leg	11.9	2.42E+07	Runout (No Failure)
5 – 2x1 Leg	12.6	2.42E+07	Runout (No Failure)
6 – PWHT	9.3	2.42E+07	Runout (No Failure)
7 – No Gap	7.6	2.42E+07	Runout (No Failure)
8 – PWHT	12.2	2.42E+07	Runout (No Failure)
9 – No Gap	10.7	7.39E+06	Root Failure

* To convert ksi to MPa, multiply the unit by 6.895.

In Test Series 1 (the 3/4-inch (1.91 cm) NPS specimens), the nine specimens failed at cycles ranging from 1 x 10^6 to 1 x 10^7. The stresses generated in the test ranged from 16 to 20.5 ksi (110.32 MPa to 141.348 MPa). Seven of the nine specimens exhibited root failures originating at the weld roots and propagating to the outside surface of the specimen on the socket side of the weld, as illustrated in Figure 4-1. The other two specimens exhibited toe failures initiating at the outside surface of the specimen near the pipe side toe of the weld and propagating to the inside surface (see Figure 4-2).



Figure 4-1
Root Failure (3/4" (1.91 cm) 2 x 1 Weld)



Figure 4-2
Toe Failure (3/4" (1.91 cm) Last Pass Improved)

The 2-inch (5.08 cm) NPS specimens, Test Series 2 and 3, also produced mostly root failures with only one toe failure, but the majority were runouts. A runout is defined as a test conducted to a large number of cycles (at least 2×10^7) in which no evidence of specimen failure was observed but the test was terminated because of time constraints. The 2-inch (5.08 cm) NPS specimens that did fail in Test Series 2 and 3 did so between 7×10^6 and 1×10^7 cycles at test stresses of 10.5 ksi (72.398 MPa) (stainless steel), and at 7×10^6 to 1×10^7 cycles at 8 to 10 ksi (55.16 MPa to 68.95 MPa) (carbon steel).

Table 4-2 is a summary of the results of Test Series 4, 5, and 6.

Table 4-2
Phase II Test Results

Test Series 4 – Repairs and Mods. - 2" (5.08 cm) SS and CS			
Specimen	Sa(ksi)*	Nf	Comments
1 – Mod. 2x1 SS	17.4	2.57E+07	Runout
2 – Mod. 2x1 SS	17.6	5.05E+06	Toe Failure
3 – Runout SS	16.3	1.33E+07	Root Failure
4 – Mod. 2x1 CS	14.7	2.57E+07	Runout
5 – Mod. 2x1 CS	11.1	2.57E+07	Runout
6 – Overlay CS	8.9	2.57E+07	Runout
7 – Overlay CS	8.0	2.57E+07	Runout
8 – Overlay SS	11.6	1.10E+07	Failure at Original Toe
9 – Overlay SS	11.0	2.57E+07	Runout
Test Series 5 – Toe Conditions - 2" (5.08 cm) SS			
Specimen	Sa(ksi)*	Nf	Comments
1 – Smooth	24.2	1.26E+06	Toe Failure
2 – Smooth	23.6	1.04E+06	Toe Failure
3 – Poor	18.2	1.62E+06	Toe Failure
4 – Poor	20.5	3.80E+05	Toe Failure
5 – Polished	21.4	3.24E+05	Toe Failure
6 – Polished	22.5	9.10E+05	Root Failure
7 – Smooth LP	22.8	3.56E+05	Toe Failure
8 – Smooth LP	23.3	1.62E+06	Root Failure
9 – Smooth LP	22.0	1.96E+06	Root Failure
Test Series 6 – 2x1 vs. Butt Weld - 2" (5.08 cm)			
Specimen	Sa(ksi)*	Nf	Comments
1 – Butt SS	23.0	1.22E+06	I. D. Root Failure
2 – Butt SS	22.3	6.61E+05	I. D. Root Failure
3 – Butt CS	15.3	2.19E+06	Toe Failure
4 – Butt CS	16.8	1.97E+06	Toe Failure
5 – Butt SS Undct	22.6	1.00E+06	Toe Failure
6 – 2x1 SS	24.0	1.04E+06	Toe Failure
7 – 2x1 SS	23.5	2.11E+07	Runout
8 – 2x1 CS	16.5	2.38E+06	Root Failure
9 – 2x1 CS	16.9	3.75E+06	Root Failure

* To convert ksi to MPa, multiply the unit by 6.895.

In view of the large number of runouts in Test Series 2 and 3, the test loads in series 4, 5, and 6 were increased over those used in series 2 and 3 by as much as a factor of 2. The toe condition tests, series 5, were tested at nominal stress levels of 22 ksi (151.69 MPa) but in some cases ended up averaging as low as 18 ksi (124.11 MPa) due to the specimen frequency shifting off resonance as toe discontinuities propagated through the pipe wall. All of the specimens failed between 0.3×10^6 and 2×10^6 cycles, with most of the failures being toe failures. In Test Series 6, the carbon steel 2 x 1 and butt weld specimens were tested at about 16 ksi (110.32 MPa) and failed between 2×10^6 and 4×10^6 cycles. The stainless steel specimens were tested at about 23 ksi (158.585 MPa) and failed between 0.6×10^6 and 1.2×10^6 cycles except for one runout. In general, the butt welds did not perform as well as the 2 x 1 welds (more on this follows). In Test Series 4 (which was run last), six of the nine specimens tested were runouts, despite extending the test to 2.6×10^7 cycles, and increasing the stress levels by 50% on all but the weld-repaired specimens.

The test results are plotted on S – N log-log plots, grouped according to the parameters being studied. Trend curves from socket weld fatigue testing [4,5,6] are also shown on the plots, labeled Higuchi Curves. The ASME mean failure curves are included for comparison purposes. Appropriate trend curves for each pipe size and material were selected. When specimens exhibited toe failures (solid points in the figures) they tended to fail somewhat prematurely, relative to the more common root failures. In general, failures at a lower number of cycles and/or higher stress tended to originate at the toe, while the higher cycle / lower stress failures tended to occur at the root.

The following sections describe in detail the test results for each of the parameters studied.

4.2 Effect of Weld Size

Figures 4-3 and 4-4 show the results of testing standard Code-size welds (1 x 1) and enhanced 2 x 1 welds, which have a leg dimension along the pipe of twice that of the Code-minimum leg dimension. Also shown for comparison are the test results for the butt welds. Figure 4-3 shows the 2-inch (5.08 cm) stainless steel data; Figure 4-4 shows the 2-inch (5.08 cm) carbon steel data.

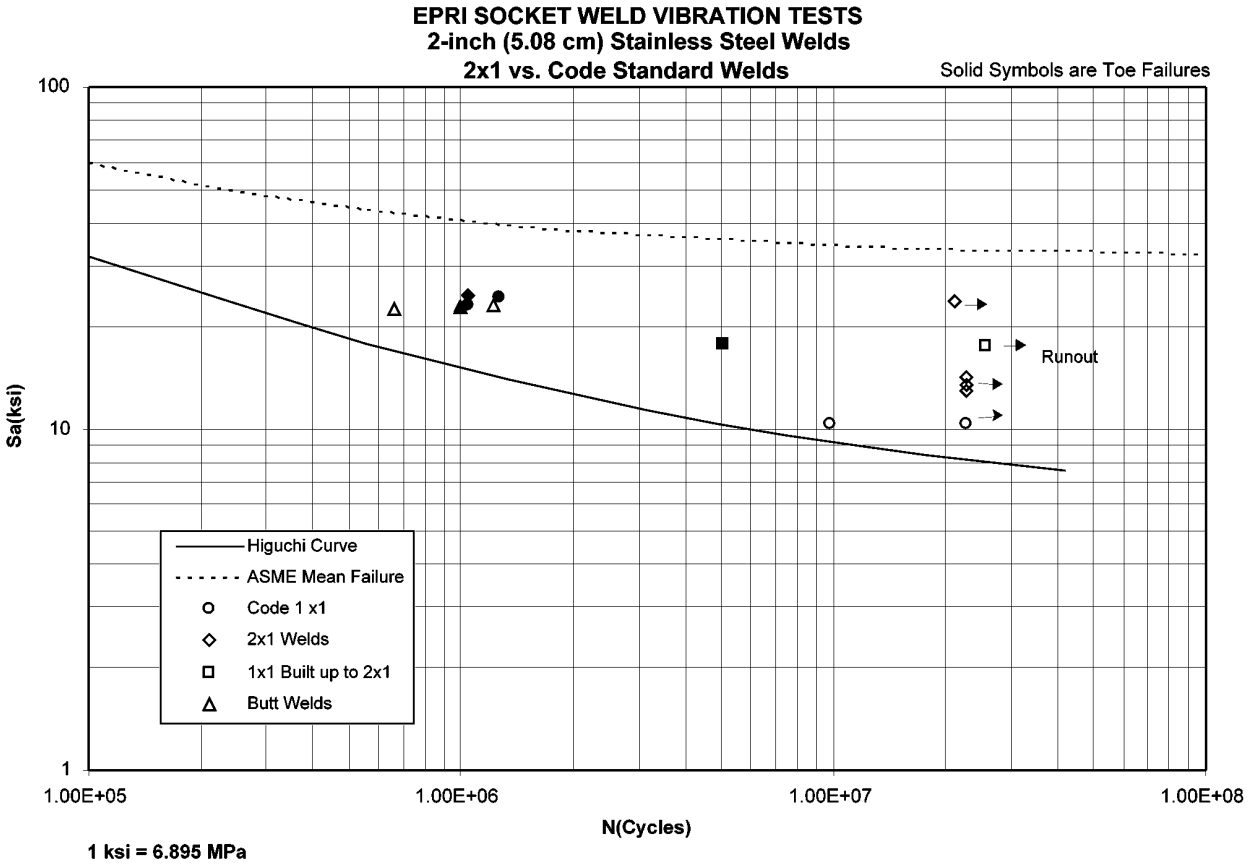


Figure 4-3
2" (5.08 cm) Stainless Steel Weld Sizes

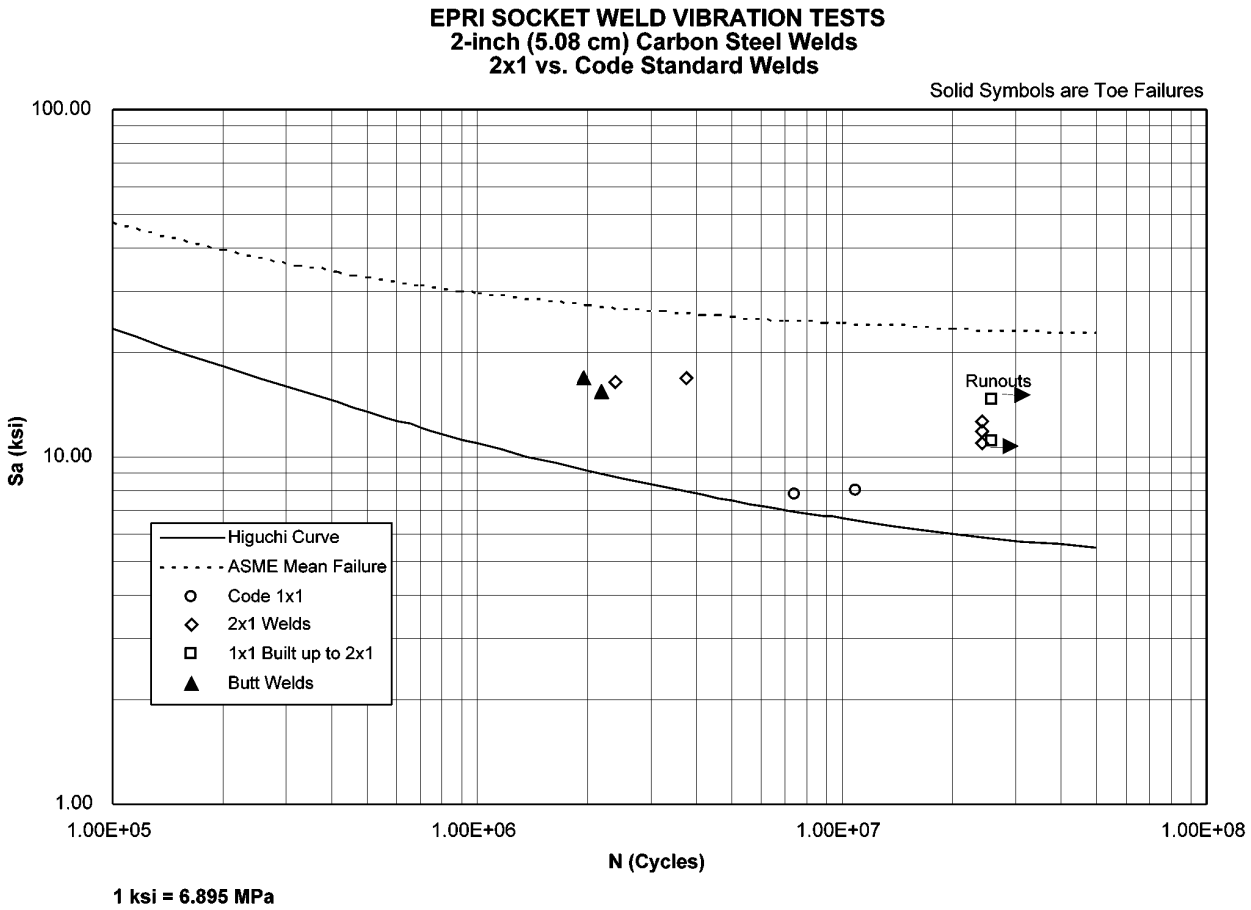


Figure 4-4
2" (5.08 cm) Carbon Steel Weld Sizes

In general, the nominal Code-dimension (1 x 1) specimens yielded data that was above the corresponding Higuchi Curve. The failures at the lower numbers of cycles were toe failures and those at higher cycles were root failures (open points in the figures). The two butt weld failures at low cycles in this figure originated in the inside diameter of the pipe, at the edge of the weld root.

The 2 x 1 specimens were significantly stronger than the standard welds. All exhibited runouts at the lower stress levels (14 ksi (96.53 MPa) stainless, 12 ksi (82.74 MPa) carbon), even though they were tested at stress amplitudes 30% higher than those applied to the standard Code specimens. At the higher stress levels, in the stainless steel tests, one was a runout at 23.5 ksi (162.033 MPa), while the other failed at only 1 x 10^6 cycles and 24 ksi (165.48 MPa). The latter specimen was a toe failure, however, and performed about the same as the standard Code specimens tested at this stress level, which also exhibited toe failures. In the carbon steel tests at higher stress levels, both of the 2 x 1 welds performed significantly better than the standard welds (Figure 4-4).

The butt welds were tested for the purpose of comparison against the 2 x 1 welds. However, the butt welds did not perform as well as expected. In the stainless steel tests, they were about as strong as the standard Code socket welds, while in the carbon steel tests, they were somewhat

better than the standard welds but not as good as the 2 x 1 welds. It was noted in Reference [9] that previous test data for carbon steel butt welds indicated lower fatigue strength reduction factors than for stainless steel butt welds.

The butt weld results can be explained by the fact that the tests were comparing a socket-welded flange to a butt-welded, weld neck flange and not to a pipe-to-pipe butt weld. The weld neck flange acts as a tapered transition, and the ASME Code stress indices reflect a reduced fatigue strength for such a joint.

For the as-welded standard socket weld (1998 Code):

$C_2K_2 = 1.93\ (2.0) = 3.86$

For the as-welded, butt-welded transition:

$C_2K_2 = 2.1\ (1.8) = 3.78$

For an as-welded, pipe-to-pipe butt weld (2-inch (5.08 cm) schedule 80):

$C_2K_2 = 1.43\ (1.8) = 2.57$

Thus, the stress indices for the butt welded transition are only slightly better than that of a socket weld. Socket welds are rarely used in pipe-to-pipe connections, but rather at elbows, branch connections, or other fittings that would result in thickness transitions if replaced with butt welds. Therefore, the practice of replacing socket welds with butt welds to “fix” vibration fatigue problems appears to be of little value, if the butt weld is located close to a transition region (see Figure 4-5).

Two of the stainless steel butt welds failed by a crack that originated at the inside diameter of the pipe, at the edge of the weld root. The crack grew perpendicular to the pipe axis, through the weld metal. This is shown in Figure 4-5. Further examination of the weld root indicated the presence of a number of discontinuities, which might have served as crack initiation sites. The other stainless steel butt weld had an undercut intentionally placed at the toe. Although the specimen failed at the toe, the fatigue strength was equivalent to the other butt welds.

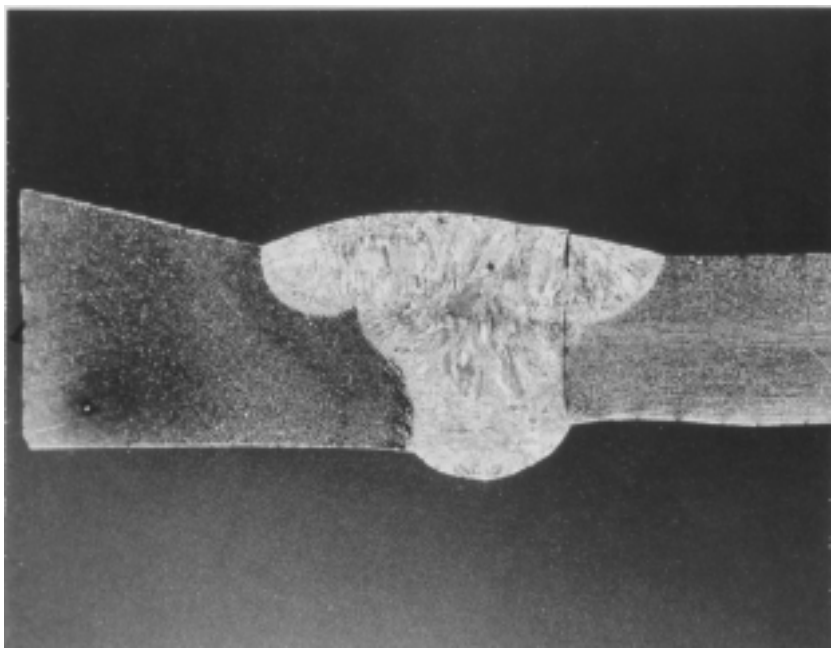


Figure 4-5
Butt Weld Failure

It was concluded from these tests that the 2 x 1 welds offer a significant improvement in fatigue strength over standard Code welds. They also provide at least as much benefit as replacement of socket welds with butt-welded fittings.

4.3 Toe Condition

Three types of toe conditions were tested:

- As-welded with a smooth transition to the pipe (intended to represent typical field welds)
- Polished toe (visible surface imperfections were removed by polishing)
- Poor toe condition (the toe had been intentionally undercut)

Also included in the smooth, as-welded group were samples in which a final weld pass was added at the toe to improve the residual stresses. All of the test samples were 2-inch (5.08 cm) stainless steel to minimize the number of variables in the test. The results are shown in Figure 4-6.

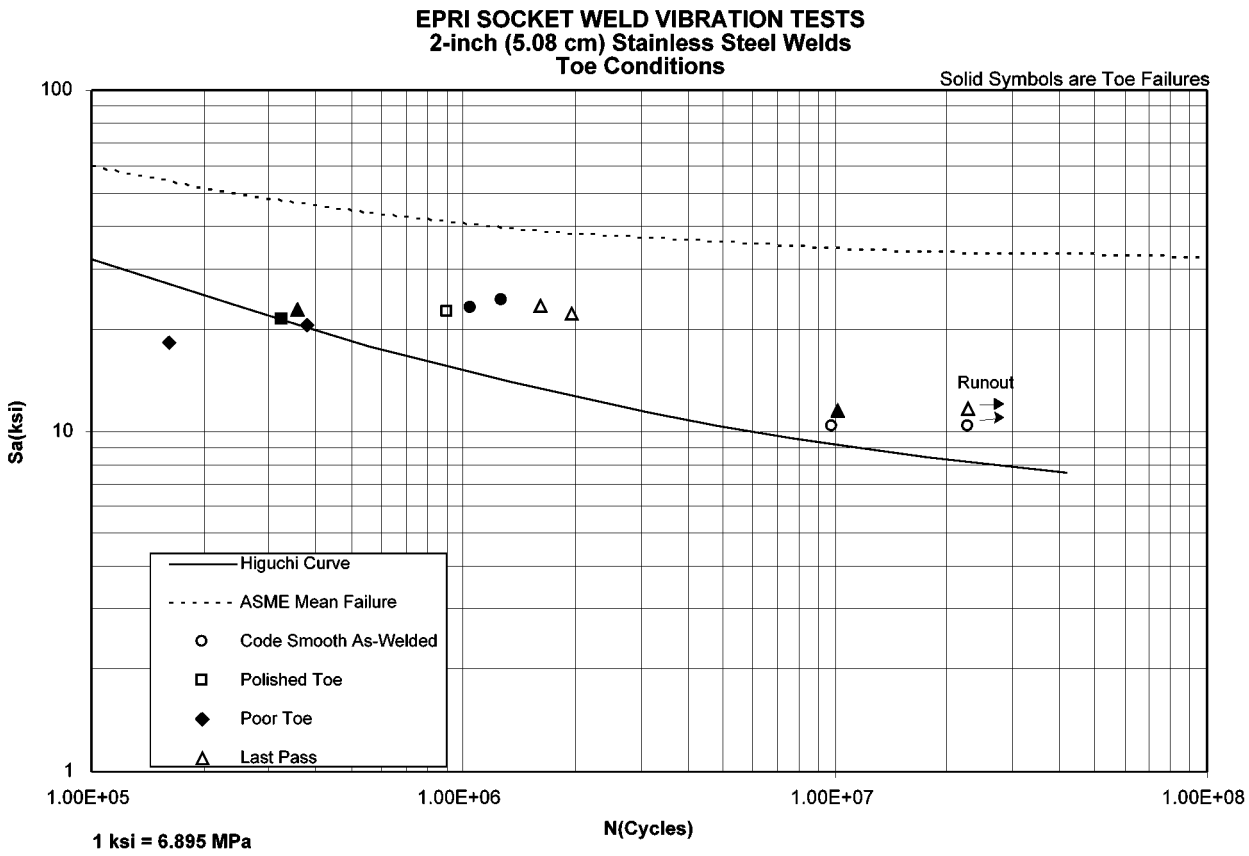


Figure 4-6
Toe Conditions

The poor toe conditions produced failures at or below the Higuchi data curve. As expected, they were toe failures. It is interesting to note that the two polished toe specimens did not show any improvement over the smooth, as-welded pieces. One of the polished toes failed at the toe right on the Higuchi trend line, which was below all of the standard, as-welded samples. A possible explanation for the lack of benefit from polishing the toe is that the polishing might have generated tensile residual stresses in the weld. Examination of the fracture surface under magnification showed multiple crack initiation sites along the scratch marks generated by the grinding. This can be seen in Figure 4-7.



Figure 4-7
Polished Toe Failure

It is concluded from these tests that, while a poor toe condition definitely reduces the fatigue life, polishing the toe does not seem to improve it. Polishing the toe is clearly not worth the effort and might even reduce the fatigue resistance. Four of the five specimens with a final weld pass at the toe performed a little better than the standard welds, with one failing early near the Higuchi trend line.

4.4 Weld Process Enhancements

Figure 4-8 compares the results of the weld process enhancements versus standard, 2-inch (5.08 cm) stainless socket welds. Figure 4-9 shows the same for the carbon steel tests. The enhancements were: adding a last pass at the weld toe on the pipe side to improve the residual stress, post-weld heat treatment of the weld, and eliminating the Code-required axial gap.

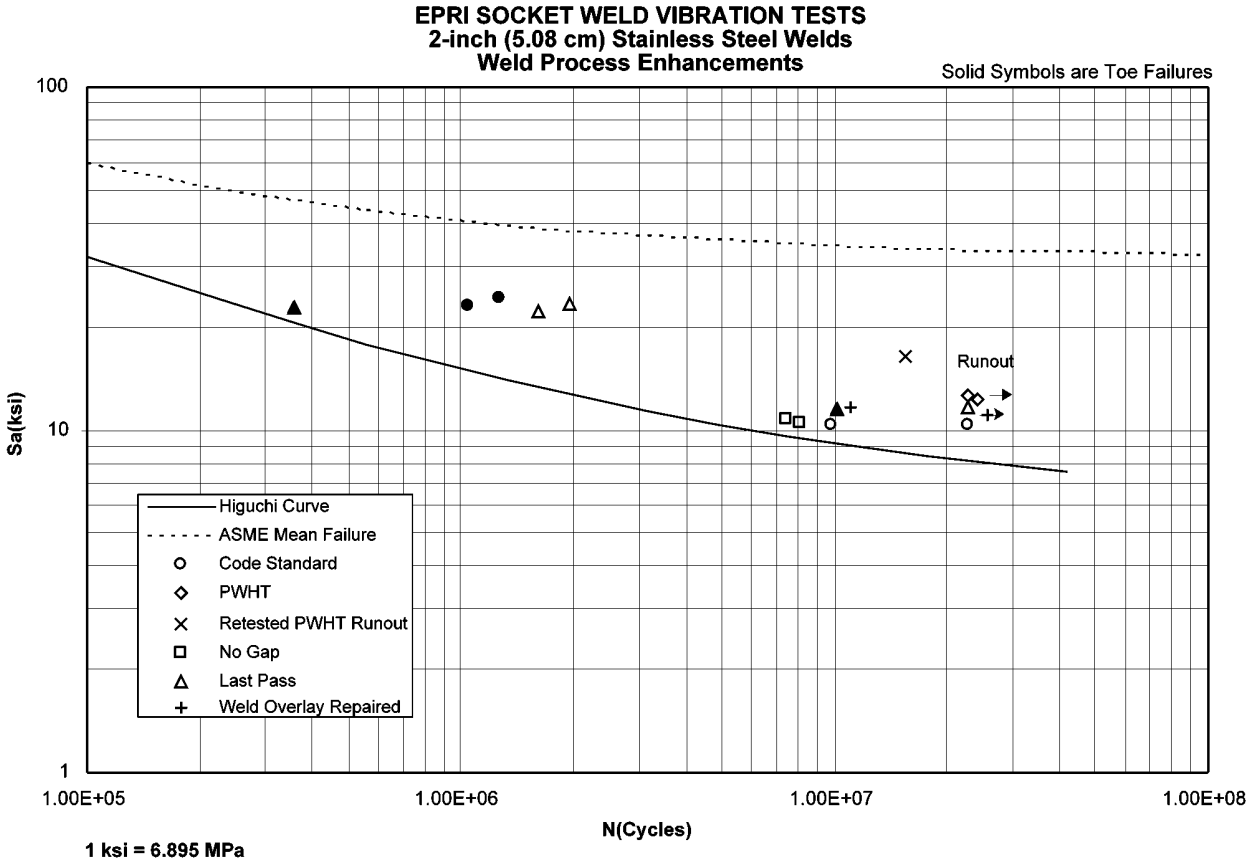


Figure 4-8
2" (5.08 cm) Stainless Steel Weld Enhancements

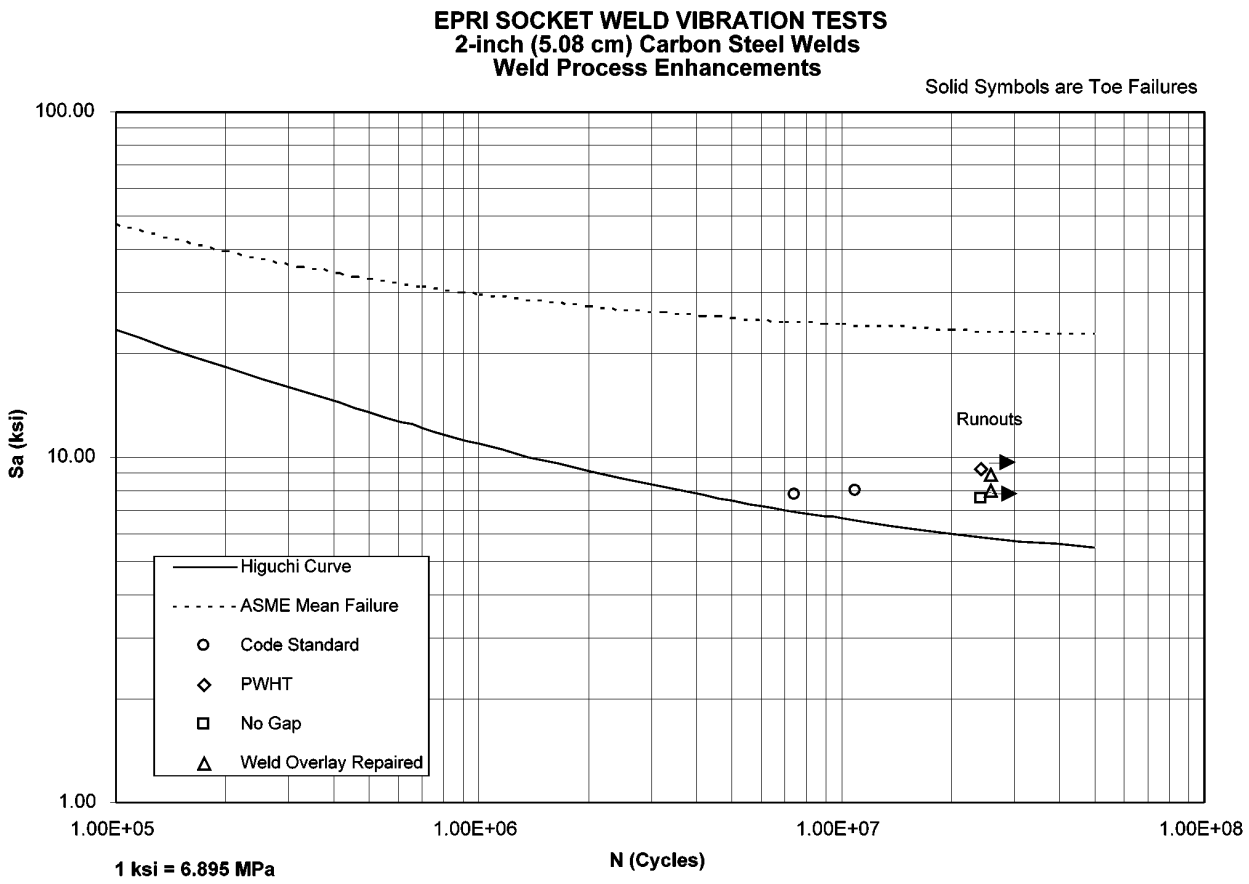


Figure 4-9
2" (5.08 cm) Carbon Steel Weld Enhancements

The last-pass-improved specimens yielded somewhat mixed results. One of the failures of these specimens occurred just above the Higuchi trend curve for normal Code specimens (the toe failure at 3.5×10^5 cycles). Other last-pass-improved specimens performed significantly better [such as the runout at 12 ksi (82.74 MPa)]. In general, where premature failures occurred in last-pass-improved specimens, they were due to toe failures, indicating that the last-pass welding might have left a discontinuity or stress raiser at the toe. Three of the five last-pass samples performed better than the standard socket welds.

Post-weld heat treatment appears to increase the fatigue life of the standard Code specimens. Both of the stainless samples tested were runouts at 12 ksi (82.74 MPa) and the carbon steel sample was a runout at 9 ksi (62.055 MPa). One of the stainless steel runouts from Test Series 2 was retested at a higher load in Test Series 4. Despite having withstood 23 million cycles at 12 ksi (82.74 MPa), it lasted another 13 million cycles at 16 ksi (110.32 MPa). The equivalent total number of cycles at 16 ksi (110.32 MPa) was estimated to be 15.4 million.

The ASME Code-required gap appears to have no consistent effect on high cycle fatigue resistance. The stainless steel, no gap specimens both failed just above the trend curve, which is below the results for standard welds. However, the carbon steel test was a runout at 8 ksi (55.16 MPa). A possible explanation is that the coefficient of thermal expansion of stainless steel is greater than that of carbon steel, thus causing more weld shrinkage and more residual stress in

the weld in the stainless steel specimens. Examination of the failure surface under magnification did not reveal anything of note, other than that the cracks originated at the root at a location with a larger radial gap. The main reason for the Code requirement of the axial gap is to avoid differential thermal expansion stresses when the pipe is carrying hot fluid. The testing was done with room temperature air so the effect of thermal expansion on fatigue strength was not tested.

4.5 3/4-Inch (1.91 cm) Pipe Diameter Tests

Figure 4-10 shows the results of the tests performed using 3/4-inch (1.91 cm) stainless steel socket weld specimens.

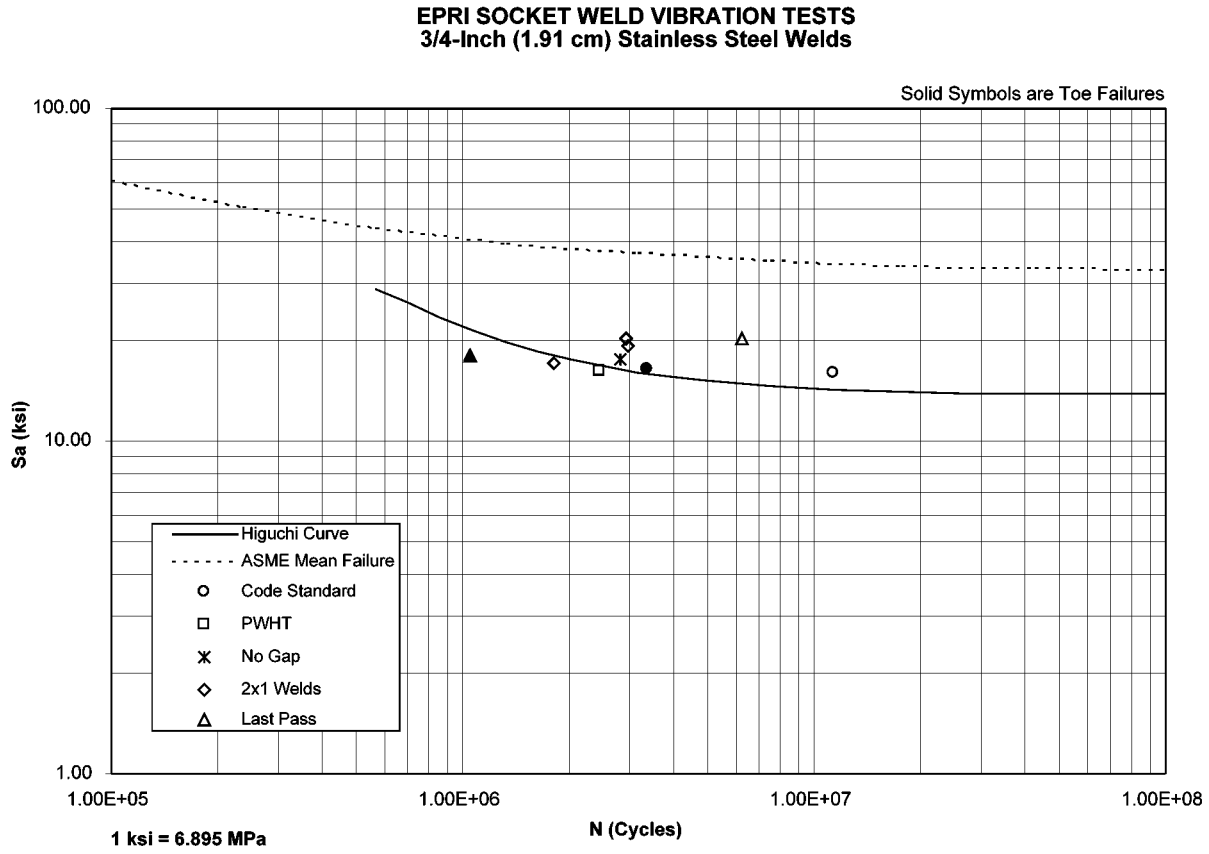


Figure 4-10
3/4" (1.91 cm) Stainless Steel Tests

The various enhanced socket weld designs showed less of an improvement over standard socket welds in the 3/4-inch (1.91 cm) sizes. The 3/4-inch (1.91 cm) 2 x 1 specimens withstood stress levels of about 15% to 20% higher than would be predicted by the corresponding Higuchi trend curve, but this was not as much of an improvement as in the 2-inch (5.08 cm) pipe. The last-pass specimens had mixed results with one case showing a significant improvement over a standard weld while the other was actually below the trend line. The 3/4-inch (1.91 cm) PWHT specimen failed right on the trend curve, but this specimen was heat-treated at too low a temperature (1150°F) (621°C) and thus the heat treatment might have been ineffective at significantly

relieving residual stresses. Elimination of the Code-required axial gap did not seem to have any impact on the fatigue strength.

Figure 4-11 is a comparison of the 3/4-inch (1.91 cm) data with the 2-inch (5.08 cm) stainless steel data.

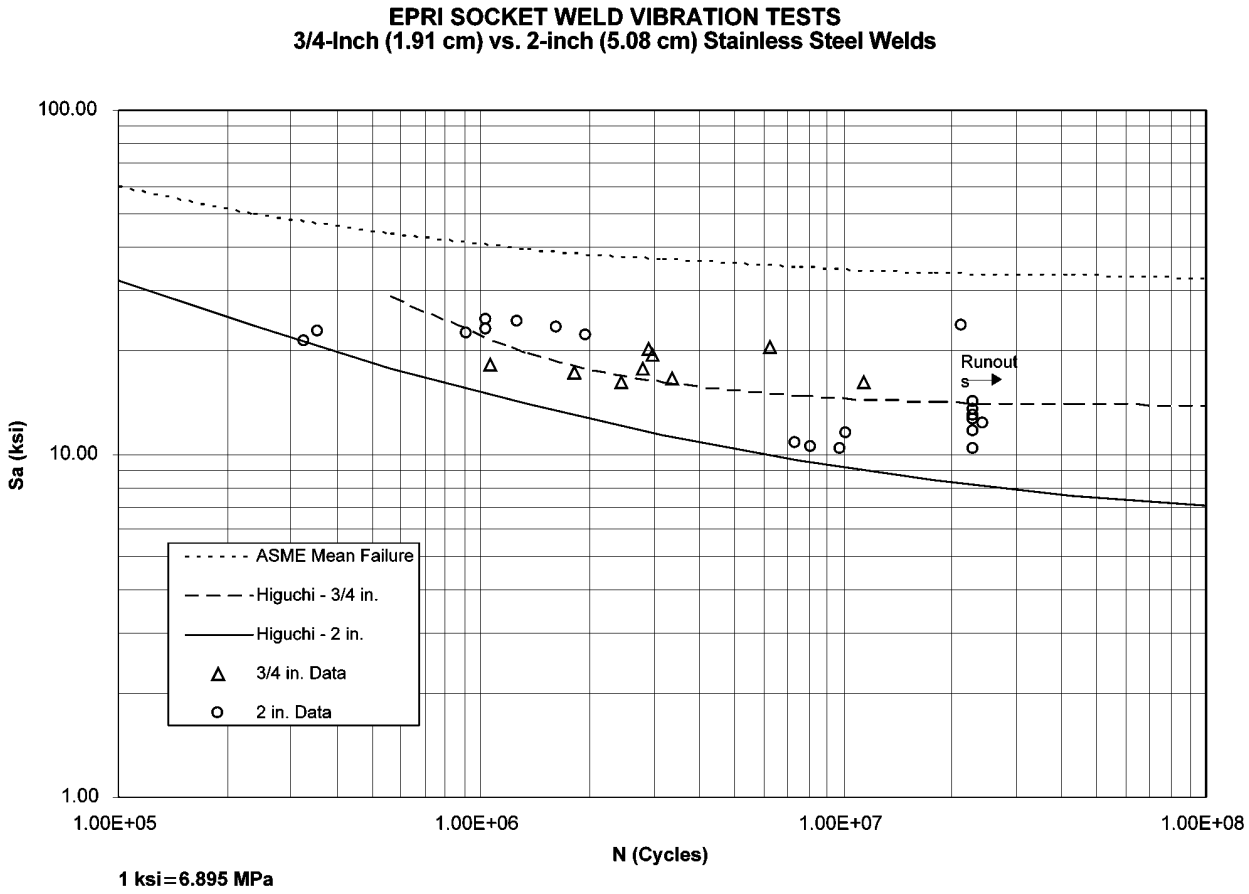


Figure 4-11
Comparison of 3/4" (1.91 cm) and 2" (5.08 cm) Data

The Higuchi trend curves for the two sizes are also shown. A comparison of the data for the two sizes indicates that the smaller size pipe generally has a higher fatigue resistance, although it is not as clear a difference as was found in Reference [5]. The reason is that this plot includes the enhanced weld designs as well as the Code standard welds. While the standard welds performed better in the 3/4-inch (1.91 cm) size, the enhancements in the 3/4-inch (1.91 cm) size resulted in less of an improvement.

4.6 Modified and Repaired Welds

Two stainless steel and two carbon steel 1x1 socket welds that had been tested to runout in the second or third test series had additional weld metal applied to them to make them 2x1 welds. The modified welds were then retested at loads that were approximately 50% higher than in the previous tests. The purpose was to determine whether an existing Code standard weld could be increased to a 2x1 weld *in situ* to improve its fatigue strength and how it would compare to a new 2x1 weld.

The results are shown in Figures 4-3 (stainless) and 4-4 (carbon steel). One of the stainless welds was a runout at 17.4 ksi (119.973 MPa). The other failed at the toe after 5 million cycles at 17.6 ksi (121.352 MPa). The first specimen was a former Code standard weld and the second was a post-weld heat treated specimen. It should be noted that the latter weld was sectioned and examined. The examination indicated that the original weld did not have any sign of cracking prior to the buildup. Both of the carbon steel welds were runouts; the first was a former post-weld heat treated specimen tested at 14.7 ksi (101.357 MPa) and the second was a no gap specimen tested at 11 ksi (75.845 MPa). In these tests, the specimens were tested for longer than in the first phase; the tests ran to about 26 million cycles. The results clearly show an improvement in fatigue strength over standard Code welds. As for comparing the built up 2x1 welds with new 2x1 welds, most of the welds of both categories were runouts so a definitive comparison was not possible. The built up welds appear to be at least as good as the new 2x1 welds.

Two stainless steel and two carbon steel socket welds that had failed (through-wall leaks) in the second and third test series were repaired and retested at their original stress levels. The repair consisted of peening and sealing the crack with water in the pipe and applying a weld overlay that provided an additional 1/4-inch (.64 cm) throat at both the pipe-side toe and the fitting-side toe. The purpose of the test was to determine whether an *in situ* weld repair would be effective in extending the life of a leaking socket weld until the next outage when it could be permanently repaired.

The results of these tests are shown in Figures 4-8 and 4-9. One of the stainless steel repaired welds lasted about 11 million cycles at 11.6 ksi (79.982 MPa). The original weld had been a last pass specimen that had failed at the toe at 10 million cycles under the same load. In the re-test, the weld failed not at the new toe but at the continuation of the original weld crack. This can be seen in Figure 4-12.



Figure 4-12
Weld Overlay of Toe Crack

Although the overlay did not arrest the original toe crack, it was still successful in restoring all of the fatigue life of the original weld. The second stainless specimen had originally been a Code standard weld that had failed at the root at 10 million cycles at 10.5 ksi (72.398 MPa). In this test, it was a runout under a load of 11 ksi (75.845 MPa). The weld overlay was successful in arresting the original crack. This can be seen in Figure 4-13.

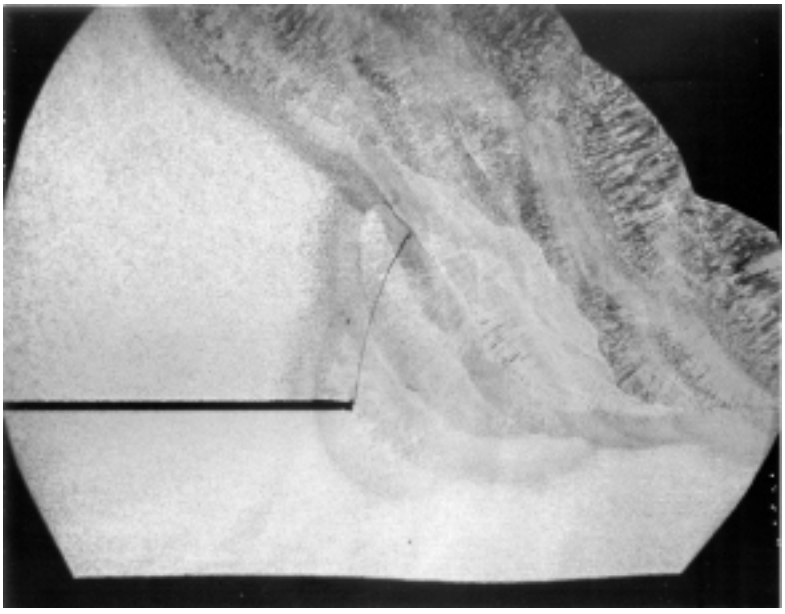


Figure 4-13
Weld Overlay of Root Crack

Thus, the repaired weld was better than the original. In the carbon steel tests, both repaired welds were runouts. They had both originally been standard Code welds that had failed at the root after 7 million and 10 million cycles at 8 ksi (55.16 MPa). The repaired welds withstood 26 million cycles at 8 and 9 ksi (55.16 MPa and 62.055 MPa), respectively, and did not show any evidence of crack initiation. It can be concluded from these tests that the weld overlay repair process was successful in not only restoring the original fatigue strength of the specimen, but it actually improved the weld's fatigue resistance. The weld overlay design used was more effective in arresting root cracks than toe cracks.

4.7 Fatigue Strength Reduction Factors

Fatigue strength reduction factors (FSRFs) were calculated as a means of quantifying the test results of the various socket weld designs. The FSRFs are approximate; they are based on estimates of the endurance limit, a number of tests that were runouts, and a limited number of test points. Table 4-3 is a summary of the FSRFs for each of the categories of tests, based on the ratio of the endurance limit from the ASME Code mean failure curve to the apparent endurance limit from the testing results. Because the testing was terminated at approximately 2×10^7 cycles, the alternating stress corresponding to this number of cycles was taken as the endurance limit for the purposes of this calculation. For the failed specimens, the endurance limit was based on graphically extending the test data point to 2×10^7 cycles along a line parallel to the Higuchi trend line. For the runouts, the tested stress level was conservatively taken as the endurance limit.

Table 4-3
Fatigue Strength Reduction Factors

Category	No. Tested	Avg. FSRF
2" (5.08 cm) Stainless Steel Tests		
Code Standard (1 x 1)	2	3.4
2 x 1	5	2.3
1 x 1 Built-up to 2 x 1	2	2.2
Butt Weld	3	2.9
Weld Overlay Repair	2	3.2
PWHT	2	2.5
Last Pass	2	3.1
No Gap	2	3.7
Polished Toe	2	3.6
Smooth As-Welded Toe	2	2.8
Smooth Last Pass Toe	3	2.9
Poor Toe	2	4.8
2" (5.08 cm) Carbon Steel Tests		
Code Standard (1 x 1)	2	3.5
2 x 1	5	2.0
1 x 1 Built-up to 2 x 1	2	1.8
Butt Weld	2	2.4
Weld Overlay Repair	2	2.8
PWHT	1	2.5
No Gap	1	3.1
3/4" (1.91 cm) Stainless Steel Tests		
Code Standard (1 x 1)	2	2.4
2 x 1	3	2.2
PWHT	1	2.6
Last Pass	2	2.3
No Gap	1	2.4

For the 2-inch (5.08 cm) stainless steel specimens, the standard Code socket welds had an FSRF of approximately 3.4. The 2 x 1 leg size specimens improved upon this to a value of 2.3 versus 2.9 for the butt-welded specimens. Similarly, for the carbon steel specimens, the standard weld FSRF was 3.5. The 2 x 1 welds reduced this value to 2.0 versus 2.4 for the butt welds. An apparent break in this trend is that, as observed previously in Reference [5], 3/4-inch (1.91 cm) standard Code specimens show less of an improvement in going to the 2x1 weld geometry. However, this might be due to the fact that the standard welds in this pipe size appear to have

significantly greater fatigue resistance than those of the larger size. Nonetheless, in general, it appears that it is reasonable to use an FSRF of 3.9 for standard Code socket welds and an FSRF of 2.6 for 2 x 1 leg size socket welds in vibration fatigue applications, independent of pipe size. This is consistent with the current ASME Section III Code requirement of $C_2K_2 = 3.9$ for standard socket welds and the lower bound of 2.6 for larger leg length welds. This is also consistent with the EPRI Fatigue Management Handbook [1] recommendation of 2.6 for "Good" welds and 4.2 for "Fair" welds. The use of a 2 x 1 weld leg configuration would, in essence, move a weld from the "Fair" to the "Good" category.

The above results apply only to welds with no root defects or lack of fusion. Prior testing and analysis [3,6] have shown that root defects can have a significant detrimental effect on socket weld high cycle fatigue resistance, and many field failures have been affected by such defects. In addition, testing of the samples with toe defects in this program resulted in an FSRF of about 5. The EPRI Handbook [1] recommends an FSRF of 8.0 for "Poor" welds, which is intended to encompass welds with root or toe defects.

A comparison of the various weld treatments indicates that post-weld heat treatment had the most consistent benefit with an FSRF of 2.5 for 2-inch (5.08 cm) stainless, 2.5 for carbon steel, and 2.6 for 3/4-inch (1.91 cm) stainless. The last-pass welds had FSRFs of about 3, and the no gap welds about 3.5.

Modification of the previously tested 1 x 1 welds, by building up the weld on the pipe side to a 2 x 1 profile, produced welds that were as good as or better than new 2 x 1 welds. For stainless steel, the FSRF for the built-up 2 x 1 welds was 2.2 versus 2.3 for new 2 x 1 welds and 3.4 for new 1 x 1 welds. For carbon steel, the FSRFs were 1.8 for the built-up 2 x 1, 2.0 for the new 2 x 1, and 3.5 for the Code-standard welds.

The weld overlay repairs were also successful in improving the fatigue strength of leaking, standard Code welds. The stainless steel welds that were repaired had an FSRF of 3.2, which is better than new standard welds at 3.4. The results were even better in the carbon steel specimens, with an FSRF of 2.8 for the repaired welds versus 3.5 for new standard Code welds.

4.8 Dynamic Load Factors (DLFs)

The tests were carried out with shaker table frequencies of about 100-120 Hz and the specimen natural frequencies were tuned to about 4-8 Hz below the table frequency. It was observed from the testing that, as a specimen began to fail, its natural frequency began to decline and, consequently, the dynamic load factor and response acceleration declined. The effect was more noticeable in the cases where the failure occurred at the toe because a crack opening at the toe reduces the stiffness of the specimen more than a crack originating at the root. Although the test plan called for removing the specimens from the table shortly after leaking, the time until the specimen was actually removed provided some data for measuring the frequency shift after the crack had grown through-wall and began to grow circumferentially. In addition, the three specimens that failed in Test Series 4 (which was actually run last) were left on the table for the duration of the test. The data indicated that, after the crack extended through-wall, the rate of decline in frequency accelerated for both toe and root failures.

Measurements of the specimen damping, which averaged about 0.5%, showed that there was very little change in damping as the specimen began to crack. Eliminating change in damping as a variable allowed the change in frequency to be directly calculated from the measured change in specimen acceleration. The result was that toe failures produced about a 4 Hz reduction in frequency up to the point where the weld began to leak. At a starting frequency of 8 Hz below the table frequency, the 4 Hz shift was enough to reduce the DLF and, consequently, the acceleration and the stress, by about 30%. If the specimen had been tuned to resonance with the excitation frequency, the reduction in DLF for a 4 Hz shift at 0.5% damping would have been as much as 80%.

After leaking through, the change in frequency accelerated as the crack grew circumferentially. The pattern for the three failed specimens in Test Series 4 was that of rapid decline in stress response in the first few million cycles after leakage, followed by a leveling off of the stress over the remaining 10 million or so cycles of the test. This corresponds to the relationship between response and frequency ratio as shown in Figure 2-2. The applied stress and the current crack size are two factors that interact to determine whether the crack will result in rupture or whether it will continue to leak indefinitely. The larger the crack, the lower the stress needed to cause additional crack growth. If the applied stress declines before the crack reaches a significant length, it can leak without breaking. This was illustrated by the varying amounts of frequency change in the three failed specimens. The two with root failures shifted by 5 Hz and 22 Hz, while the one with the toe failure shifted as much as 70 Hz. The amount of frequency shift is an indication of crack length. A surface examination of the latter specimen indicated that the crack length had grown to more than half of the circumference. The frequency of the other two specimens had stopped declining toward the end of the testing, while the frequency of the third continued to decline. This indicates that most likely the first two would continue to leak without breaking under continued cycling, while the third would eventually break. This result is also dependent on the level of the applied stress versus the endurance limit and how close the initial, uncracked natural frequency was to the vibration source frequency. Nevertheless, this indicates that there would be quite a bit of conservatism in assuming a constant stress level in a crack growth analysis of these specimens.

Thus, the shifting in frequency suggests that for vents and drains that are excited by a single frequency source of vibration, such as pumps, as the weld begins to crack, the attachment will tend to detune itself from the excitation frequency causing a reduction in stress at the weld. The attachment might then continue to leak without breaking until an opportunity becomes available to repair it. This might not be true in cases of flow-induced vibration where the vibration is broad-band and the declining attachment frequency might resonate with other lower excitation frequencies.

5
CONCLUSIONS AND RECOMMENDATIONS

On the basis of the testing, it is concluded that socket welds with a 2 to 1 weld leg configuration (weld leg along the pipe side of the weld equal to twice the Code-required weld leg dimension) offer a significant high cycle fatigue improvement over standard ASME Code socket welds (in which both weld legs are equal to the Code-required dimension). This weld design offers a superior improvement in fatigue resistance than does replacement of socket-welded fittings with butt-welded fittings. Since vibration fatigue of socket welds has been a significant industry problem, it is recommended that this improved configuration be used for all socket welds in vibration-critical applications.

The majority of the test failures occurred due to cracks that initiated at weld roots. However, toe-initiated failures occurred in tests at higher stress levels that were premature in comparison with identical tests in which root failures prevailed. Therefore, care must be taken with socket welds of any design to avoid metallurgical or geometric discontinuities at the toes of the welds (such as undercut or non-smooth transitions). Such discontinuities promote a tendency for toe failures, which greatly reduce fatigue life. Tests of welds with intentionally poor toes clearly demonstrated the early failures that such discontinuities can produce. Polishing the toes not only did not provide any benefit, but actually caused earlier cracking, which originated at the scratch marks. Because of the importance of the toe condition, the last pass improvement process (in which a final pass is added to the pipe side toe of a standard Code weld) cannot be given an unqualified recommendation at this time. The last-pass-improved specimens had a tendency to develop toe failures.

Other conclusions drawn from this program are that the Code-required axial gap in socket welds [1/16-inch (.16 cm)] appears to have little or no effect on high cycle fatigue resistance, and that post-weld heat treatment appears to increase the fatigue resistance of standard Code specimens. Although post-weld heat treatment consistently showed improved results, it has the downside of potentially sensitizing austenitic welds for IGSCC in certain environments. Therefore, PWHT is not recommended for situations where IGSCC might be an active damage mechanism.

The test data supports the use of the ASME Section III fatigue strength reduction factor for standard Code welds (currently $C_2K_2 = 3.9$). It also indicates that this factor can be reduced to two-thirds that value (2.6) for 2 to 1 leg size welds. (The current Code lower bound of $C_2K_2 = 2.6$ is based on weld leg length but it is a function of the shortest leg length.) Both of these values are appropriate only if the weld roots are free of defects such as lack of fusion or lack of penetration. Testing has indicated that weld root defects can cause as much as a factor of 2 increase in the fatigue strength reduction factor.

Testing of modification and repair concepts indicated that these approaches were successful in improving the strength of already-installed socket welds without having to replace them with

butt welds. Code standard 1x1 welds that were built up to a 2x1 profile performed as well as new 2x1 welds. Weld overlay repairs of leaking standard welds not only provided enough fatigue resistance for the welds to last to the next outage, but actually improved their fatigue strength to better-than-new standard Code welds. The weld overlay process was somewhat more successful repairing root failures than toe failures.

It was observed that as a fatigue crack in a socket-welded, cantilevered attachment grows in depth and length under continued cycling, the natural frequency of the attachment reduces. This can result in a significant decline in the response when the excitation is at a constant frequency, such as from pump vibration. The stresses that drive crack growth might decrease sharply due to the component frequency moving off resonance with the excitation frequency. This suggests that a fatigue crack in the weld attaching the vent or drain to the run pipe will tend to leak but not break.

6
REFERENCES

1. *EPRI Fatigue Management Handbook.* EPRI, Palo Alto, CA: December 1994. TR-104534-V1, -V2, -V3.

2. J. K. Smith, "Vibrational Fatigue Failures in Short Cantilevered Piping with Socket-Welding Fittings," *ASME PVP*. Vol. 338-1 (1996).

3. *Vibration Fatigue of Small Bore Socket-Welded Pipe Joints.* EPRI, Palo Alto, CA: June 1997. TR-107455.

4. M. Higuchi et al., "Fatigue Strength of Socket Welded Pipe Joints," *ASME PVP*. Vol. 313-1 (1995).

5. M. Higuchi et al., "A study on Fatigue Strength Reduction Factor for Small Diameter Socket Welded Pipe Joints," *ASME PVP*. Vol. 338-1 (1996).

6. M. Higuchi et al., "Effects of Weld Defects at Root on Rotating Bending Fatigue Strength of Small Diameter Socket Welded Pipe Joints," *ASME PVP*. Vol. 338-1 (1996).

7. *Vibration Fatigue Testing of Socket Welds.* EPRI, Palo Alto, CA: December 1998. TR-111188.

8. *ASME Boiler and Pressure Vessel Code*, Section III, Subsection NB, 1998 Edition.

9. Welding Research Council Bulletin 432, "Fatigue Strength Reduction Factors and Stress Concentration Factors for Welds in Pressure Vessels and Piping," June 1998.

10. "Criteria of the ASME Boiler and Pressure Vessel Code for Design by Analysis," Sections III and VIII, Division 2, ASME, 1969.

11. C. E. Jaske and W. J. O'Donnell, Trans. ASME, J. Pressure Vessel Technology, pp. 584-592 (1977).

A
TEST ASSEMBLY

This appendix describes the details of the test specimens and specifications for each component of the test assembly used in this program.

The basic configuration of a test specimen is shown in Figure A-1. The “test weld” is located between the pipe and the socket weld flange as shown in Figure A-1. The complete assembly is mounted to a specially fabricated plate, which is bolted directly to a shaker table.

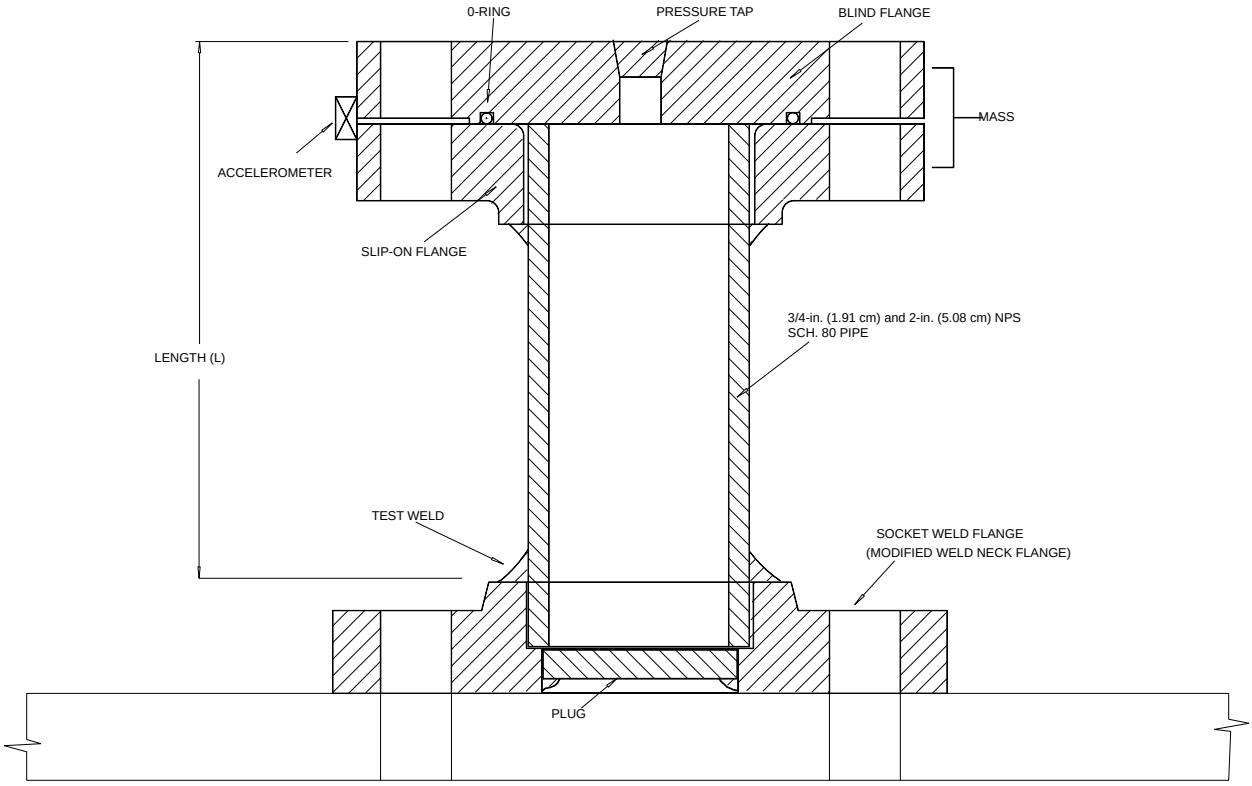
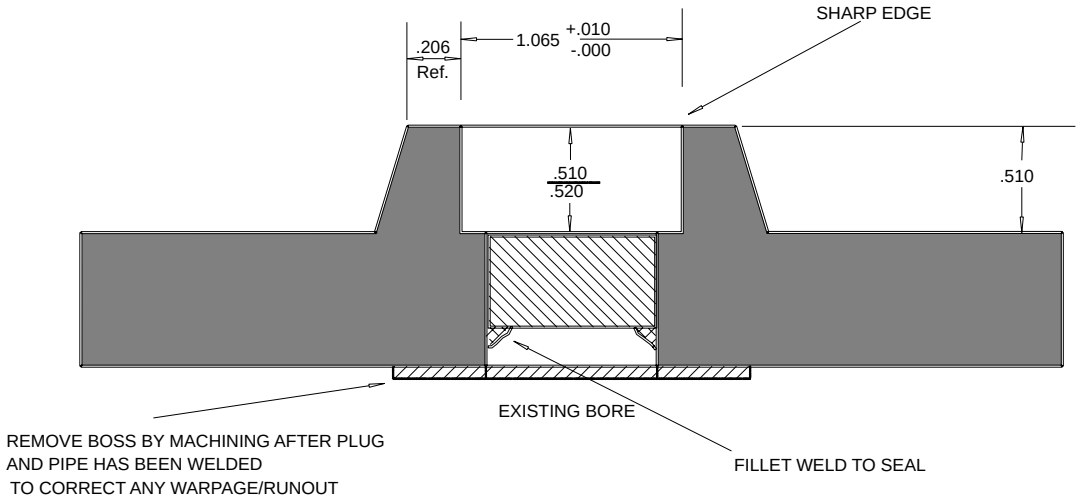


Figure A-1
Drawing of Typical Test Specimen for Vibration Fatigue Test Evaluation

Test Assembly

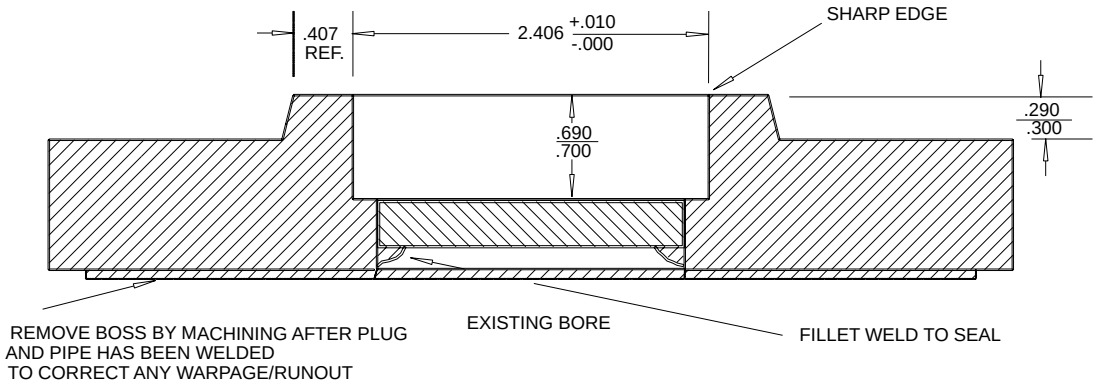
A.1 Socket Weld Flange

The socket weld flanges were machined from standard 300 lb. (136.1 kg) weld neck pipe flanges. This was done to reduce dimensional inconsistencies between each test specimen. Dimensional details for the modified welded-neck pipe flanges are shown in Figures A-2 and A-3 for 3/4-inch (1.91 cm) and 2-inch (5.08 cm) test specimens, respectively, and were used for both stainless steel and carbon steel flanges. The machined components provided a consistent radial and axial gap to reduce the effects of variations in clearances at the test weld location.



NOTE: All dimensions are in inches. To convert inches to centimeters, multiply the unit by 2.54.

Figure A-2
Socket-Welded Flange Specifications for 3/4-Inch (1.91 cm) Test Specimens



NOTE: All dimensions are in inches. To convert inches to centimeters, multiply the unit by 2.54.

Figure A-3
Socket-Welded Flange Specifications for 2-Inch (5.08 cm) Test Specimens

Both ends of the test assembly were sealed to allow the test specimens to be pressurized [(approximately 50 psi (344.8 Kpa)]during the fatigue tests. A plug was welded into the bore of the modified socket weld flange of all test assemblies and an O-ring slot was machined into the upper blind flanges as shown in Figure A-1. The plugs were recessed below the insertion depth of the pipe to ensure clearance between the pipe and plug.

The bottom of the socket-welded flange was machined flat after all welding was completed. This ensured that solid contact with the mounting plate was achieved and that the test specimens remained perpendicular to the mounting plate. The flatness of the completed assembly was verified on a granite table prior to fitting it on the breadboard. The fully assembled component was pressure-checked to verify the integrity of the plug weld after final machining.

A.2 Pipe Section

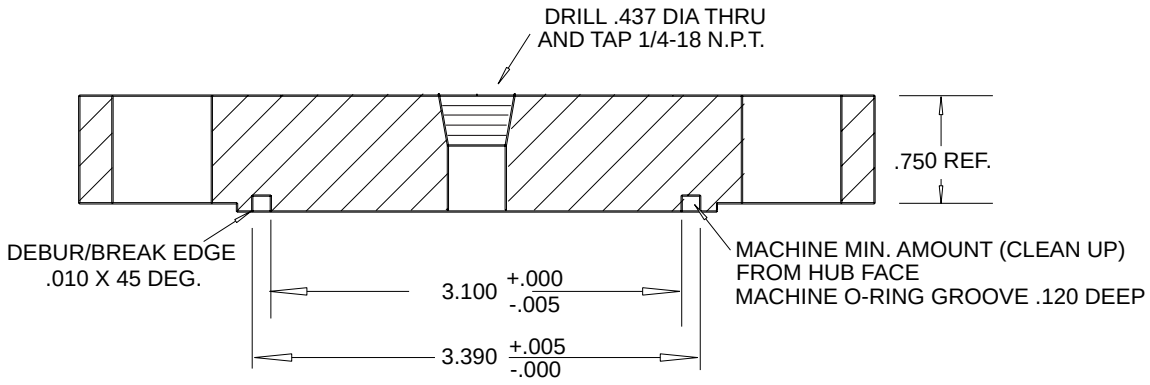
The pipe sections consisted of 2-inch (5.08 cm) and 3/4-inch (1.91 cm) NPS, Schedule 80 pipe. The materials used were stainless steel and carbon steel. The nominal wall thickness for 2-inch (1.91 cm) Schedule 80 is 0.218 inch (0.554 cm) and, for 3/4-inch Schedule 80, is 0.154 inch (0.391 cm). The pipe sections and mass at the opposite end of the test assembly were sized to achieve failure in the test weld within $1x10^7$cycles. The overall lengths of the 2-inch (5.08 cm) and 3/4-inch (1.91 cm) diameter pipes were 16.5 inches (41.9 cm) and 9.5 inches (24.13 cm), respectively. The use of a slip-on flange on the opposite end of the assembly allowed the overall length to remain constant for specimens without the typical [1/16-inch (0.16 cm)] axial gap requirements.

The weld-to-weld length of the butt weld test specimens matched the dimensions of the socket-welded configurations.

A.3 Slip-On Flange and Blind Flange

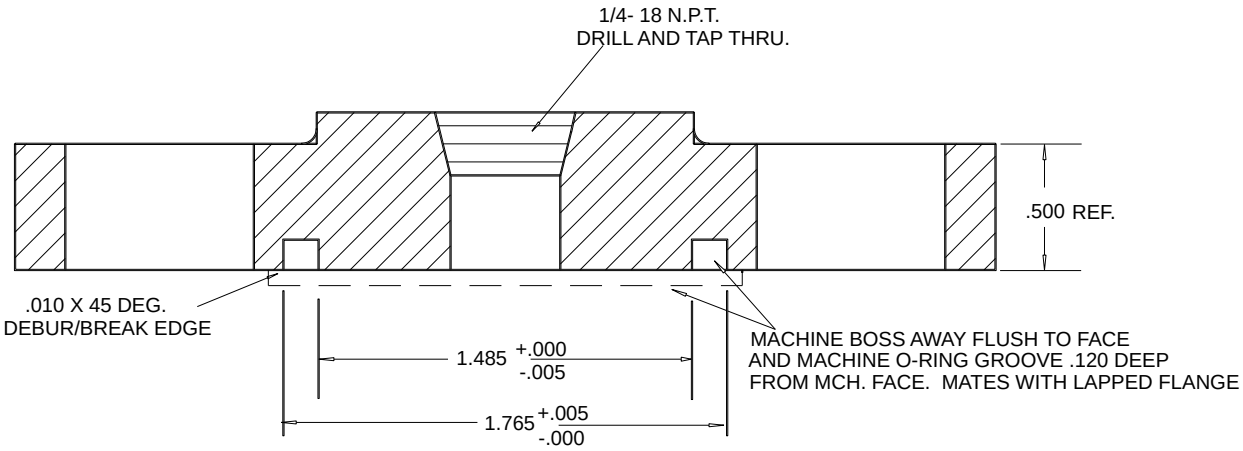
The mass required for the test was fabricated by combining a slip-on welded flange and a blind flange as shown in Figure A-1. The slip-on flange and blind flange were used to seal and pressurize the test assembly during the duration of the test. The boss was machined flush with the face of the blind flange and an O-ring groove was machined into a set of nine blind flanges for both 2-inch (5.08 cm) and 3/4-inch (1.91 cm) test assemblies as shown in Figures A-4 and A-5. The blind flanges were also drilled and tapped to support individual pressure taps on each test assembly. This allowed each set of blind flanges to be reused for subsequent tests. The pressure taps were used to independently monitor the internal pressure of the test assemblies. Failure of the test weld was determined by a 20% drop in the internal pressure.

Test Assembly



NOTE: All dimensions are in inches. To convert inches to centimeters, multiply the unit by 2.54.

Figure A-4
Blind Flange for 2-Inch (5.08 cm) Test Specimens with O-Ring Groove



NOTE: All dimensions are in inches. To convert inches to centimeters, multiply the unit by 2.54.

Figure A-5
Blind Flange for 3/4-Inch (1.91 cm) Test Specimens with O-Ring Groove

B
WELD SPECIFICATIONS

This appendix provides details of the welding and repair procedures for the test welds.

The test specimens in this program included remediation-type welds, which were fabricated from Phase I specimens that had either failed or were terminated prior to failure. These specimens were used to verify improvements or the life expectancy that could be achieved by repairing or modifying existing socket welds. Remediated welds included the repair of leaking socket welds by a complete overlay process or the modification of susceptible welds from a 1 x 1 to 2 x 1 weld dimension. Specimens were also used to determine the effects of toe discontinuities of both socket welds and butt-welded configurations.

From Phase I and II, ten categories were selected to examine remedial treatment, each having its own specifications for welding, processing, and/or assembly. Table B-1 lists each category along with the test specimen labeled according to identification numbers assigned in Tables 3-1 and 3-2. All welding was completed with semi-automatic gas tungsten arc welding (GTAW), with the pipe/fitting rotating at a constant speed. Filler material and torch manipulation were applied manually with the exception of repair welds, which were manually seal-welded and overlaid using the shielded metal arc welding (SMAW) process. Welding parameters, assembly, and welding procedures are outlined in the following sections for each category.

Table B-1
Test Matrix—Weld Categories

Category	Mockup Identification	Pipe Size*	Material	Bead Sequence	Axial Gap*	Comments
1x1 Standard Configuration Section B.1	B2-2SS-1 B2-2SS-2 B1-3/4SS-1 B1-3/4SS-2 B3-2CS-1 B3-2CS-2 B5-2SS-1 B5-2SS-2	2-in., Schedule 80 2-in., Schedule 80 3/4-in., Schedule 80 3/4-in., Schedule 80 2-in., Schedule 80 2-in., Schedule 80 2-in., Schedule 80 2-in., Schedule 80	Type 304 Type 304 Type 304 Type 304 Carbon Steel Carbon Steel Type 304 Type 304	L1 = L2 = 1.09 x wall thickness. Three consecutive beads. (Figure B-1)	1/8-inch	Typical bead sequence
2x1 Modified Configuration Section B.2	B1-3/4SS-3 B1-3/4SS-4 B1-3/4SS-5 B2-2SS-3 B2-2SS-4 B2-2SS-5 B3-2CS-3 B3-2CS-4 B3-2CS-5 B6-2SS-6 B6-2SS-7 B6-2CS-8 B6-2CS-9	3/4-in., Schedule 80 3/4-in., Schedule 80 3/4-in., Schedule 80 2-in., Schedule 80 2-in., Schedule 80 2-in., Schedule 80 2-in., Schedule 80 2-in., Schedule 80 2-in., Schedule 80 2-in., Schedule 80 2-in., Schedule 80 2-in., Schedule 80 2-in., Schedule 80	Type 304 Type 304 Type 304 Type 304 Type 304 Type 304 Carbon Steel Carbon Steel Carbon Steel Type 304 Type 304 Carbon Steel Carbon Steel	Last pass intentionally placed on the fitting side. (Figures B-2 and B-3)	1/8-inch	Variation in the 3/4-inch and 2-inch weld sequence.
Last Pass Improved (LPI) Section B.3	B1-3/4SS-7 B1-3/4SS-8 B2-2SS-7 B2-2SS-8 B5-2SS-7 B5-2SS-8 B5-2SS-9	3/4-in., Schedule 80 3/4-in., Schedule 80 2-in., Schedule 80 2-in., Schedule 80 2-in., Schedule 80 2-in., Schedule 80 2-in., Schedule 80	Type 304 Type 304 Type 304 Type 304 Type 304 Type 304 Type 304	L2 > L1= 1.09 x wall thickness. (Figure B4)	1/8-inch	Standard L1 = L2 with an additional pass on the pipe side. Smooth transition was maintained from the pipe to the weld. L2 approximately equal to 1.5 x L1.

* To convert inches to centimeters, multiply the unit by 2.54.

Table B-1 (cont.)
Test Matrix—Weld Categories

Category	Mockup Identification	Pipe Size*	Material	Bead Sequence	Axial Gap*	Comments
Post Weld Heat Treat (PWHT) Section B.4	B1-3/4SS-6 B2-2SS-6 B3-2SS-8 B3-2CS-6 B4-2SS-3 (B2-6)	3/4-in., Schedule 80 2-in., Schedule 80 2-in., Schedule 80 2-in., Schedule 80 2-in., Schedule 80	Type 304 Type 304 Type 304 Carbon Steel Type 304	L1 = L2 = 1.09 x wall thickness. Three consecutive beads. (Figure B-1)	1/8-inch	Typical bead sequence
No Axial Gap Configuration Section B.5	B1-3/4SS-9 B2-2SS-9 B3-2SS-9 B3-2CS-7	3/4-in., Schedule 80 2-in., Schedule 80 2-in., Schedule 80 2-in., Schedule 80	Type 304 Type 304 Type 304 Carbon Steel	L1 = L2 = 1.09 x wall thickness. Three consecutive beads. (Figure B-5)	No axial gap	Typical bead sequence. Full contact or engagement between the fitting and the pipe.
Welds with Toe Discontinuities Section B.6	B5-2SS-3 B5-2SS-4 B5-2SS-5 B5-2SS-6	2-in., Schedule 80 2-in., Schedule 80 2-in., Schedule 80 2-in., Schedule 80	Type 304 Type 304 Type 304 Type 304	Typical bead sequence for 1x1 configuration with alterations of the last pass. (Figure B-1)	1/8-inch	Toe modifications were produced by altering the welding technique on the pipe side or by blend grinding the toe.
1x1 to 2x1 Modified Weld Configuration Section B.7	B4-2SS-1 (B2-1) B4-2SS-2 (B3-8) B4-2CS-4 (B3-6) B4-2CS-5 (B3-7)	2-in., Schedule 80 2-in., Schedule 80 2-in., Schedule 80 2-in., Schedule 80	Type 304 Type 304 Carbon Steel Carbon Steel	Three beads starting from the pipe side working toward the fitting. (Figures B-6 and B-7))	1/8-inch	Modification of Phase I (1x1) test specimens to a 2x1 configuration.
Overlay Repair Weld Configuration Section B.8	B4-2CS-6 (B3-1) B4-2CS-7 (B3-2) B4-2SS-8 (B2-8) B4-2SS-9 (B2-2)	2-in., Schedule 80 2-in., Schedule 80 2-in., Schedule 80 2-in., Schedule 80	Carbon Steel Carbon Steel Type 304 Type 304	Bead sequence varied per seal weld requirements. (Figures B-8 through B-16)	1/8-inch	Localized seal weld and full overlay buildup. (Figure B-8)
Standard Butt Weld Configuration Section B.9	B6-2SS-1 B6-2SS-2 B6-2CS-3 B6-2CS-4 B6-2SS-5	2-in., Schedule 80 2-in., Schedule 80 2-in., Schedule 80 2-in., Schedule 80 2-in., Schedule 80	Type 304 Type 304 Carbon Steel Carbon Steel Type 304	Typical bead sequence. (Figure B-18)	1/8-inch	Standard
Butt Weld with Toe Discontinuities Section B.10	B6-2SS-6	2-in., Schedule 80	Type 304	Typical bead sequence for a butt weld with undercut at the toe. (Figure B-19)	1/8-inch	Undercut was produced by modifying the joint geometry.

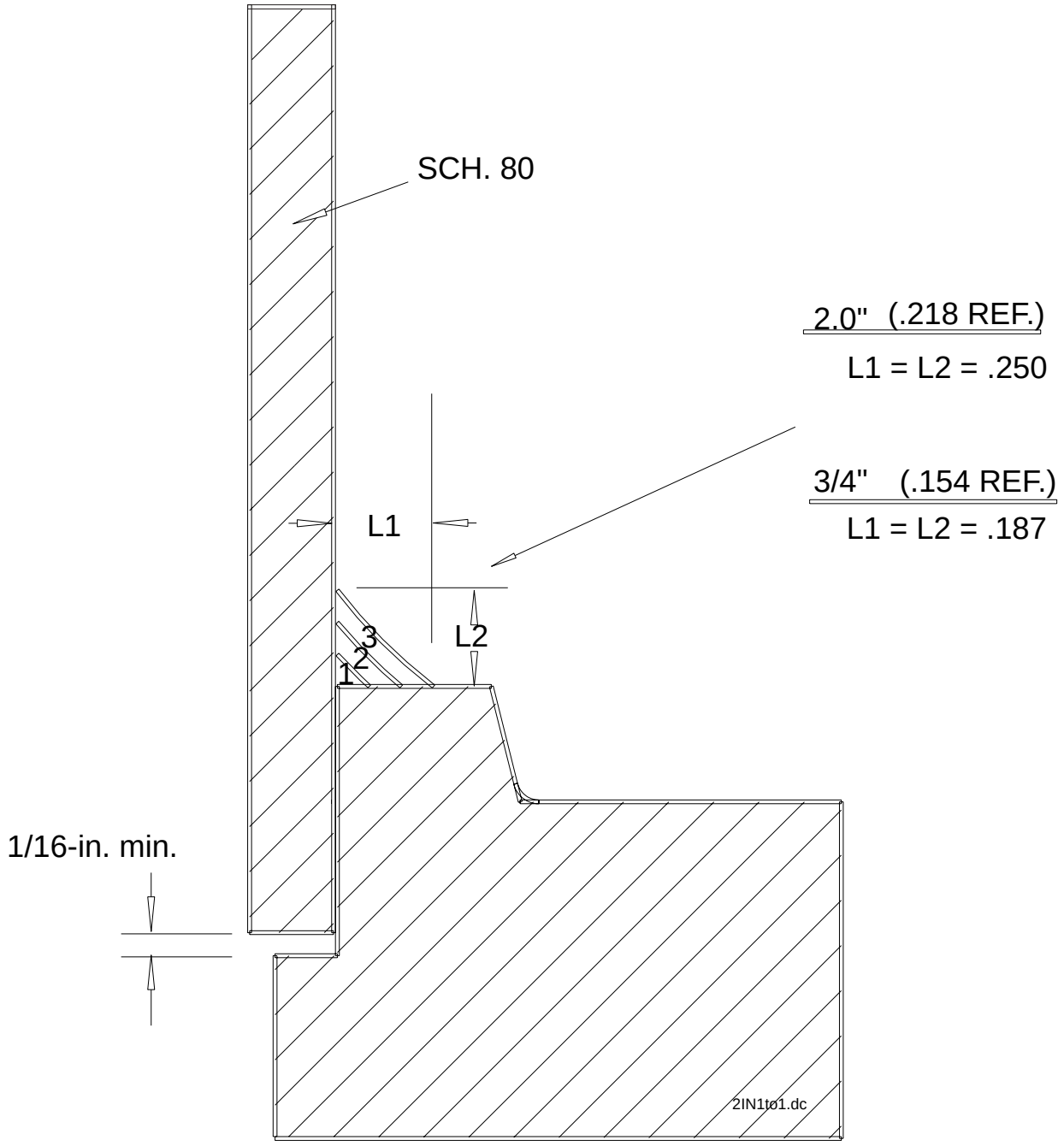
* To convert inches to centimeters, multiply the unit by 2.54.

B.1 Standard 1x1 Configuration

The standard 1x1 configuration was used as the baseline test for all test specimens. The 1x1 configuration consisted of equal leg lengths specified per Code requirements (L1 = L2 = pipe wall thickness × 1.09) as shown in Figure B-1. The weld leg lengths were maintained at or slightly greater than the minimum leg length on both the pipe side and fitting side of the weld. A slightly concave final weld bead geometry, with smooth transitions into the pipe and fitting, was specified for all the welds of this configuration. The pipe sections were tacked to the fittings with a 1/8-in. (0.318 cm) standoff between the pipe and fitting to maintain a minimum 1/16-inch (0.16 cm) axial gap after welding. Lines were scribed on both the fitting and pipe side of the assembly to assist the welder in maintaining the correct leg length and to control the gap requirements. Weld specifications for this configuration are listed in Table B-2.

Table B-2
Weld Specifications for Standard 1x1 Configuration

Weld Geometry	Standard 1x1 weld (1.09 x wall thickness = L2 = L1)
Pipe Size	2-inch (5.08 cm). and 3/4-inch (1.91 cm) Schedule 80
Pipe Material	Carbon Steel and Type 304 Stainless Steel
Filler Metal	3/32-in. (0.238 cm) (root) and 1/8-in. (0.318 cm) ER308L Sandvik 3/32-in. (0.238 cm) (root) and 1/8-in. (0.318 cm) ER 70S-2 Lincoln
GTAW Sequence	(Figure B-1) Three beads, each bead extends from the pipe to the fitting with equal leg lengths (45°). The same sequence was used for both the 3/4-in. (1.91 cm) and the 2-in. (5.08 cm) test specimens.
Electrode Diameter	3/32-in. (0.238 cm) tungsten
Purge	ID argon purge during entire weld sequence
Technique	Walking the cup except for the root pass. Pipe rotating at constant speed.
Amperage (DCSP) and Voltage	125-135 amps and 19-20 volts for stainless steel 160-170 amps and 21-22 volts for the carbon steel
Welding Power Supply	Hobart Cyber-TigII
Travel Speed	5–6 ipm (12.7–15.24 cm/minute) for root pass, 1.5–2 ipm (3.81–5.08 cm/minute) for cap passes
Cup Size	#5 cup



NOTE: All dimensions are in inches. To convert inches to centimeters, multiply the unit by 2.54.

Figure B-1
Drawing of Standard Weld Sequence with Equal Leg Lengths (L2 = L1)

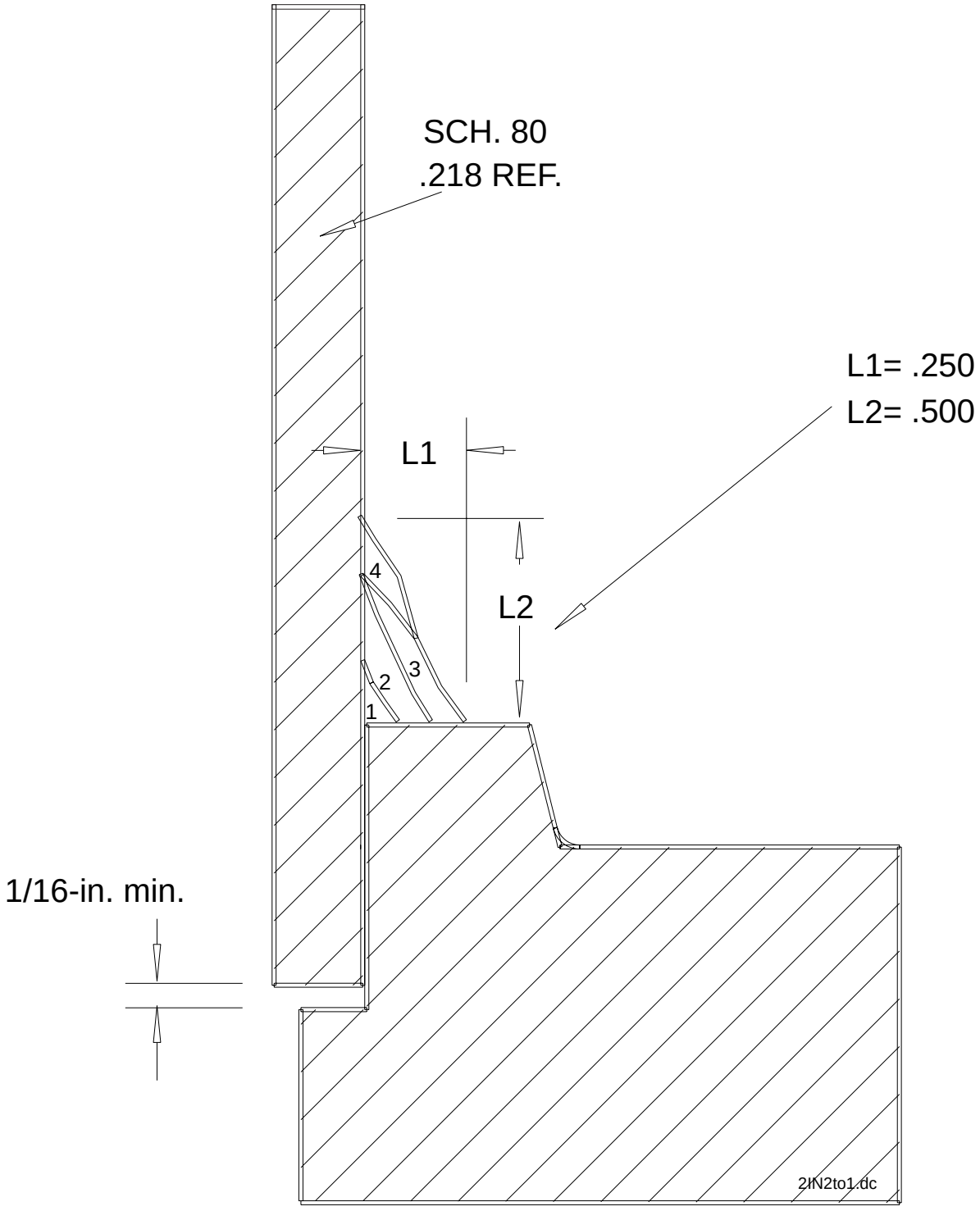
B.2 2x1 Modified Configuration

The 2x1 modified configuration consisted of a weld profile that exceeds the Code-required minimum. The 2x1 configuration consisted of a fillet weld with L2 = 2 × L1 where L1 is the weld leg length on the fitting. Similar to the standard 1x1 configuration, the weld leg on the fitting side was maintained at the minimum length (wall thickness x 1.09) allowed by the Code as shown in Figures B-2 and B-3. A slightly concave final weld bead geometry, with smooth transitions into the pipe and fitting, was specified for all the welds of this configuration. To maintain a minimum 1/16-inch (0.16 cm) axial gap after welding, the pipe sections were tacked to the fittings with a 1/8-inch (0.318 cm) standoff between the pipe and fitting. Lines were scribed on both the fitting and pipe side of the assembly to assist the welder in maintaining the correct leg length and to control the gap requirements.

The weld sequence differed between the 2-inch (5.08 cm) and 3/4-inch (1.91 cm) specimens due to the leg length requirements relative to wall thickness. The 2-in. (5.08 cm) specimen required a 0.5-inch (1.27 cm) leg length on the pipe side while the 3/4-in. (1.91 cm) specimen only required a 0.375-inch (0.953 cm) leg length on the pipe side. The 2-inch (5.08 cm) specimens used a series of weld beads with unequal leg lengths to extend the weld on the pipe side. A fourth bead was then applied with a 50% overlap on bead 3, which extended L2 to the required length as shown in Figure B-2. The 3/4-inch (1.91 cm) specimen used two equal leg welds followed by a third bead, which extended the weld geometry further up the wall of the pipe. A single cover pass was then applied across the existing weld beads to complete the weld sequence as shown in Figure B-3. Weld specifications for this configuration are listed in Table B-3.

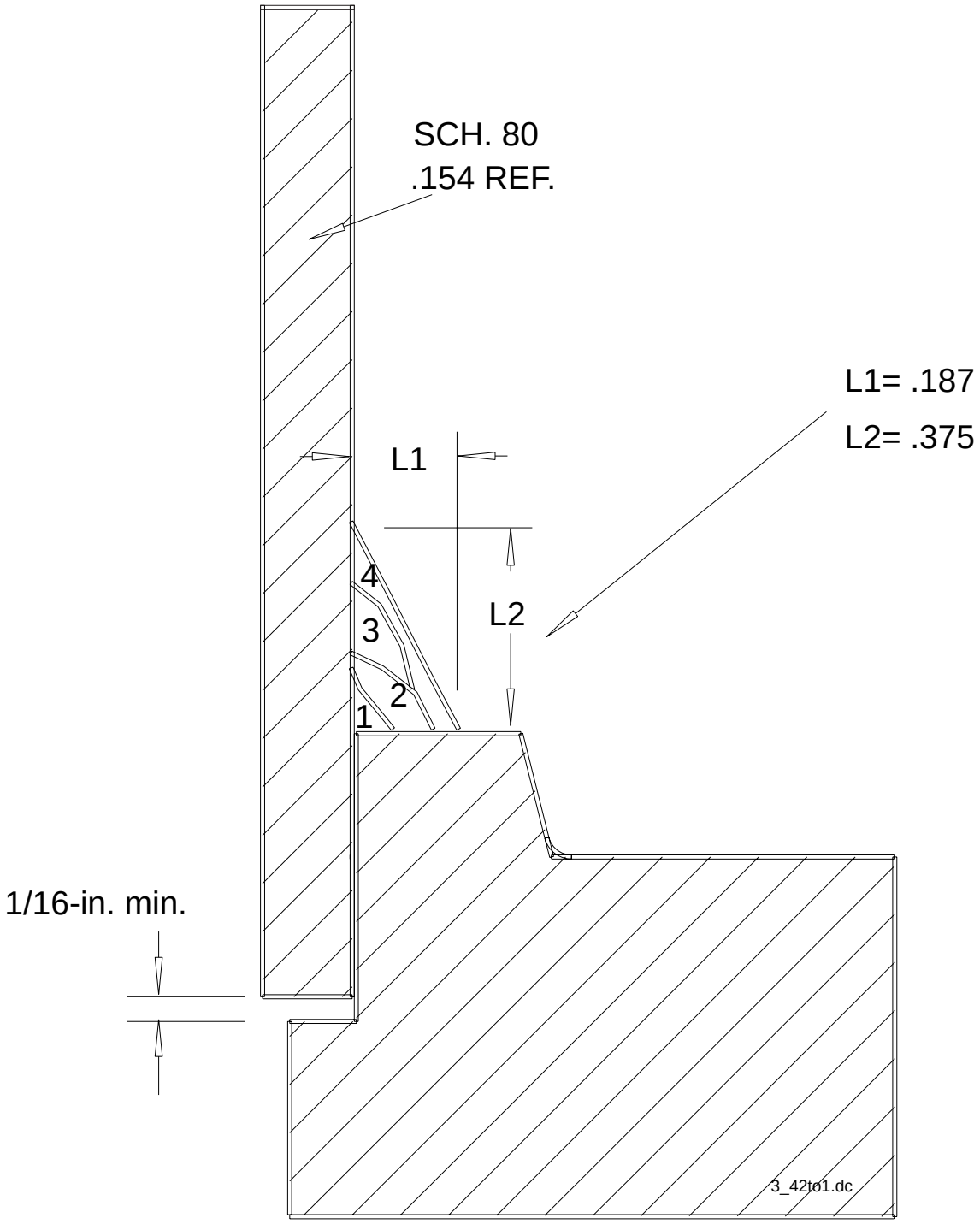
Table B-3
Weld Specifications for 2x1 Modified Configuration

Weld Geometry	2x1 weld. L2 = 2L1; L1 = 1.09 x wall thickness
Pipe Size	2-in. (5.08 cm) and 3/4-in. (1.91 cm) Schedule 80
Pipe Material	Carbon Steel and Type 304 Stainless Steel
Filler Metal	3/32-in. (0.238 cm) (root) and 1/8-in. (0.318 cm) ER308L Sandvik 3/32-in. (0.238 cm) (root) and 1/8-in. (0.318 cm) ER 70S-2 Lincoln
GTAW Sequence for 2-inch (5.08 cm) specimens	(Figure B-1) Four weld beads. Beads 1, 2, and 3 extend from the pipe to the fitting with unequal leg lengths (L2 > L1). Bead 4 extends from bead 3 to the desired 2 x L1.
GTAW Sequence for 3/4-inch (1.91 cm) specimens	(Figure B-2) Four weld beads. Bead 1 and 2 extend from the pipe to the fitting with equal leg lengths. Bead 3 extends from bead 2 up the wall of the pipe. Bead 4 covers the entire weld and extends L2.
Electrode Diameter	3/32-in. (0.238 cm) tungsten
Purge	ID argon purge during entire weld sequence
Technique	Walking the cup except for the root pass. Pipe rotating at constant speed.
Amperage (DCSP) and Voltage	125-135 amps and 19-20 volts for stainless steel 160- 170 amps and 21-22 volts for the carbon steel
Welding Power Supply	Hobart Cyber-TigII
Travel Speed	5–6 ipm (12.7–15.24 cm/minute) for root pass, 1.5–2 ipm (3.81–5.08 cm/minute) for cap passes.
Cup Size	#5 cup



NOTE: All dimensions are in inches. To convert inches to centimeters, multiply the unit by 2.54.

Figure B-2
Drawing of Modified Weld Sequence for Vibration Fatigue Test Matrix with Fillet Weld Leg L2 > L1 for 2-Inch (5.08 cm) Specimen



NOTE: All dimensions are in inches. To convert inches to centimeters, multiply the unit by 2.54.

Figure B-3
Drawing of Modified Weld Sequence with Unequal Fillet Weld Leg Length (L2 = 2 x L1) for 3/4-Inch (1.91 cm) Test Specimen

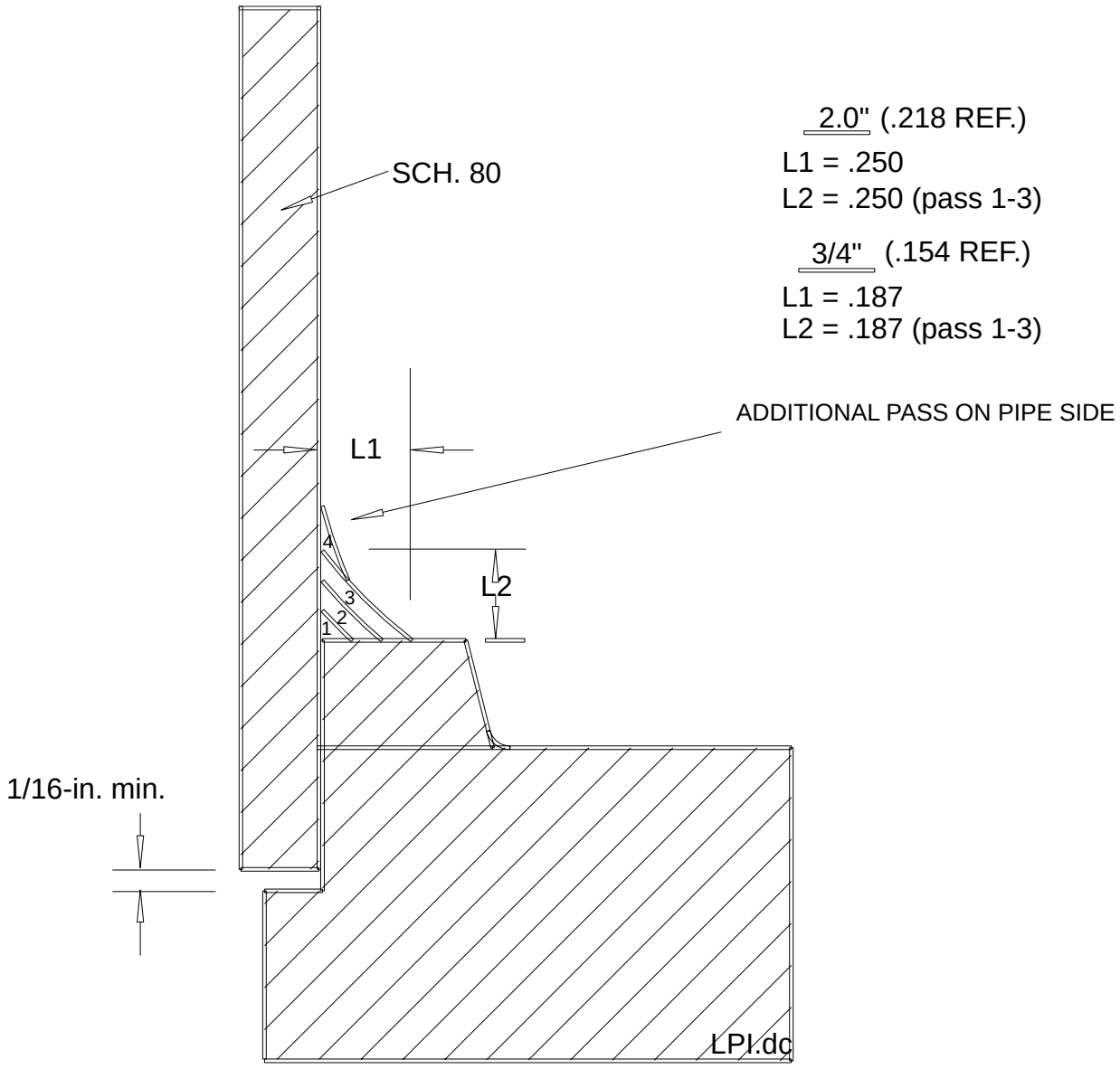
B.3 Last Pass Improved (LPI)

The LPI weld configuration consisted of a standard 1x1 configuration with an additional weld pass on the pipe side, as shown in Figure B-4. The weld sequence consisted of three beads to produce equal leg lengths. The additional pass on the pipe side produced a weld geometry with a leg length of less than 2 x L1 but greater than L1. A slightly concave final weld bead geometry, with smooth transitions into the pipe and fitting, was specified for all of the welds of this configuration. The weld was positioned precisely at the toe of the last weld and applied with a minimal oscillation of the weld torch to create a smooth transition into the pipe. The overall weld geometry was approximately 1.5 x L1 = L2.

The pipe sections were tacked to the fittings with a 1/8-in. (0.318 cm) standoff between the pipe and fitting to maintain a minimum 1/16-in. (0.16 cm) axial gap after welding. Lines were scribed on both the fitting and pipe side of the assembly to assist the welder in maintaining the correct leg length and to control the gap. Weld specifications for this configuration are listed in Table B-4.

Table B-4
Weld Specifications for LPI Configuration

Weld Geometry	Last pass improved 1 x 1 weld (1.09 x wall thickness) plus additional pass on the pipe side
Pipe Size	2-inch (5.08 cm) and 3/4-inch (1.91 cm) Schedule 80
Pipe Material	Type 304 Stainless Steel
Filler Metal	3/32-in. (0.238 cm) (root) and 1/8-in. (0.318 cm) ER308L Sandvik
GTAW Sequence	(Figure B-4) Four weld beads. Beads 1-3 are identical to the standard 1x1 weld geometry. Bead 4 is applied at the toe of bead 3 and the pipe to maintain a smooth transition. The overall geometry is approximately L2 = 1.5 x L1.
Electrode Diameter	3/32-in. (0.238 cm) tungsten
Purge	ID argon purge during entire weld sequence
Technique	Walking the cup except for the root pass. Pipe rotating at constant speed.
Amperage (DCSP) and Voltage	125-135 amps and 19-20 volts
Welding Power Supply	Hobart Cyber-TigII
Travel Speed	5–6 ipm (12.7–15.24 cm/minute) for root pass, 1.5–2 ipm (3.81–5.08 cm/minute) for cap passes.
Cup Size	#5 cup



NOTE: All dimensions are in inches. To convert inches to centimeters, multiply the unit by 2.54.

Figure B-4
Drawing of Modified Weld Sequence with Last-Pass-Improved Weld Pass on the Pipe Side (L2 > L1)

B.4 Post-Weld Heat Treat (PWHT)

Several standard 1 x 1 test specimens (Figure B-1) were post-weld heat treated (PWHT). All PWHT test specimens were welded with the standard minimum gap requirement of 1/16-inch (0.16 cm) after welding. The PWHT was performed prior to the final machining of the socket weld flange to assure flatness on the test stand. The specifications of the PWHT were as follows:

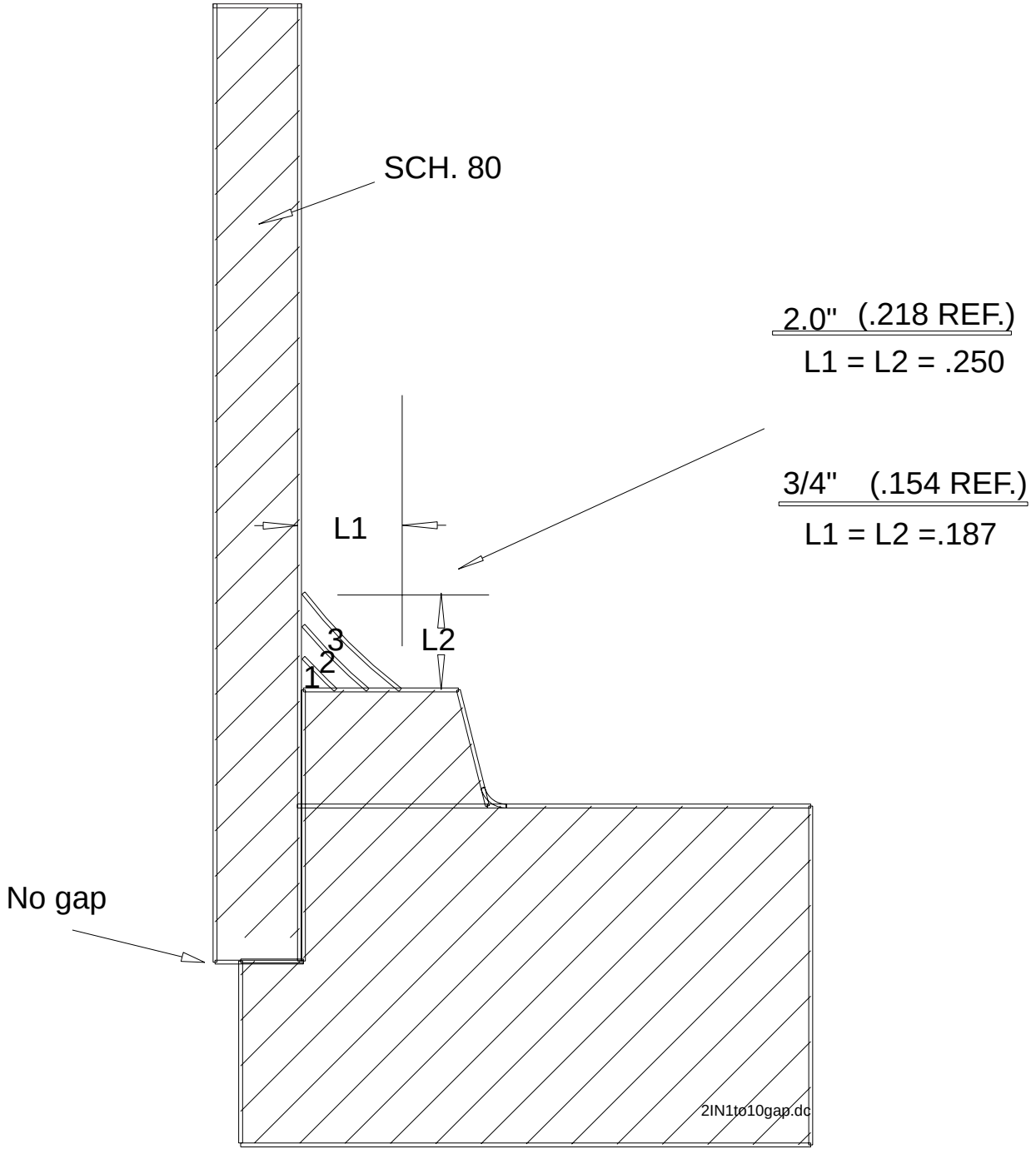
- 1150°F (621°C) for one hour for the 3/4-in. (1.91 cm) stainless steel specimen
- 1650°F (899°C) for one hour for the 2-in. (5.08 cm) stainless steel specimens
- 1150°F–1200°F (621°C–649°C) for one hour for the 2-in. (5.08 cm) carbon steel specimen

The weld specifications for the PWHT specimens were the same as the standard 1x1 configuration listed in Table B-2. The temperature of the PWHT was altered to 1650°F (899°C) for the stainless steel specimens after the 3/4-in. (1.91 cm) stainless steel specimen was tested and showed no improvement over the non-PWHT specimen.

B.5 No Axial Gap Configuration

Another variation of the standard configuration consisted of specimens with no axial gap before welding as shown in Figure B-5. Test specimens with no axial gap were fabricated according to the same welding specifications used with the standard 1x1 specimens.

The specimens were fabricated such that the pipe and fitting made solid contact before the welding process. Lines were scribed on both the fitting and pipe side of the assembly, according to the desired standoff and required leg lengths, to assist the welder in maintaining the required weld geometry. Weld specifications for the no-gap specimens were the same as the standard 1x1 configuration listed in Table B-2.



NOTE: All dimensions are in inches. To convert inches to centimeters, multiply the unit by 2.54.

Figure B-5
Drawing of Standard Weld Sequence with Equal Leg Lengths (L2 = L1)

B.6 Welds with Toe Discontinuity

A number of test specimens in Phase II were produced with specific design criteria for the toe discontinuities on the pipe side to define acceptance standards for toe discontinuities. The test specimens consisted of standard 1x1 configuration and were welded with the standard minimum gap requirement of 1/16-inch (0.16 cm) after welding.

The intention of these test specimens was to insert toe discontinuities that were representative of typical flaws found in welds but are considered acceptable by industry code and workmanship standards. Two specimens were welded with intentional irregularities in the solidification pattern at the toe. This was accomplished by controlling the oscillation of the weld torch on the third pass in a manner that did not allow the weld to tie in consistently at the toe. This produced a scalloped toe and a slight undercut. The weld quality was considered acceptable and the leg lengths remained consistent with the 1x1 specifications.

Two additional samples were welded identically to the standard 1x1 configuration, followed by blend grinding or polishing the toe on the pipe side. A pneumatic polisher with 80-grit sandpaper was used to blend the weld with the pipe. The specimens were polished until the ripples in the solidification pattern of the weld were entirely removed. The weld leg lengths remained consistent with the 1x1 specifications after polishing. Weld specifications for the modified toe configurations are the same as the standard 1x1 configuration listed in Table B-2.

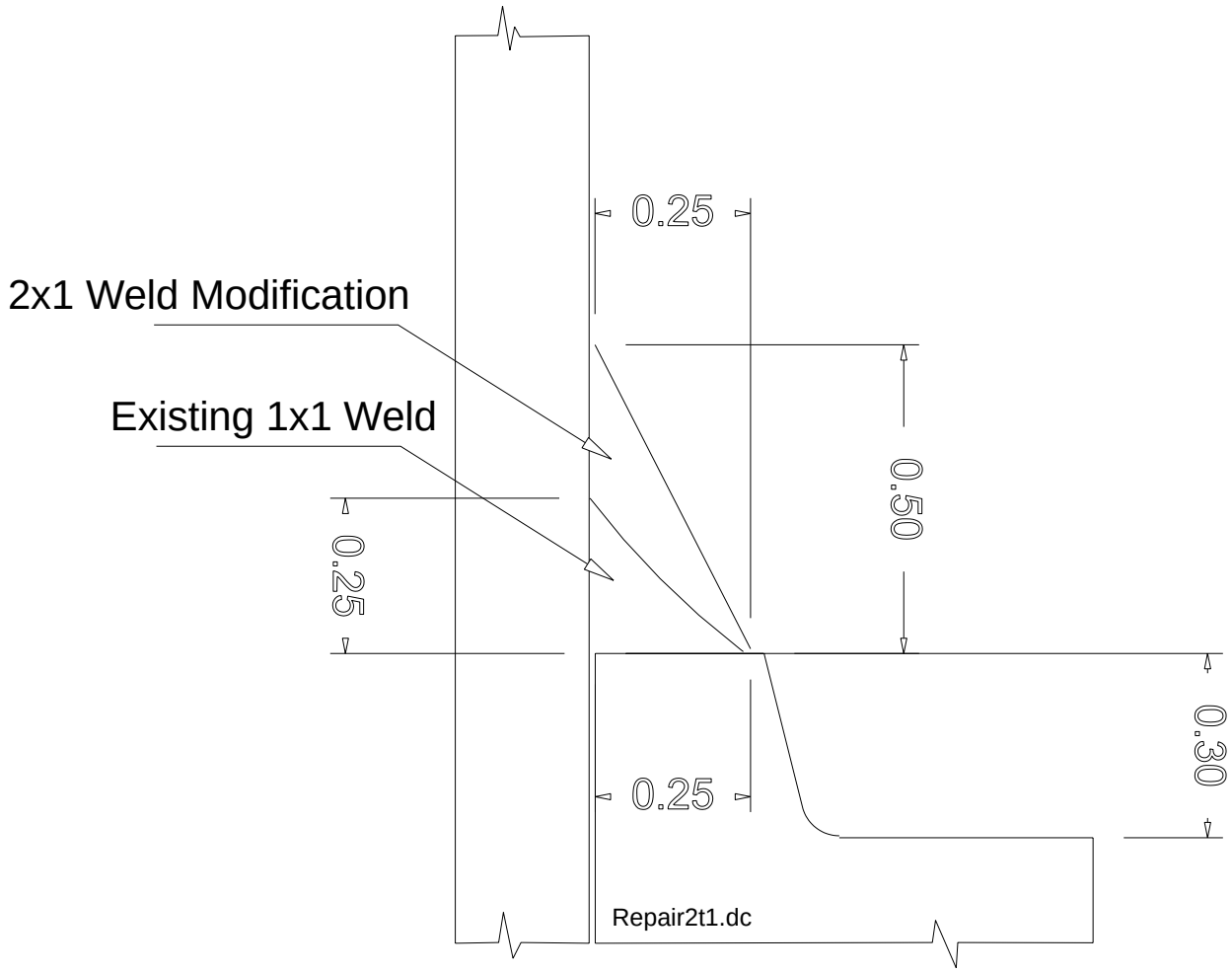
B.7 1x1 to 2x1 Modified Configuration

Phase I test results demonstrated that a weld geometry with a modified 2x1 configuration offered significantly higher resistance to high cycle fatigue. To confirm these results, standard 1x1 configurations from Phase I that did not fail in the allotted test cycle were modified to the 2x1 configuration as shown in Figure B-6. Two carbon steel and two stainless steel standard 1x1 configurations were used from Phase I, as shown in Table B-1. One specimen of each material was originally post-weld heat treated under the Phase I testing specification (Section B.4).

Mockups were used to establish a weld sequence that would result in modifying a 1x1 configuration to a 2x1 configuration. The weld tests concluded that three additional weld beads over the existing weld would provide the appropriate geometry as shown in Figure B-7. The bead sequence started on the pipe side and worked toward the fitting to completely overlay the existing weld. The first bead was applied to the existing 1x1 configuration and extended the weld to the rquired length on the pipe side as shown in Figure B-7. The second and third beads were applied primarily to blend the weld geometry into the fitting, maintaining a slightly concave geometry. Weld specifications for this configuration are listed in Table B-5.

Table B-5
Weld Specifications for 1x1 to 2x1 Modified Configuration

Weld Geometry	2x1 weld configuration. L2 = 2L1; L1 = 1.09 x wall thickness. (Figure B-7)
Pipe Size	2-inch (5.08 cm) Schedule 80
Pipe Material	Carbon Steel and Type 304 Stainless Steel
Filler Metal	3/32-in. (0.238 cm) (bead 3) and 1/8-in. (0.318 cm) (bead 1 & 2) ER308L Sandvik. 3/32-in. (0.238 cm) (bead 3) and 1/8-in. (0.318 cm) (bead 1 & 2) ER 70S-2 Lincoln.
GTAW Sequence for 2-inch (5.08 cm) specimens	(Figure B-7) Four weld beads. Bead 1 extends L2 to the full length of 2 x L1. Bead 2 was used to blend bead 1 with the existing 1x1 weld. Bead 3 was used to blend bead 2 to the toe of the existing 1x1 weld on the fitting side. A smaller diameter filler rod 3/32-in. (0.238 cm) was used for bead 3.
Electrode Diameter	3/32-in. (0.238 cm) tungsten
Purge	ID argon purge during entire weld sequence
Technique	Walking the cup. Pipe rotating at constant speed.
Amperage (DCSP) and Voltage	125-135 amps and 19-20 volts for stainless steel 160- 170 amps and 21-22 volts for the carbon steel
Welding Power Supply	Hobart Cyber-TigII
Travel Speed	1.5 –2 ipm (3.81–5.08 cm/minute) for cap passes.
Cup Size	#5 cup



NOTE: All dimensions are in inches. To convert inches to centimeters, multiply the unit by 2.54.

Figure B-6
Drawing of Modified Weld Geometry from the Standard L1 = L2 to L2 = 2L1

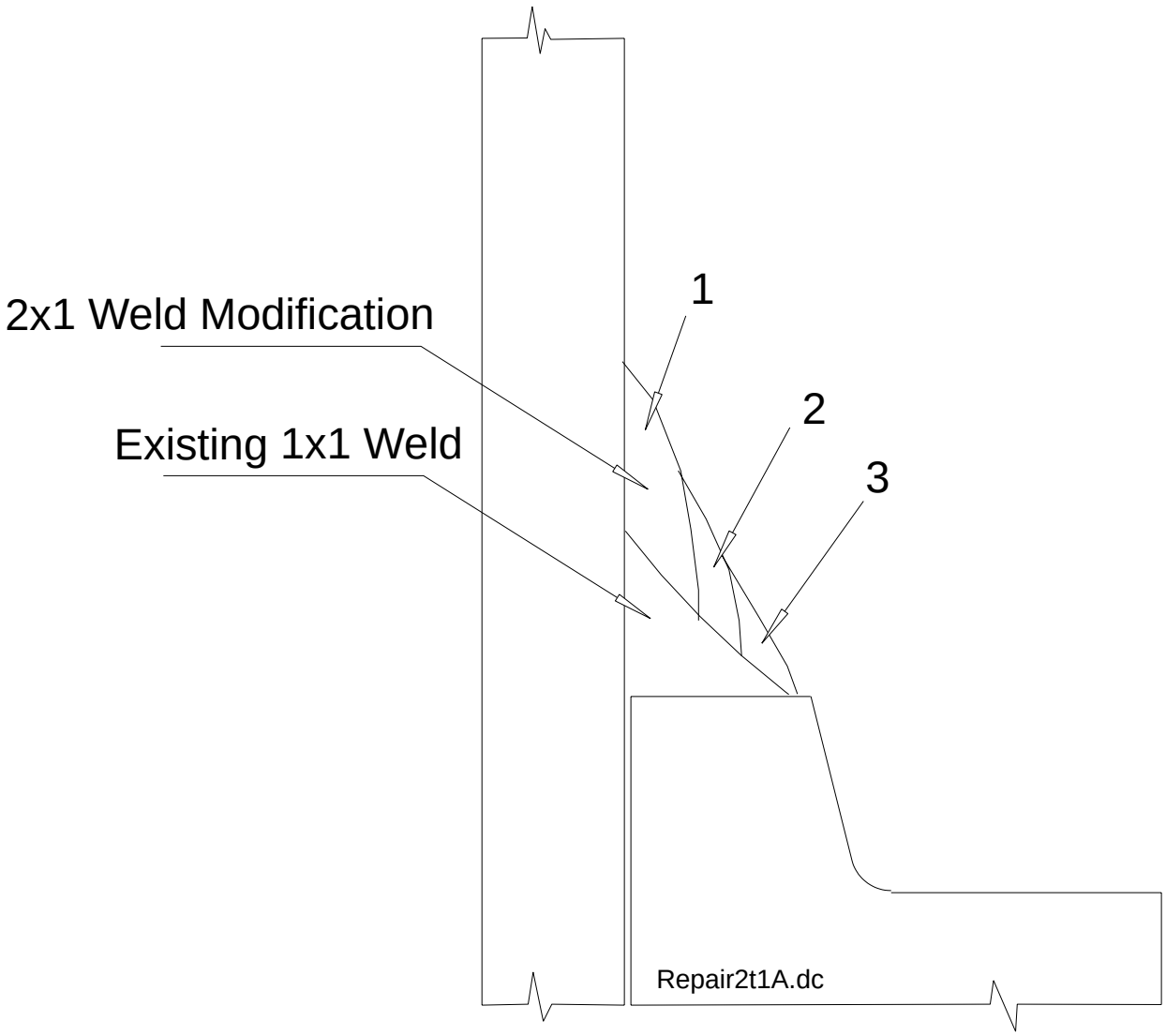


Figure B-7
Weld Sequence for 1x1 to 2x1 Modified Configuration

B.8 Overlay Repair Weld Configuration

A number of specimens in Phase I resulted in through wall cracks initiating at either the toe or the root of the weld. The failed specimen included standard 1x1 and LPI configurations discussed in Sections B.1 and B.3. The overlay repair process consisted of two specific repair steps. The first step was primarily used to seal the crack and stop the flow of water. This step included a peening and seal welding process that allowed a sound weld to be applied over the crack location. All welding was done over the crack with no attempt to remove the crack prior to welding. The second step was a complete overlay of the existing cracked weld to replace the structural properties of the existing socket weld. The overlay weld was applied around the entire circumference of the pipe and fitting.

The geometry of the overlay was designed by drawing a circle with a radius exceeding the minimum leg length of 1.09 times wall thickness at both toes of the original weld. The geometry of the weld overlay was developed by connecting the two circles and extending the overlay from the fitting to the pipe, as seen in Figure B-8. The geometry assured the weld thickness was equal to or greater than the original leg lengths in all directions of either potential crack location. This allowed the geometry of the overlay to remain constant for both failure modes (toe or root). Unlike the previous test specimens, all seal welding and overlay repair welds used the shielded metal arc welding (SMAW) process.

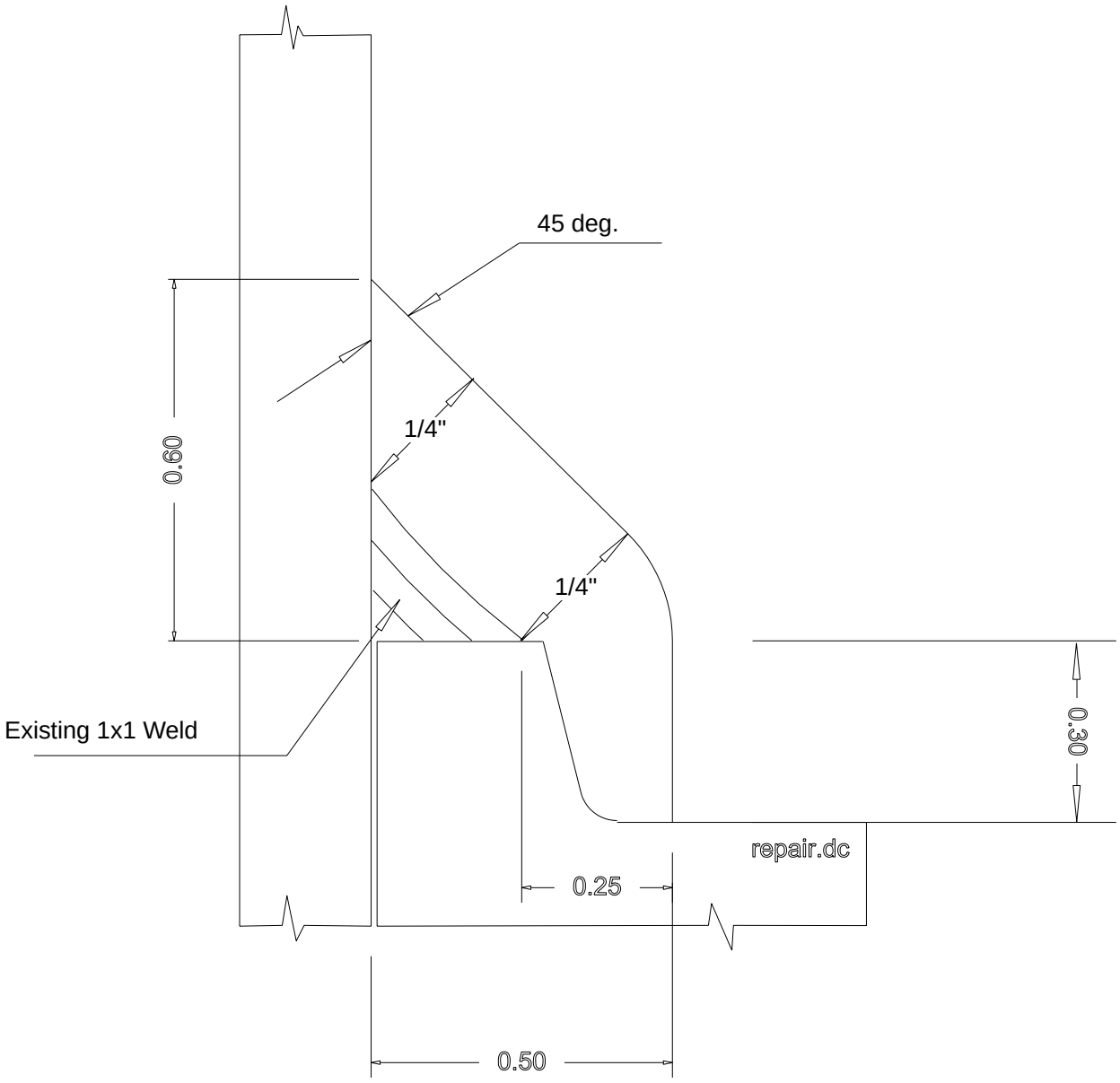
Prior to repairing the test specimens from Phase I, mockups were used to establish welding and peening guidelines for the seal welding process. As seen in Figures B-9, B-11, B-13, and B-16, the weld sequence for sealing the crack was not predictable and resulted in various weld sequences and bead placements to seal the crack. The basic seal welding process was as follows:

- Each specimen was examined by dye penetrant (PT) to identify the ends of the crack. The crack location and length were recorded and photographed.
- The specimens were pressurized to 300 psi–400 psi (2069 kPa–2758 kPa) with water prior to peening.
- Closure of the crack was initiated using a pneumatic peening hammer with a blunt-ended tip [radius of app. 3/8-in. (0.953 cm)]. Peening continued until the water flow was completely stopped. Peening was either directly over the crack or approximately 1/8-in (0.318 cm) removed from the crack with the tip directed toward the crack, depending on the severity of the crack.
- Seal welds were applied directly over the crack location (in the direction of the crack length) using the welding specifications stated in Table B-6. Welding was terminated if a leak reinitiated during the welding process. The seal welding technique utilized a small diameter electrode that maintained a stable arc at low amperage settings with very little penetration.
- Subsequent peening was continued after each seal weld until the water flow completely subsided. The weld metal was removed by grinding if porosity resulted or if pinhole leaking persisted.
- The seal welds were typically capped with additional weld beads to ensure moisture was completely eliminated and that sufficient material was available to allow standard welding procedures to be used for applying the engineered overlay. The starts and stops of the seal welds were often ground prior to initiating the overlay weld buildup.
- Before the overlay was applied with the SMAW process, the flange was secured or restrained to minimize distortion and the overlay was laid out by scribe lines on the specimen. Water remained in the pipe during the overlay procedure and an interpass temperature of 350°F (177°C) was maintained.

Mockups were used to establish a basic welding sequence and welding parameters for applying the weld overlay per the specifications in Figure B-8. Scribe lines and gages were fabricated to assist the welders in maintaining the specified geometry of the overlay. The gages allowed the welder to measure the buildup of the weld to assure minimum thickness was achieved. Inevitably, each overlay was slightly different due to the seal weld geometry and welder consistency. Figures B-10, B-12, B-14, and B-16 illustrate the bead sequence applied to each test specimen. Weld specifications for the overlay configuration are listed in Table B-6.

Table B-6
Weld Specifications for Overlay and Seal Weld Repair Configuration

Weld Geometry	1x1 and LPI weld configuration. L2=L1=L1=1.09 x wall thickness. Figures B-1 and B-4.
Pipe Size	2-inch (5.08 cm) Schedule 80
Pipe Material	Carbon Steel and Type 304 Stainless Steel
Filler Metal	.069-inch (1.75-mm) x 11.81-inch (300-mm) Lincoln Omnia E6013 3/32-in. (0.238 cm) ESAB E7018 3/32-in. (0.238 cm) ESAB ARCALOY 308L-17
SMAW Sequence for Seal and Overlay Weld Specimens	B4-2CS-6 (B3-1): Six stringer beads for seal weld of root crack. Beads 1 and 2 were followed by additional peening. Bead 3 completely sealed the crack. Beads 4 through 6 were reinforcement of seal weld, Figure B-9. Eighteen beads for overlay as seen in Figure B-10 with a slight weave pattern. B4-2CS-7 (B3-2): Seven stringer beads for seal weld of root crack [length approximately 1 5/8-in. (4.13 cm)]. Beads 1 through 3 were followed by additional peening. Bead 4 completely sealed the crack. Beads 5 through 7 were reinforcement of seal weld, Figure B-11. Eighteen beads for overlay as seen in Figure B-12 with a slight weave pattern. B4-2SS-9 (B2-2): Six stringer beads for seal weld of root crack (length approximately 2-inch (5.08 cm)]. Beads 1 and 2 were followed by additional peening. Bead 3 completely sealed the crack. Beads 4 through 6 were reinforcement of seal weld, Figure B-13. Eighteen beads for overlay as seen in Figure B-14 with a slight weave pattern. B4-2SS-8 (B2-8): Six stringer beads for seal weld of toe crack [length approximately 1 3/4-in. (4.45 cm)]. Beads 1 and 4 were followed by additional peening. Bead 5 completely sealed the crack. Bead 6 was reinforcement of the seal weld, Figure B-15. Fifteen beads for overlay as seen in Figure B-16 with a slight weave pattern.
Technique	Pipe stationary, slight weave on overlay, stringer beads on seal weld.
Amperage and Voltage	E6013 - DCSP @ 51 amps and 28 volts E7018 - DCRP @ 88 amps and 21 volts ER308L – DCRP @ 60–61 amps and 23-25 volts for seal weld and 73 amps and 24-25 volts for overlay.
Welding Power Supply	Miller Aerowave
Travel Speed	Manual



NOTE: All dimensions are in inches. To convert inches to centimeters, multiply the unit by 2.54.

Figure B-8
Geometry for Repair Overlay Sequence for Standard 1x1 Weld

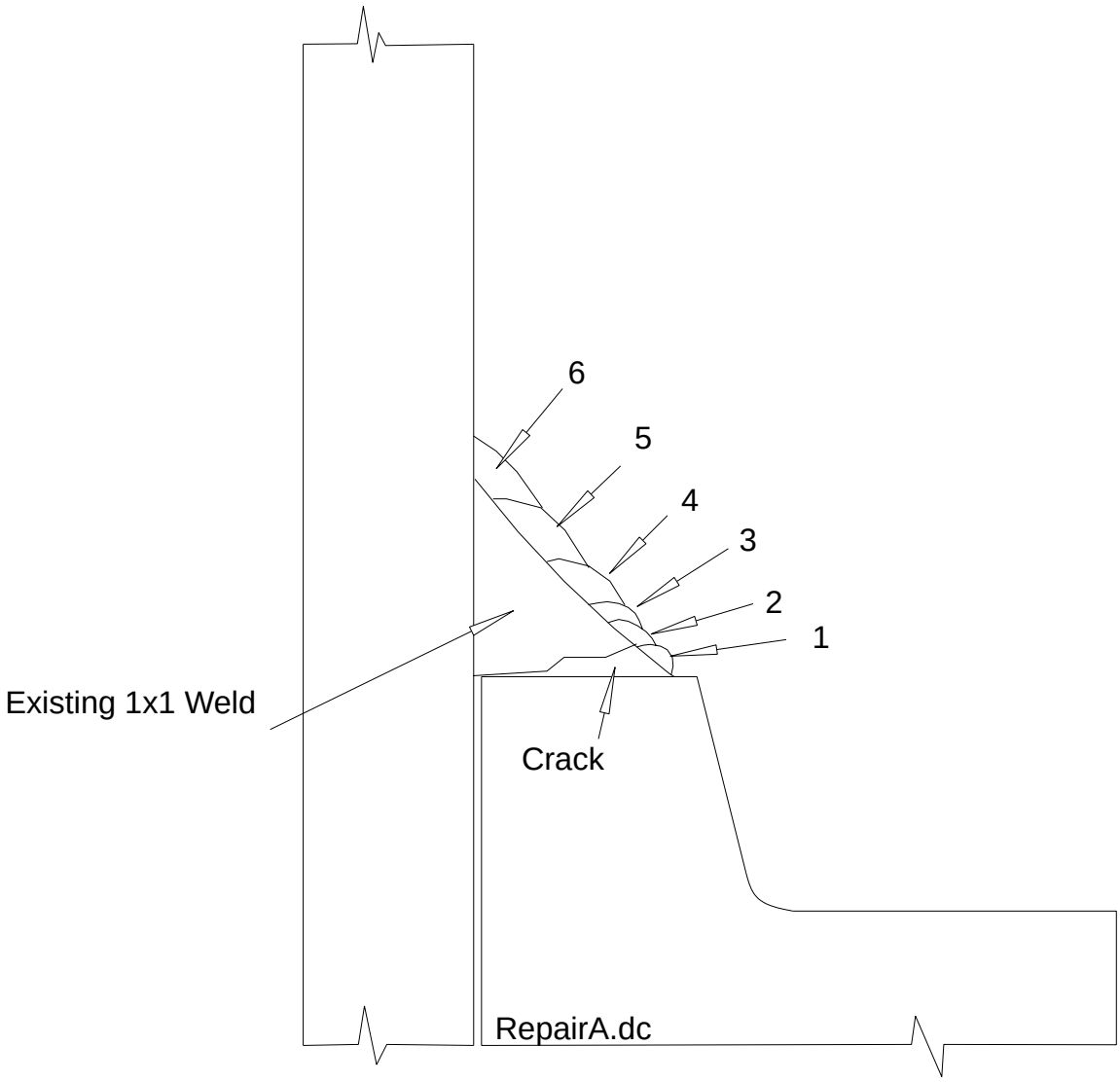


Figure B-9
Seal Welds for Cracked Specimen B3-2CS-1 (B4-2CS-6)

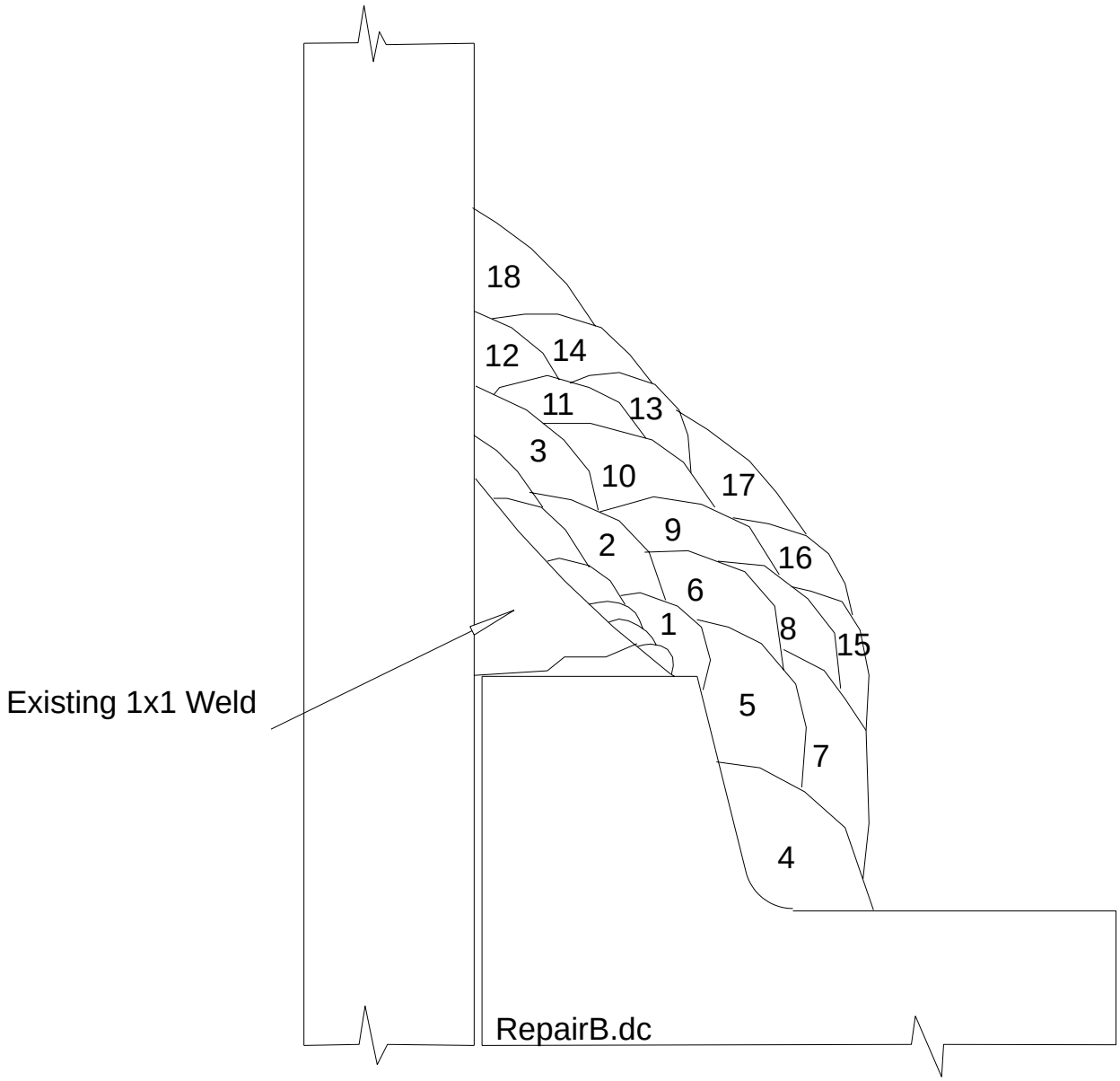


Figure B-10
Overlay Sequence for Cracked Specimen B3-2CS-1 (B4-2CS-6)

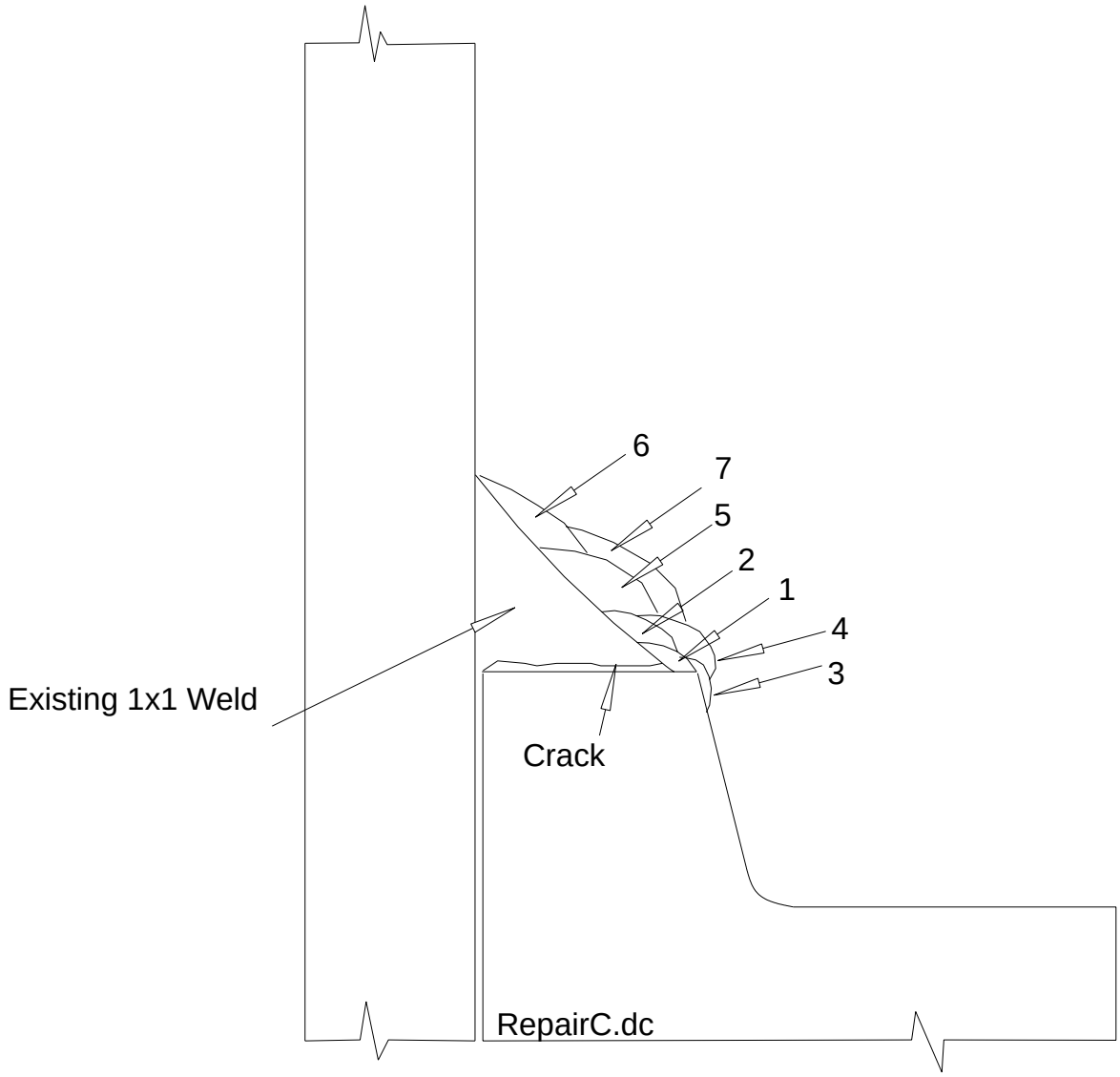


Figure B-11
Seal Welds for Cracked Specimen B3-2CS-2 (B4-2CS-7)

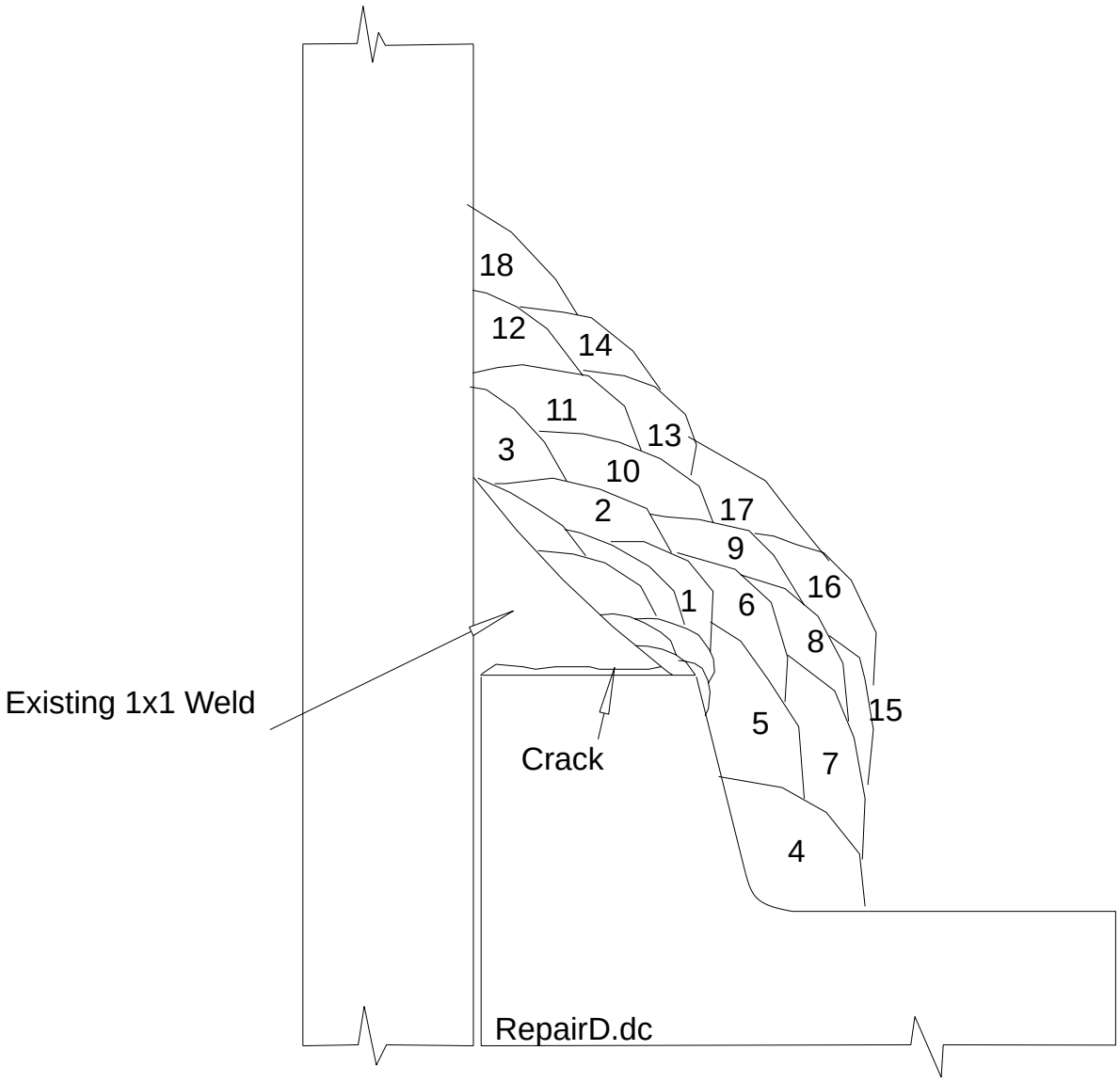


Figure B-12
Overlay Sequence for Cracked Specimen B3-2CS-2 (B4-2CS-7)

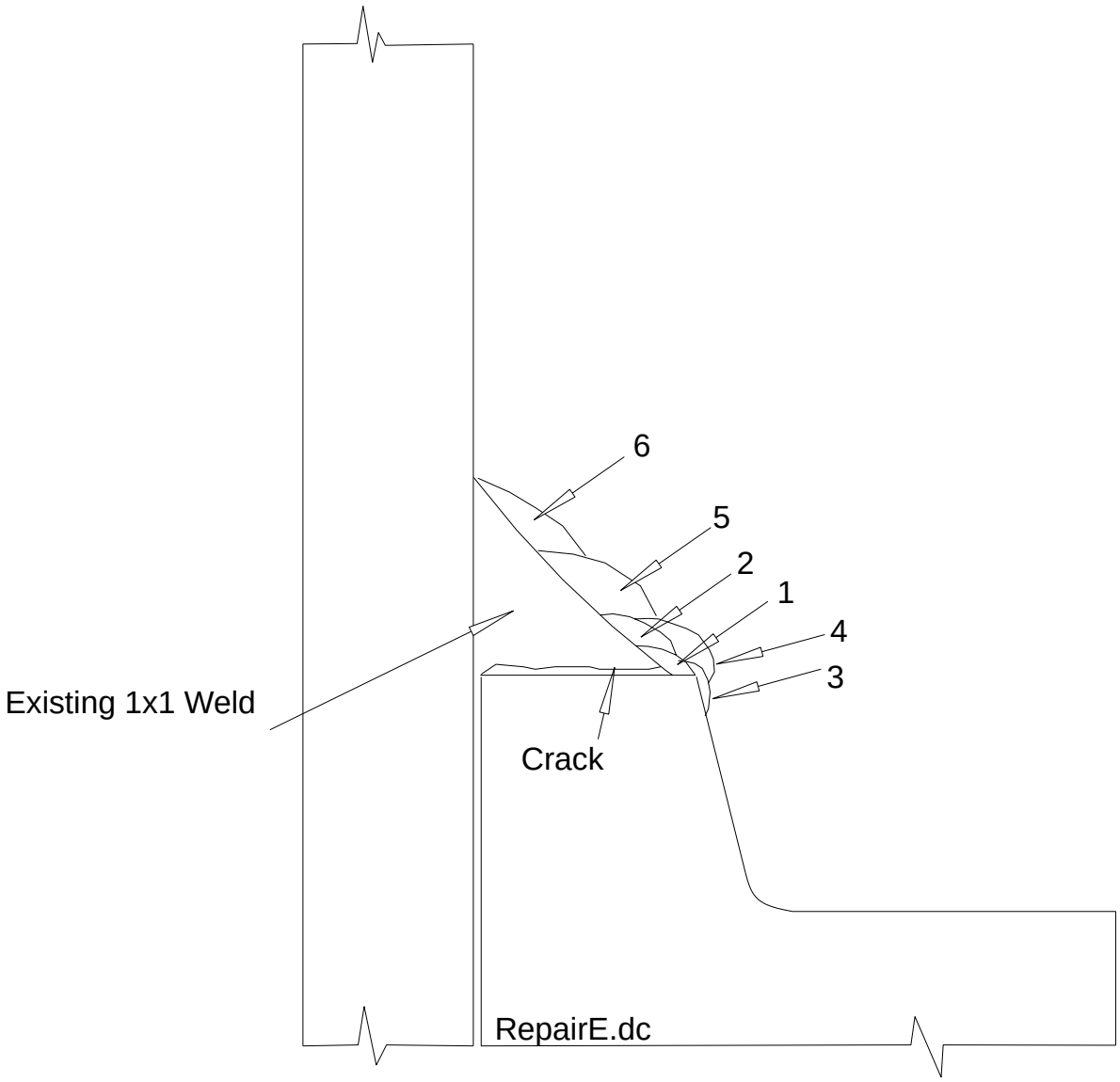


Figure B-13
Seal Welds for Cracked Specimen B2-2SS-2 (B4-2SS-9)

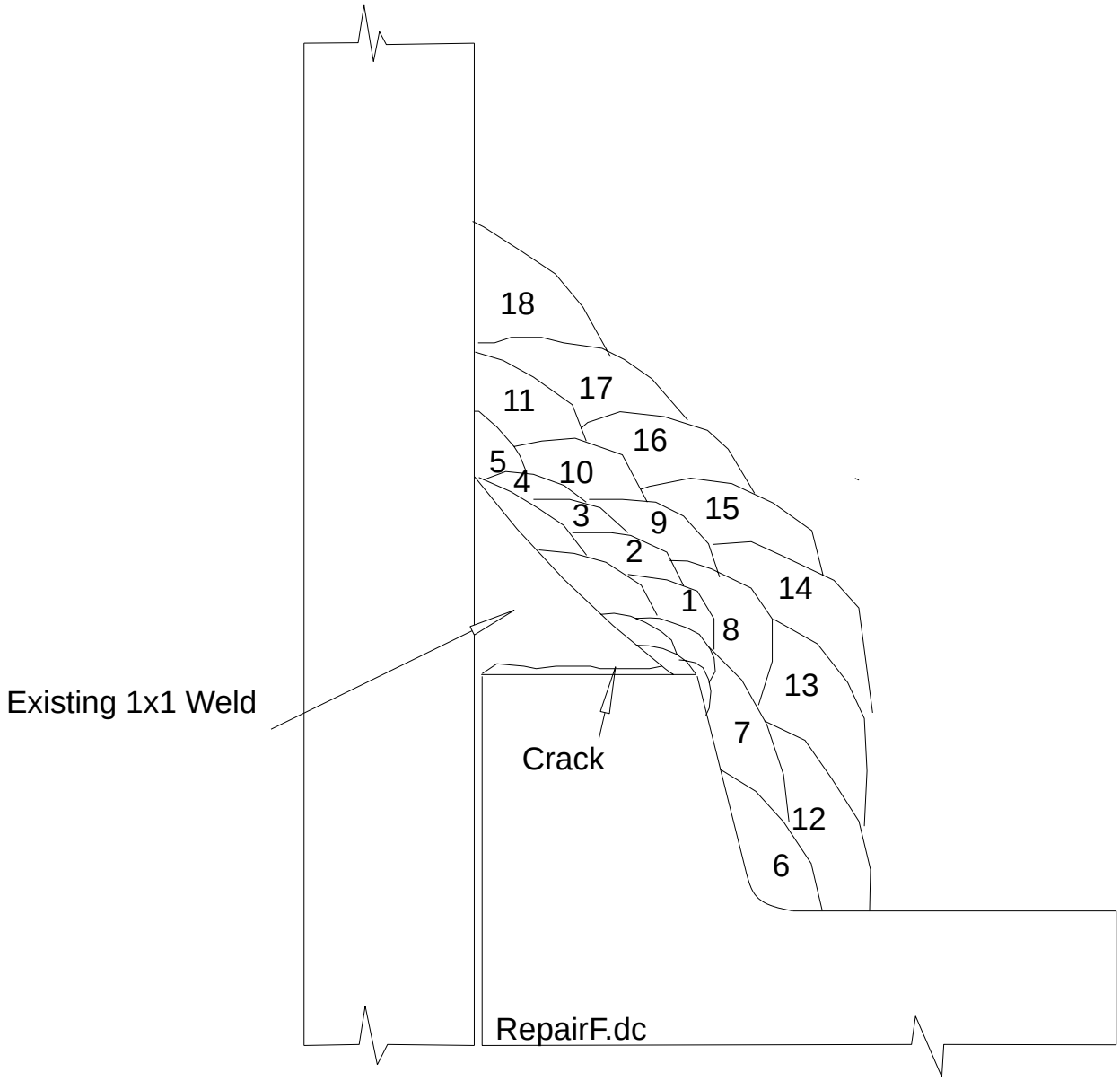


Figure B-14
Overlay Sequence for Cracked Specimen B2-2SS-2 (B4-2SS-9)

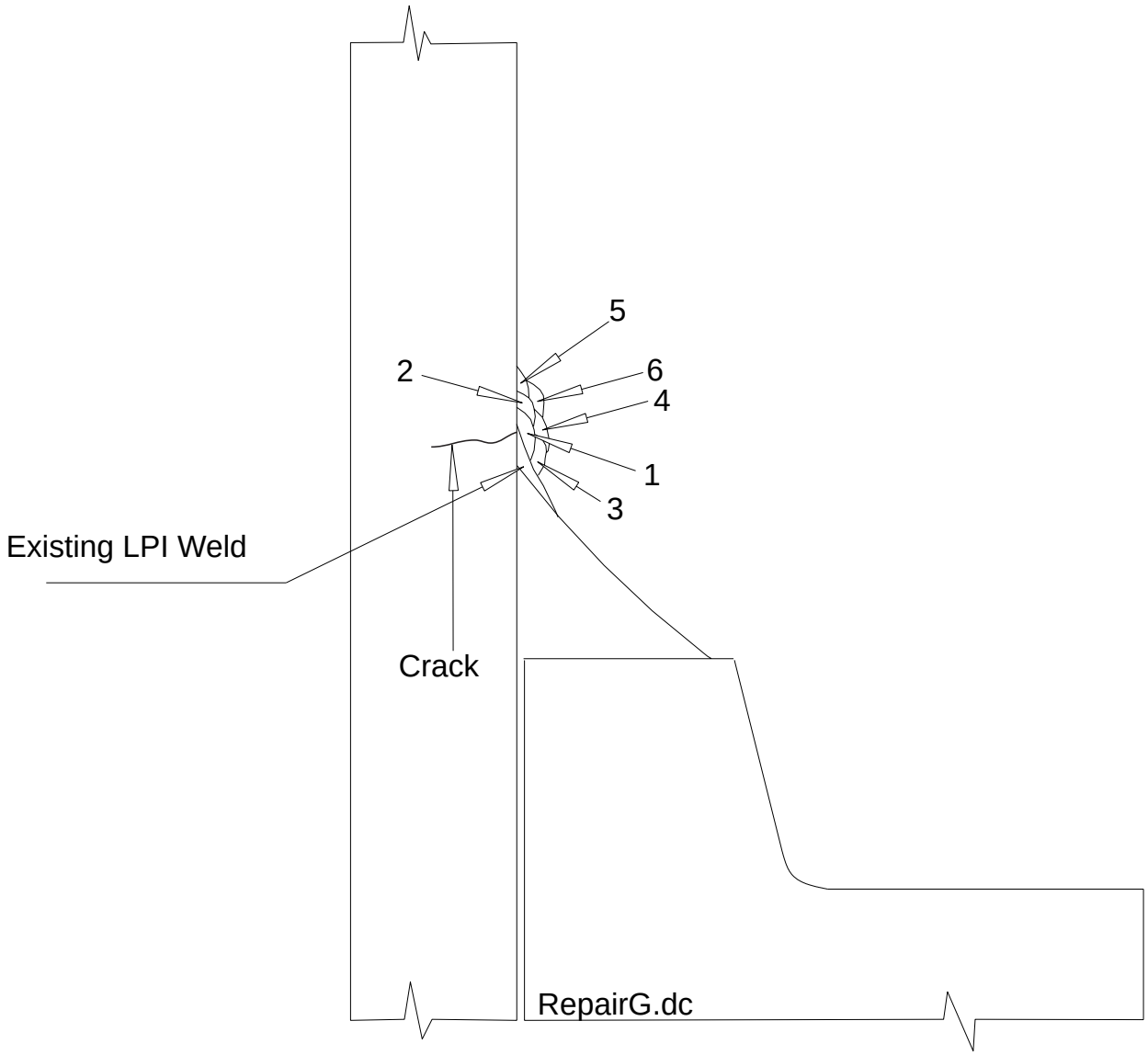


Figure B-15
Seal Welds for Cracked Specimen B2-2SS-8 (B4-2SS-8)

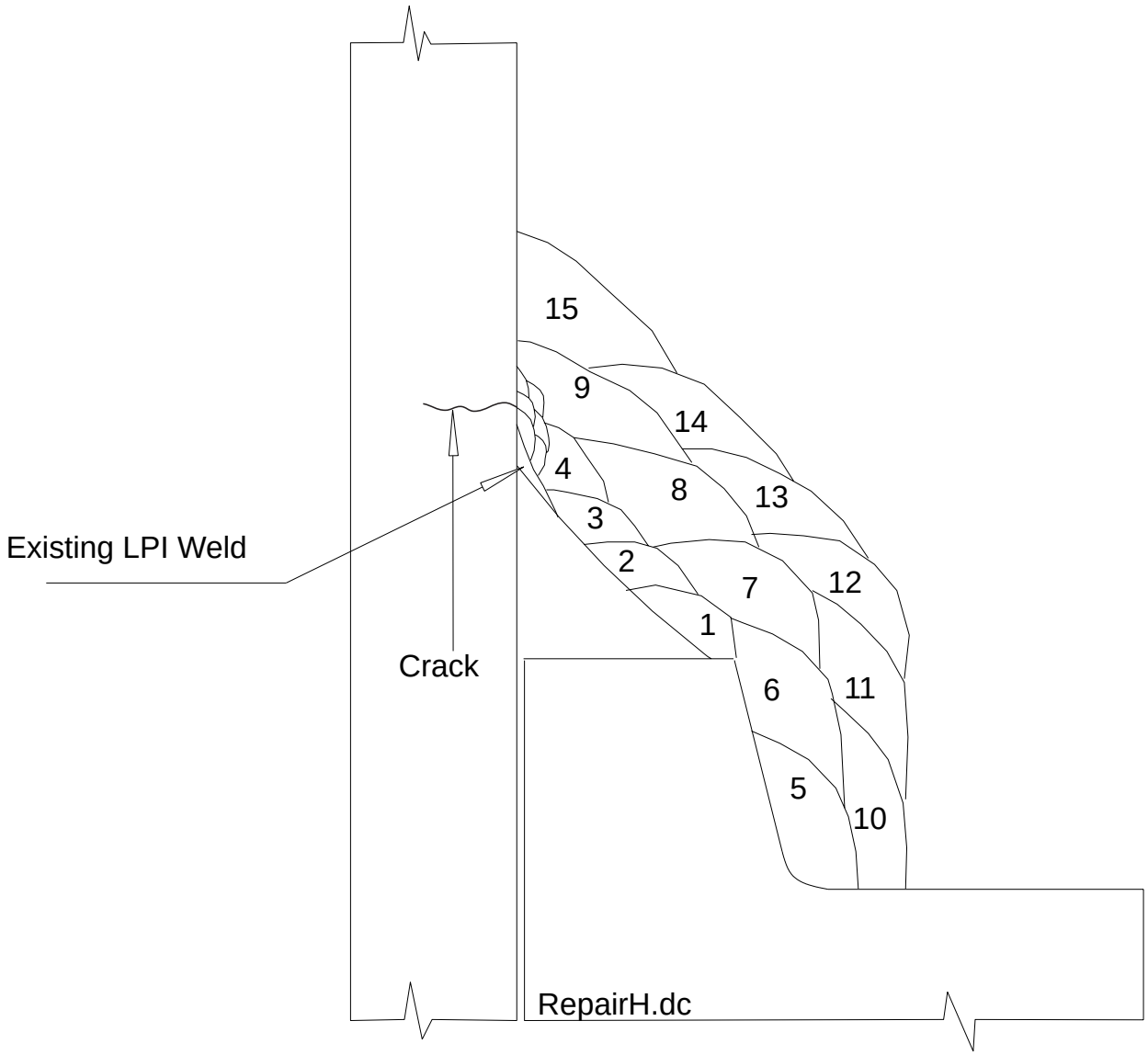


Figure B-16
Overlay Sequence for Cracked Specimen B2-2SS-8 (B4-2SS-8)

B.9 Standard Butt Weld Configuration

Test assemblies were fabricated and tested under similar conditions as the socket-welded joint configurations to allow a direct comparison of conventional small bore butt welds to the new 2x1 configurations and remediated socket-welded specimens. The overall length of the specimens was increased to allow the length-to-mass ratio of the weld to remain constant for all test assemblies, as shown in Figure B-17.

The standard butt weld configuration is a typical weld profile consisting of three weld beads (root pass and two cover passes), as shown in Figure B-18. The joint configuration consists of a v-groove configuration with 0.060-in. (0.152 cm) land and a 37.5-degree bevel. The weld neck flange and pipe are tacked together with a 1/32-in. (0.08 cm) gap and with the pipe section held perpendicular to the face of the flange. A slightly convex final weld bead geometry, with smooth transitions into the pipe and fitting, was specified for all of the welds with this configuration. Mock-ups were fabricated to establish welding parameters and assure consistency of all of the butt weld specimens. The weld specifications for the butt weld configurations are listed in Table B-7.

Table B-7
Weld Specifications for Standard Butt Weld Configurations

Weld Geometry	Standard Butt Weld Configuration
Pipe Size	2-inch (5.08 cm) Schedule 80
Pipe Material	Carbon Steel and Type 304 Stainless Steel
Filler Metal	3/32-in. (0.238 cm) (root) and 1/8-in. (0.318 cm) ER308L Sandvik 3/32-in. (0.238 cm) (root) and 1/8-in. (0.318 cm) ER 70S-2 Lincoln
GTAW Sequence	Figure B-18. Three beads. Each bead extends from the pipe to the fitting.
	3/32-in. (0.238 cm) tungsten
Electrode Diameter	ID argon purge during entire weld sequence
	Walking the cup except for the root pass. Pipe rotating at constant speed.
Technique	125-135 amps and 19-20 volts for the stainless steel 160-170 amps and 21-22 volts for the carbon steel
Amperage	Hobart Cyber-TigII
Travel Speed	5–6 ipm (12.7–15.24 cm/minute) for root pass, 1.5–2 ipm (3.81–5.08 cm/minute) for cap passes
Cup Size	#5 cup

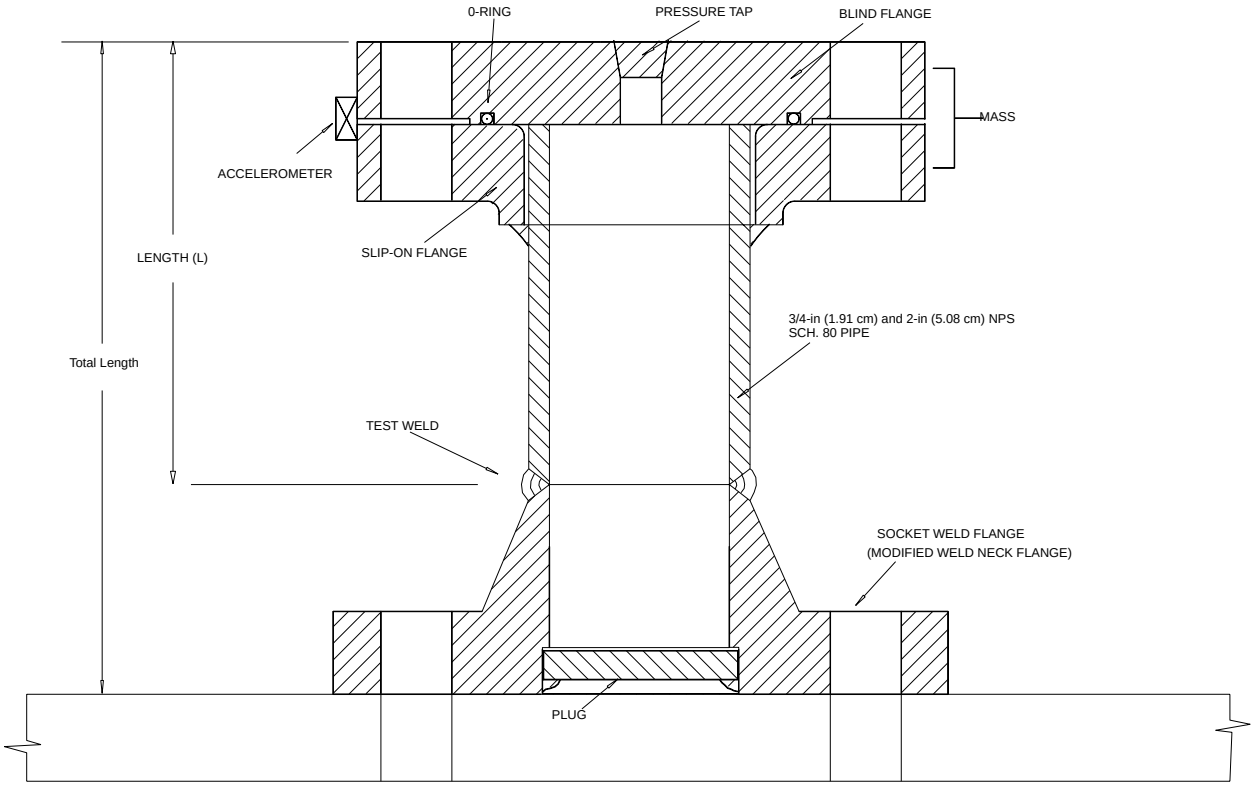
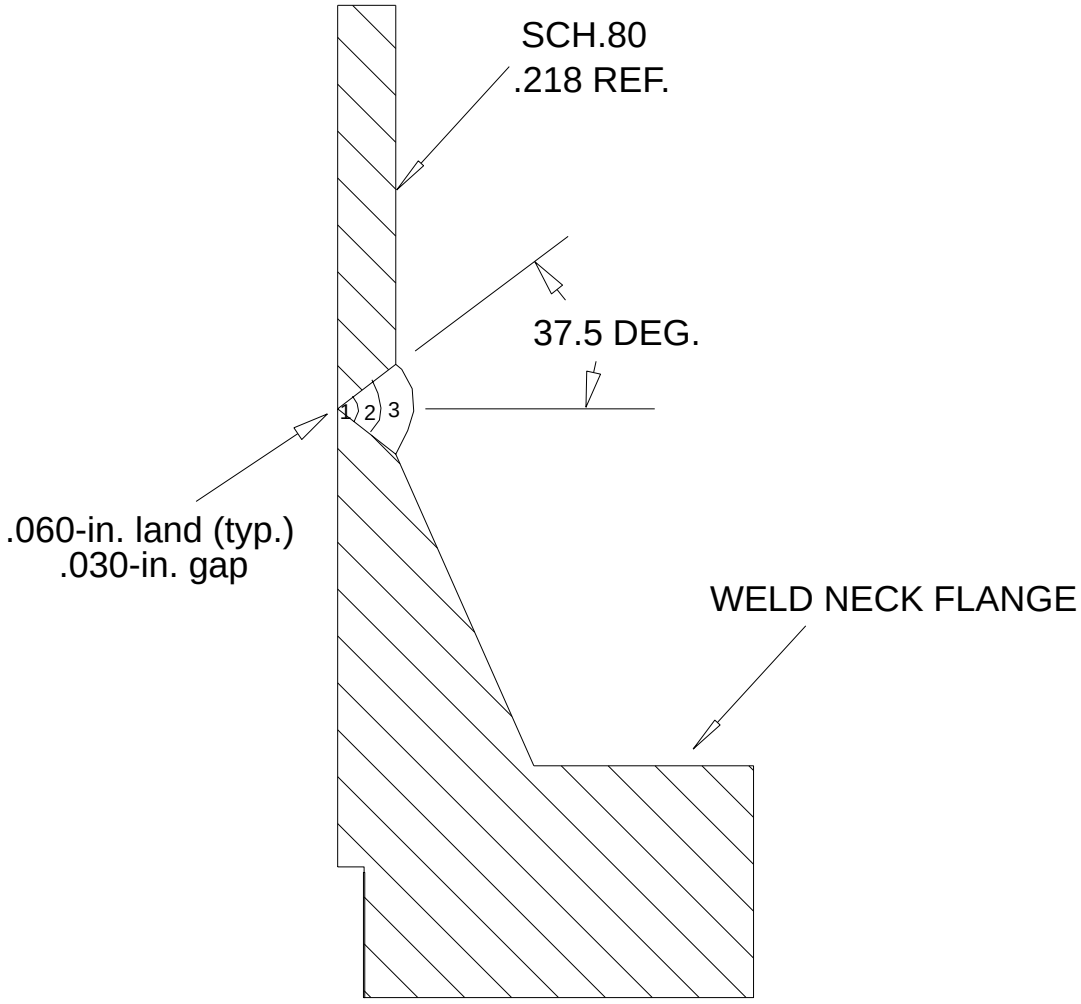


Figure B-17
Drawing of Typical Mockup Configuration with Standard Weld Neck Flange for Butt Weld Evaluation



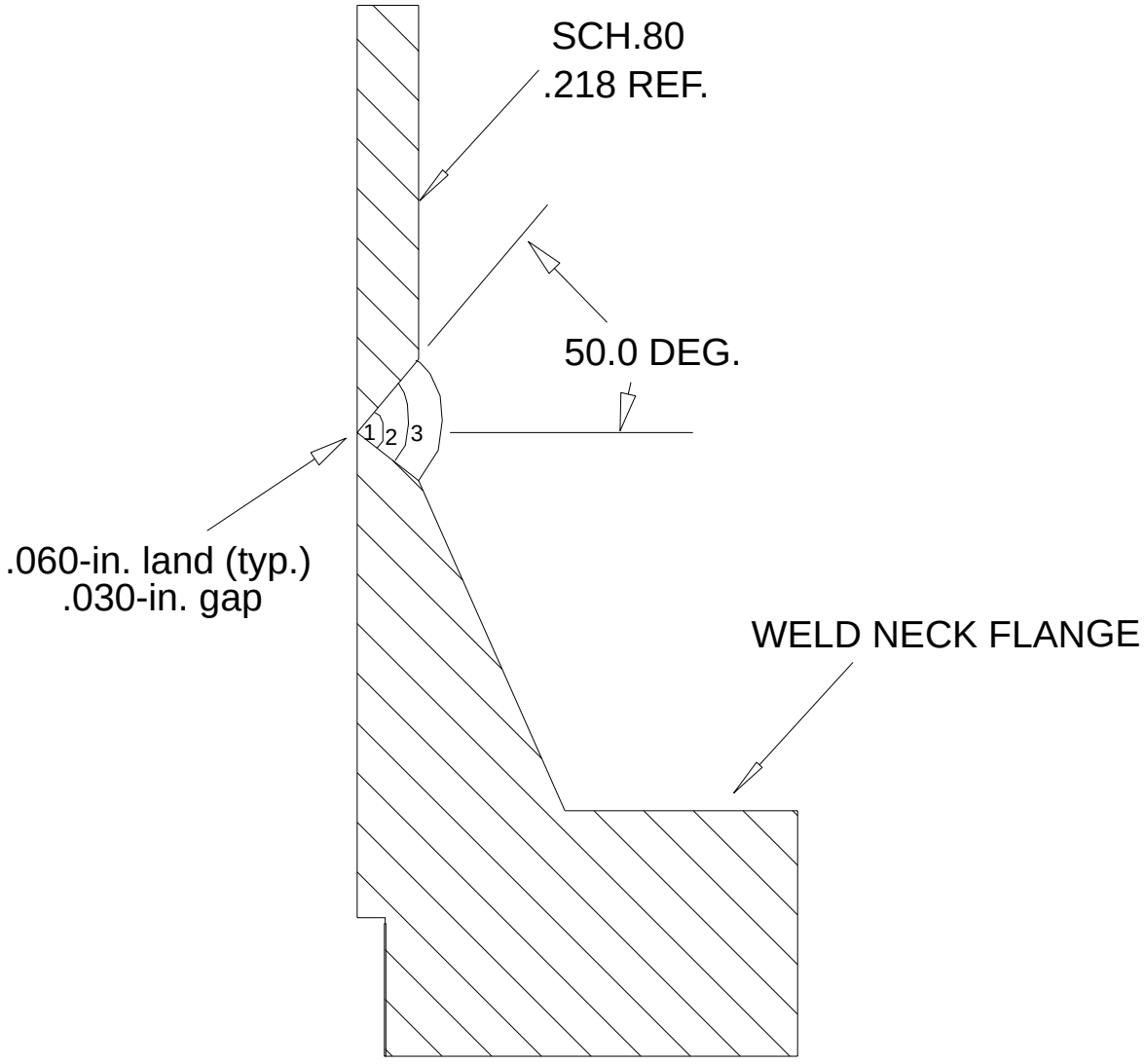
NOTE: All dimensions are in inches. To convert inches to centimeters, multiply the unit by 2.54.

Figure B-18
Drawing of Standard Weld Sequence for Butt Weld Geometry

B.10 Butt Weld with Flaw

Phase II included butt welds with intentional toe discontinuities.

The butt-welded configuration with toe discontinuity had the same weld sequence as the standard butt weld configuration, with the exception of the joint geometry. The joint configuration consisted of a v-groove configuration with 0.060-in. (0.152 cm) land and a 37.5-degree bevel on the fitting side and a 50-degree bevel on the pipe side. The 50-degree bevel extended the v-groove along the pipe side. The weld profile remained a typical three-bead sequence as seen in Figure B-19. The toe discontinuity was achieved by slightly underfilling the groove geometry on the pipe side (50-degree bevel) to achieve the appearance of an undercut. The slight undercut was considered acceptable by normal workmanship standards. The weld specifications for the butt weld configurations are listed in Table B-7.



NOTE: All dimensions are in inches. To convert inches to centimeters, multiply the unit by 2.54.

Figure B-19
Drawing of Standard Weld Sequence for Butt Weld Geometry with Flaw